



NEXOGENESIS

STREAMLINING WATER RELATED POLICIES

Future Trends and Validation of biophysical data for uncertainty assessment

Lead: Euro-Mediterranean Centre on Climate Change (CMCC)

Date: 23/02/2024



Project

Project Number	Project Acronym	Project Title
101003881	NEXOGENESIS	Facilitating the next generation of effective and intelligent water-related policies, utilizing artificial intelligence and reinforcement learning to assess the water-energy-food-ecosystem (WEFE) nexus

Instrument:	Thematic Priority
H2020RIA	LC-CLA-14-2020

Title
Future Trends and Validation of biophysical data for uncertainty assessment

Contractual Delivery Date	Actual Delivery Date
29.02.2024	29.02.2024

Start Date of the project	Duration
01 September 2021	48 months

Organisation name of lead contractor for this deliverable	Document version
CMCC	1

Dissemination level	Deliverable Type
Public	Report

Authors (organisations)
Antonio Trabucco (CMCC), Andrea Rivosecchi (CMCC), Sara Masia (CMCC/IHE), Muhammad Faizan Aslam (CMCC), Walter Rossi Cervi (WUR), Linderhof, Vincent (WUR)
Stefano Terzi (EURAC)



Abstract

The Deliverable 2.5 presents an overview and scoping of uncertainty linked to results of biophysical macro data/general trends for the case studies in the NEXOGENESIS project, aiming to facilitate screening and validation of results. Among biophysical modelling results made available through D2.2 (“*Nexus data vector of biophysical data for each case study [M30]*”), several variables and trends in line with a set of selected IPCC emission scenarios have been considered, discussed and reported for preliminary validation, following progress already established in MS18 (“*Internal Report of preliminary validation results for selected case studies [M26]*”). Several key variables consolidated in D2.2 repository data have been screened for uncertainty assessment and validation according to specific WEF nexus dimensions and modelling tools, in order to facilitate implementation of complexity science tools. This deliverable, combined with D3.6 (“*Sensitivity/Uncertainty Analysis Report [M30]*”) will characterize effective and representative uncertainty evaluations to facilitate the finalization of System Dynamic Modelling and its implementation for policy evaluation through Artificial Intelligence in WP4.

Keywords

RCP, SSP, WEF nexus, Coherency, Modelling, Socio-Economic, Biophysical, Climate, Hydrology, Agriculture, Water Demand, Ecosystem Functions

Disclaimer:

This report is prepared solely for the purpose of fulfilling the deliverables of this project and is based on the information and datasets available at the time of preparation. The data used reflects the most recent updates to the relevant databases and models at the time of release. The authors are not responsible for any changes or updates to the data or information that may occur after the report's completion.



Abbreviation/Acronyms

AGMIP	Agricultural Model Intercomparison and Improvement Project
CGE	Computable general equilibrium
CMIP	Coupled Model Intercomparison Project
CLC	CORINE Land Cover
GDP	Gross Domestic Product
GHGs	GreenHouse Gases
GTAP	Global Trade Analysis Project
IPCC	Intergovernmental Panel on Climate Change
ISIMIP	Inter-Sectoral Impact Model Intercomparison Project
RCP	Representative Concentration Pathway
SDM	System Dynamic Model
SLNAE	Self-Learning Nexus Assessment Engine
SSP	Shared Socioeconomic Pathways
WEFE	Water-Energy-Food-Ecosystem



Contents

Project	2
Abbreviation/Acronyms	4
Executive Summary	6
1 Introduction	7
1.1 Project summary	7
1.2 Case studies	7
1.3 Bio-Physical human modelling in NXG	8
2 Climate / Biophysical modelling data trends and uncertainty assessment	9
2.1 Modelling climate change	9
2.2 The Inter-Sectoral Impact Model Intercomparison Project (ISIMIP)	10
3 Trends and uncertainties in the NEXUS Sectors	13
3.1 Climate	13
3.2 Agriculture	22
3.3 Water	38
3.4 Ecosystems/Biomes	53
4 Land Use	66
4.1 Land Use Sources Data	66
4.2 Uncertainties in land use downscaling	67
5 Conclusions and contribution to other project activities	69
References:	70
ANNEX I. land use products	2



Executive Summary

The Deliverable 2.5 (Retrospective analysis and validation of biophysical data for uncertainty assessment [M30]) presents an overview of uncertainty linked to biophysical modelling data trends for the case studies in the NEXOGENESIS project. Several biophysical modelling variables and their trends in line with selected IPCC emission scenarios have been aggregated, harmonized and made available through D2.2 (Nexus data vector of biophysical data for each case study [M24]) for System Dynamic Modelling and Artificial Intelligence tasks in NEXOGENESIS. These modelling results inherently present uncertainty due to modelling biases, underlying climate drivers, emission scenarios, that altogether define multiple trajectories and pathways of development for each or most of the biophysical variables. Several key variables consolidated in D2.2 repository data have been screened according to specific WEF nexus dimensions and modelling tools, in order to facilitate and support the implementation of complexity science tools. **In particular, the biophysical modelling variables considered include: mean daily precipitation flux [mm/day], daily maximum and minimum temperature [C] (climate); crop yields [t/ha] and irrigation requirement [kg/m²] (agriculture); surface runoff [mm/day] and groundwater recharge [mm/day] (water); soil carbon storage [kg/m²] and vegetation carbon storage [kg/m²] (ecosystems).** Summary tables of mean values and uncertainty ranges are provided for all the studied variables in each case study region. Temperature and precipitation uncertainty ranges are consistent across regions, with model projections mostly agreeing with each other. As expected, higher uncertainty appears for the bio-physical variables, especially those related to water and agriculture. This is due to the higher number of factors affecting the models projections, including model parameterization and design, as well as different response to climatological uncertainty. In most cases the uncertainty range is increased by the presence of one or two models acting as outliers and projecting values significantly different from the rest of the ensemble. Moreover, differences in models behaviour across regions could be dictated by different local conditions, the extent of the studied area and biases in the choice of grid-cells. Defining and describing uncertainty ranges of modelling results facilitate a preliminary understanding of both conservative and outlying projections for preliminary validation and screening. ~~while flagging potential mistakes.~~



1 Introduction

1.1 Project summary

Water, Energy, Food, and Ecosystems are interconnected and part of a complex system referred to as the Water-Energy-Food-Ecosystem (WEFE) nexus. The assessment of the interactions between these components through the nexus approach is crucial to enhance synergies and minimize trade-offs between sectors, thus to inform decision makers with feasible strategies to accelerate sustainable and inclusive socio-economic development. The Nexogenesis (NXG) project aims at improving policies related to water, energy, food and ecosystems and contribute to the operationalization of the WEFE nexus approach by developing and validating three main solutions: i) the self-learning nexus assessment engine (SLNAE) that exploits artificial intelligence to provide a series of possible actions that maximise nexus performance; ii) a WEFE Nexus Footprint, i.e., a composite indicator that will contribute to monitor sustainability of resource management; iii) policy packages developed per each case study for streamlining water-related policy into the nexus which include the impact of external drivers such as the climate and the socio-economic system. The project aims at developing a coherent, consistent and replicable framework - co-created and validated by local experts and stakeholders - that will support out-scaling of the project's outcomes to wider regions.

1.2 Case studies

NEXOGENESIS (NXG) will develop and apply a coherent and consistent framework in five case studies characterised by a large variety of nexus policy issues.

The project case studies are located in different geographical areas (Figure 1) and each of them address different challenges:

- Nestos River Basin (BG-EL): ecologically significant delta, hydropower, water diplomacy up-/downstream countries;
- Lielupe River Basin (LT-LV): increased fertiliser use, pollutant runoff, hydropower impacts, water diplomacy issues;
- Lower Danube Basin (SRB-BG-RO): iron gates hydropower, significant (80%) wetland loss, agriculture;
- Adige River Basin (IT): ecosystem services support, equitable resource distribution, lack of trust/collaboration, peculiar governance regime due to cultural and historical reasons;



- Inkomoti-Usuthu Water Management Area (ZA-SZ-MZ): strategic management of water sources, three-nation, complex water diplomacy issues



Fig 1. Case studies geographical location.

The case studies represent: (i) diverse spatial, social, cultural, and development situations; (ii) strong WEF nexus relations, with the potential for disruption from policy implementation; (iii) allow assessment of how water-related policy can be streamlined into the nexus; and (iv) project outcomes are potentially transferable to other regions.

1.3 Bio-Physical human modelling in NXG

The NXG WP2 aims at providing a portfolio of consolidated future biophysical and socio-economic data trends for each case study to characterize climatic, hydrological, environmental, and socio-economic variables, in line with a set of selected IPCC scenarios, as combination of shared socioeconomic pathway (SSP) and representative concentration pathway (RCP) scenarios. The framework of macro data/general trends has been structured, listing significant available variables that can be generated under uniform methodology, assumptions and modelling across all case studies. The inventory list is formulated and about to be presented to describe potential support for SDM development for the different case studies.

2 Climate / Biophysical modelling data trends and uncertainty assessment

2.1 Modelling climate change

General Circulation Models (GCMs) have been used to simulate physical processes within the atmosphere, ocean, cryosphere and land surface systems, to understand how the climate has changed in the past and may change in the future, for simulating and predicting the response of the planet climate system to increasing concentration of Green-House Gasses (GHGs). They normally simulate climate processes using 3-dimensional planetary grids, with a spatial horizontal resolution between 70 and 300 km, 10 to 20 vertical layers in the atmosphere and sometimes as many as 30 layers in the oceans. Still, GCMs are extremely demanding in processing time and require some of the largest computing facilities in order to generate their projections. The complexity, and high level of interactions involved to represent accurately the climate system, and processing limitations lead to still quite coarse resolution (70-100 km over land) for most impact assessments.

Thus, with such coarse pixel resolution many physical processes must be averaged over larger scale, and many physical processes related to clouds formation and interaction with orography and shorelines cannot be modelled accurately. Downscaling is a post-processing analytical method widely used to increase resolution and better represent spatial variability, but often only available to limited regions with consistent delay in terms of product production. Thus, several sources of modelling errors and divergences among model outputs (i.e. uncertainties) are present, for which improvement of reliability and confidence of climate modelling outputs are needed. To this end, climate models are constantly updated and improved, both in terms of increased spatial resolution and more accurate parameterization and simulation of biophysical processes and biogeochemical cycles. A coordinated modelling effort is part of the Coupled Model Intercomparison Project (CMIP), aiming to improve climate models by cross-comparing different simulations and coordinate modelling results update around the schedule of the Intergovernmental Panel on Climate Change (IPCC) assessment reports. Thus, sets of CMIP model results, known as runs, are released in the lead-up of and to support IPCC reports: 2013 IPCC fifth assessment report (AR5) was based on climate models from CMIP5, while the 2021 IPCC sixth assessment report (AR6) features new state-of-the-art CMIP6 models. CMIP working timeline currently suggests scenario availability from CMIP7 in late 2025/early 2026.

Evaluating results from most CMIP6 model runs, it has become evident that they have a notably higher climate sensitivity than models in CMIP5, which contributes to projections of greater warming this century – around 0.4C warmer than similar scenarios run in CMIP5.

2.2 The Inter-Sectoral Impact Model Intercomparison Project (ISIMIP)

Inter-Sectoral Impact Model Intercomparison Project (ISIMIP) outcomes in combination with climate drivers from the Coupled Model Intercomparison Project (CMIP) have been consolidated to provide relevant and harmonized modelling outputs for different sectors (Climate, Water, Agriculture, Forest, Biomes, terrestrial biodiversity, etc.) following common standard protocols and underlying climate forcing/scenarios. Thus, ISIMIP modelling outcomes provides a consistent framework of the impact of climate change across sectors. To this end, ISIMIP is organised in “simulation rounds” around specific CMIP runs. For each round, a simulation protocol defines a set of common simulation scenarios (e.g. climate projections as driver) and other global drivers. ISIMIP simulation rounds have been mostly established in combination and based on CMIP simulation rounds. These ISIMIP implementations create a coherent impact modelling chains around CMIP simulation rounds with impact established following common standard protocol and underlying climate scenarios for different sectors. Each simulation round covers specific sectors namely: global and regional water, fisheries and marine ecosystems, energy supply and demand, regional forests, global biomes, and agriculture, agro-economic modelling, terrestrial biodiversity, permafrost, coastal systems, health, lakes, and fire. The sectors screened so far are the climate, water, agriculture, terrestrial biodiversity, and biomes sectors ([Annex 1](#)).

Selected climate projections established from CMIP runs, and used as underlying climate input/drivers at global scale for pre-industrial, historical, and future conditions in ISIMIP, are both bias corrected and downscaled to a spatial resolution of 0.5 degrees (i.e. 50-60 km) using ERA5 observational data (W5E5), according to following methodology:

https://www.isimip.org/documents/16/Fact_Sheet_Bias_Correction.pdf

As mentioned, the ISIMIP is organized in simulation rounds: simulation round 2b is consolidated on CMIP5, while simulation round 3b is consolidated on CMIP6. Being established earlier on, CMIP5 and CMIP6 have some substantial differences between the relative historical and future (projections) time periods. CMIP5 historical projection based on observed GHG concentrations end in 2005, and thereafter projections start from 2006 with different emission scenarios (RCPs). Likewise, CMIP6 historical projections, end in 2014, and projections start thereafter, from 2015 onward. At the beginning of the project (2021) only ISIMIP modelling results from simulation round 2b were available, and have been used to populate preliminary time series and variable vector lists for the different case studies. From summer 2023, however, modelling impact results from most recent ISIMIP round 3b (following CMIP6) on different sectors have become available. Thereafter, results from ISIMIP 3b have been included in the biophysical vector list in addition to results from ISIMIP 2b, and made available to NEXOGENESIS SDM development.

Data in the biophysical vector list are available therefore for

ISIMIP 2b for the historical (1971-2005) and future (2006-2070) time periods under climate scenarios RCP 2.6, RCP 6, RCP 8.5.

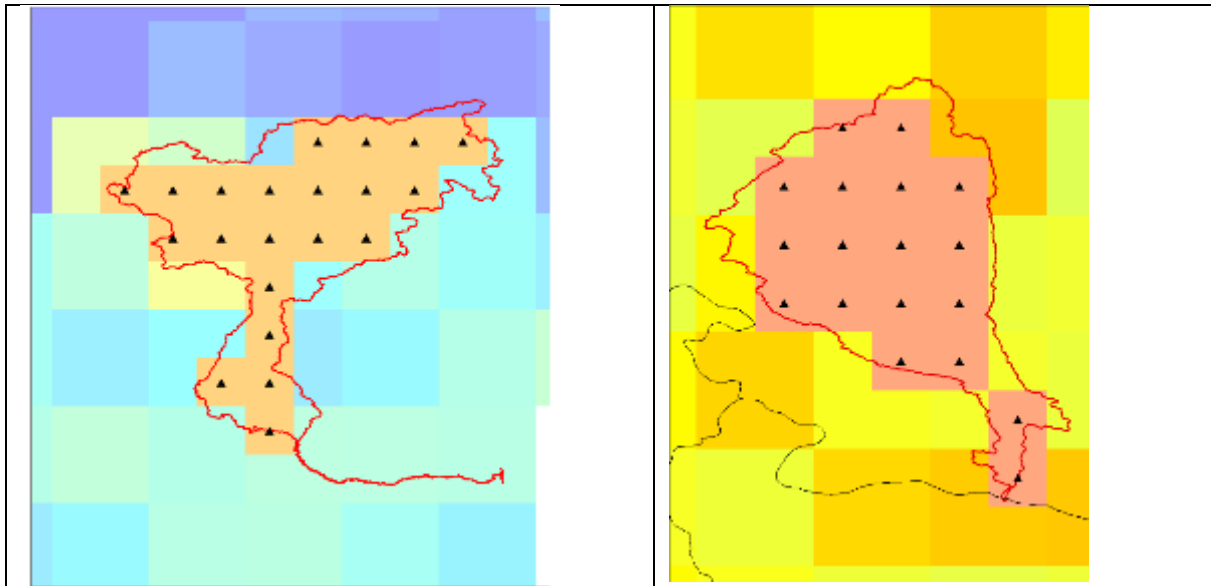
ISIMIP 3b for the historical (1971-2014) and future (2015-2070) time periods under climate scenarios ssp_{x26} (formally replacing RCP2.6 of CMIP5) and ssp_{x85} (formally replacing RCP8.5 of CMIP5)

All the climate and biophysical data ISIMIP data proposed for the development of the System Dynamics Models (SDMs) within the NXG project are bias corrected and are made available with a spatial resolution of 0.5°x0.5°. In order to facilitate weighting and subsampling more accurately pixel portions within the boundaries of project case studies, original 0.5 degrees raster grids have been subset to 0.25 pixels from which basin-wide average for each variable have been sampled for the whole time series. Data series are available for historical and future time frames. The temporal frequency of the available climate and biophysical data ranges from monthly (for sectors Climate, Water, Biomes Monthly), to yearly (for sectors Agriculture, Biomes yearly) to 30-yr mean (for sector Biodiversity) temporal resolution depending on the variable.

Accordingly, data projections have been consolidated from different hydrological and land use modelling tools (e.g. WaterGAP, JULES, LPJmL, H08), as harmonized to provide robust information, and data values extracted for each case study for several variables most relevant to characterize processes and interlinkages across NEXUS dimensions: Climate (Min and max Temperature, Precipitation, Relative Humidity, Surface downwelling longwave and shortwave Radiation, Wind Speed, Snowfall, Snowdepth), Water (Potential/Reference Evapotranspiration, Surface/Subsurface Runoff, Soil Moisture, groundwater recharge, water demand from different sectors), Food (Crop Yield, biomass yield, irrigation requirements, Nitrogen application rate for about 12 main crops), Ecosystem (Net & Gross Primary Productivity, Leaf Area Index, Above and Belowground Carbon stock for combination of 10-20 landuse-ecosystem types, Biodiversity metrics).

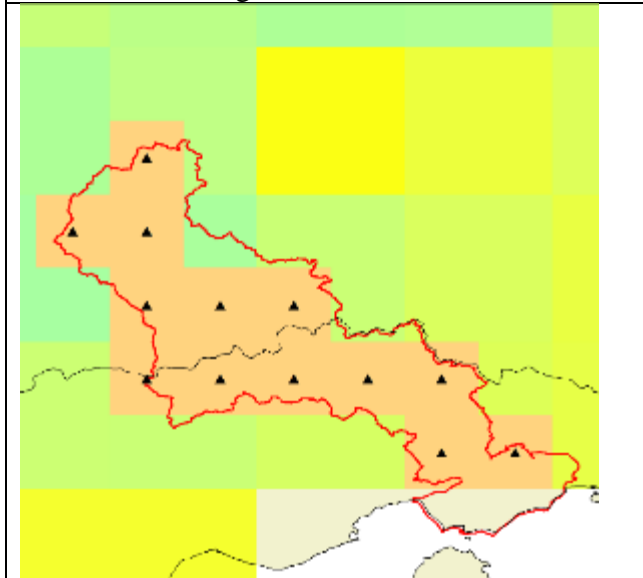
In addition, projections for the aforementioned climate variables, except for snowdepth, have been downscaled to 0.1 degrees with statistical downscaling using the ISIMIP3BADS method (Lange 2019, 2021) for the Nestos and Adige case studies. These variables are available at a daily resolution providing inputs for further additional hydrological modelling in these case studies for a more detailed simulation of hydrological processes for the present and the future.



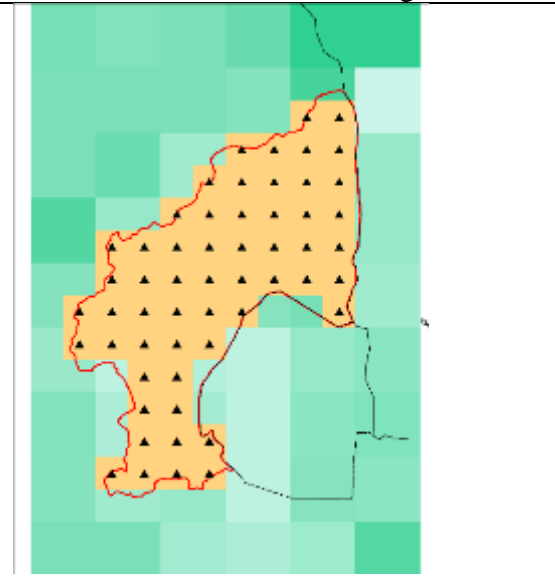


Adige Case Study, subsampling of ISIMIP 0.5 degrees pixels at 0.25 degrees for extraction of basin wide average values

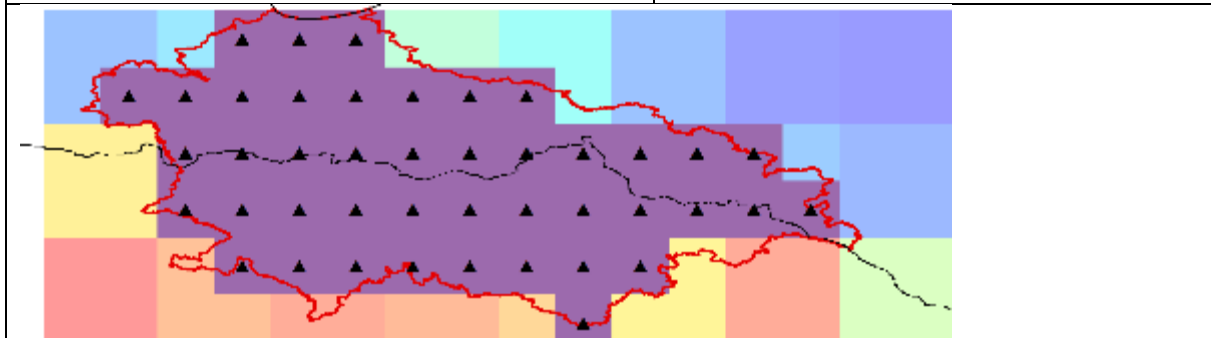
Jiu Case Study, subsampling of ISIMIP 0.5 degrees pixels at 0.25 degrees for extraction of basin wide average values



Nestos Case Study, subsampling of ISIMIP 0.5 degrees pixels at 0.25 degrees for extraction of basin wide average values



Limpopo Case Study, subsampling of ISIMIP 0.5 degrees pixels at 0.25 degrees for extraction of basin wide average values



Lielupe Case Study, subsampling of ISIMIP 0.5 degrees pixels at 0.25 degrees for extraction of basin wide average values



3 Trends and uncertainties in the NEXUS Sectors

The climate and biophysical variables screened from the ISIMIP 2b and ISIMIP 3b database cover climate, water, agriculture, terrestrial biodiversity and biomes sectors (see details in [Annex 1](#)). The SIMETAW_GIS model complement the biophysical variable for agricultural and water sector provided by the ISIMIP.

3.1 Climate

Climate scenarios projections are representations of various possible future states of the climate system, based on numerical model simulations. These models describe the complex processes and interactions affecting the climate system, but also use information about anthropogenic climate forcing. Different factors of anthropogenic activity like socio-economic, technological, demographic and environmental development are characterized in climate models, such as changes in GHG concentrations, land use, etc. The climate trajectories of different emission scenarios (e.g. between RCP2.6, RCP4.5 and RCP6.0) do not substantially diverge before the middle of the 21st century, therefore it is advisable that the most remarkable and expected differences for assessments are inferred following scenarios on the low-high end.

An implicit downscaling was implemented to the finer resolution of a 0.5° using the WATCH Forcing Data (WFD, Weedon et al. 2011) for CMIP5 and W5E5 forcing data for CMIP6, as observation-based reference data. The applied bias correction method preserves the long-term trends of the variables. In a first step, only the monthly variability and mean are corrected using a constant offset or multiplicative correction factor that corrects for long-term differences between the simulated and observed monthly mean data in the historical period. Then the daily variability of the simulated data is modified about their monthly means to match the observed daily variability.

Bias corrected data are based on simulations of five GCMs for ISIMIP 2b from CMIP5 archive and three GCMs for ISIMIP 3b from CMIP6 (see Table 1).

The projections for several model consist of historical model runs from 1971 and following emission scenarios from 2014 till 2070. From each model, two scenario based on the Representative Concentration Pathway (RCP) emission scenarios (Moss et al. 2010, van Vuuren et al. 2011, Meinshausen et al. 2011) are available: RCP2.6 and RCP8.5, which have been renamed as ssp26 and ssp85 under CMIP6. Thus, there are 10 different ISI-MIP 2b and 6 different ISI-MIP 3b climate driving projection scenarios, for a combination of 8 climate models and 2 emission scenarios. A model ensemble with a high number of endmembers ensures better coverage of model uncertainty and allows for quantile and other statistical analyses. The selected models cover a broad response space defined by global temperature. (Portman et al., 2013).

Table 1. Climate projections of five GCMs for ISIMIP 2b from CMIP5 archive and three GCMs for ISIMIP 3b from CMIP6 archive

Run	Acronym	Origin
ISIMIP 2b (CMIP5)	HadGEM2-ES	Met Office Hadley Centre (UK) and Instituto Nacional de Pesquisas Espaciais (BR)
	IPSL-CM5A.LR	Institut Pierre-Simon Laplace (FR)
	MIROC-ESM-CHEM	Japan Agency for Marine-Earth Science and Technology, Atmosphere and Ocean Research Institute (U Tokyo), and National Institute for Environmental Studies (JP)
	GFDL-ESM2M	NOAA Geophysical Fluid Dynamics Laboratory (US)
	NorESM1-M	Norwegian Climate Centre (NO)
ISIMIP 3b (CMIP6)	mpi-esm1-2-hr	Max Planck Institute Earth System Model (Germany)
	gfdl-esm4	NOAA Geophysical Fluid Dynamics Laboratory Earth System Model v 4.1 (US)
	ipsl-cm6a-lr	Institut Pierre-Simon Laplace Climate Model 6A (FR)

The variable consolidated from the ISIMP database for the development of the climate vectors list for the NXG case studies are:

Total Precipitation (short_name *pr*) Total precipitation is expressed as kg m⁻² s⁻¹ or mm day⁻¹ and is available at daily or monthly temporal resolution for CMIP5 (under RCP2.6, RCP6.0 and RCP8.5) and for CMIP6 (under ssp26 and ssp85).

Average Temperature (short_name *tas*) Near-Surface Air average Temperature is expressed as K° or C° and is available at daily or monthly temporal resolution for CMIP5 (under RCP2.6, RCP6.0 and RCP8.5) and for CMIP6 (under ssp26 and ssp85).

Maximum Temperature (short_name *tasmax*) Near-Surface Air Maximum Temperature is expressed as K° or C° and is available at daily or monthly temporal resolution for CMIP5 (under RCP2.6, RCP6.0 and RCP8.5) and for CMIP6 (under ssp26 and ssp85).

Minimum Temperature (short_name *tasmin*) Near-Surface Air Minimum Temperature is expressed as K° or C° and is available at daily or monthly temporal resolution for CMIP5 (under RCP2.6, RCP6.0 and RCP8.5) and for CMIP6 (under ssp26 and ssp85).

Snowfall (short_name *prsn*) Total snowfall is expressed as kg m⁻² s⁻¹ or mm day⁻¹ and is available at daily or monthly temporal resolution for CMIP5 (under RCP2.6, RCP6.0 and RCP8.5) and for CMIP6 (under ssp26 and ssp85).

Relative Humidity (short_name *rhs*) Near-Surface Average Relative Humidity is expressed as % and is available at daily or monthly temporal resolution for CMIP5 (under RCP2.6, RCP6.0 and RCP8.5) and for CMIP6 (under ssp26 and ssp85).

Shortwave Radiation (short_name *rsds*) Surface Downwelling or Incoming Shortwave Radiation is expressed as W m⁻² and is available at daily or monthly temporal resolution for CMIP5 (under RCP2.6, RCP6.0 and RCP8.5) and for CMIP6 (under ssp26 and ssp85).

Longwave Radiation (short_name *rsds*) Surface Downwelling or Incoming Longwave Radiation is expressed as W m⁻² and is available at daily or monthly temporal resolution for CMIP5 (under RCP2.6, RCP6.0 and RCP8.5) and for CMIP6 (under ssp26 and ssp85).

Wind Speed (short_name *wind*) near surface wind speed (m s⁻¹) is expressed as m s⁻¹ and is available at daily or monthly temporal resolution for CMIP5 (under RCP2.6, RCP6.0 and RCP8.5) and for CMIP6 (under ssp26 and ssp85).



Table 2. Average changes of pr (mm per day and difference in %), tasmax and tasmin (degrees °C and change as difference in degree °C) are reported for each case study, emission scenarios (RCP2.6 vs RCP8.5) and CMIP run (CMIP5 vs CMIP6), between baseline (average over 1985-2014) and future (average over 2036-2065) time frames.

		Historical 1985-2014		rcp26 2036-2065		rcp85 2036-2065	
		cmip5	cmip6	cmip5	cmip6	cmip5	cmip6
		Adige	pr (mm day-1)	2.63	2.65	2.71	2.72
	tasmax (°C)	6.96	6.84	8.39	8.35	9.53	9.09
	tasmin (°C)	0.28	0.03	1.55	1.30	2.58	2.20
Inkomati	pr (mm day-1)	2.24	2.19	2.38	2.19	2.27	2.21
	tasmax (°C)	25.89	26.32	27.00	27.50	28.02	28.28
	tasmin (°C)	12.65	12.98	13.64	13.92	14.62	14.74
Jiu	pr (mm day-1)	2.03	2.10	2.05	2.14	1.98	2.02
	tasmax (°C)	14.66	14.64	16.41	16.29	17.59	17.20
	tasmin (°C)	5.48	5.31	6.80	6.56	7.90	7.52
Lielupe	pr (mm day-1)	1.93	1.93	1.96	2.04	1.96	2.12
	tasmax (°C)	10.87	10.54	12.85	12.24	13.85	13.01
	tasmin (°C)	2.95	2.79	4.84	4.37	5.89	5.32
Nestos	pr (mm day-1)	1.72	1.85	1.71	1.89	1.61	1.73
	tasmax (°C)	14.81	14.94	16.31	16.48	17.46	17.40
	tasmin (°C)	5.47	5.04	6.71	6.21	7.63	6.98

		2036-2065 vs 1985-2014			
		rcp26		rcp85	
		cmip5	cmip6	cmip5	cmip6
Adige	pr (diff %)	3.2	2.7	1.2	2.8
	tasmax (diff °C)	1.4	1.5	2.6	2.2
	tasmin (diff °C)	1.3	1.3	2.3	2.2
Inkomati	pr (diff %)	6.5	0.0	1.5	0.9
	tasmax (diff °C)	1.1	1.2	2.1	2.0
	tasmin (diff °C)	1.0	0.9	2.0	1.8
Jiu	pr (diff %)	1.0	1.8	-2.5	-4.0
	tasmax (diff °C)	1.7	1.7	2.9	2.6
	tasmin (diff °C)	1.3	1.3	2.4	2.2
Lielupe	pr (diff %)	1.5	5.4	1.8	9.6
	tasmax (diff °C)	2.0	1.7	3.0	2.5
	tasmin (diff °C)	1.9	1.6	2.9	2.5
Nestos	pr (diff %)	-0.4	2.3	-6.2	-6.2
	tasmax (diff °C)	1.5	1.5	2.6	2.5
	tasmin (diff °C)	1.2	1.2	2.2	1.9



Variable trends and uncertainty

The three CMIP6 climate models show good agreement among each other for both average temperature (tas) and total precipitation (pr), as their trend overlap in all regions for the entire studied period. The magnitude and long-term trends highlighted by the three models for both total precipitation and average temperature are consistent with the most recent literature (Almazroui et al., 2020; Coppola et al., 2021). Thus, from this analysis it emerges that all climate models within the dataset can be used interchangeably, with no significant difference in the outcome. As a general rule, in the absence of a reference observational dataset, the preferred model should be the one with the highest correlation with the inter-model mean. In this case, no model appears to behave better than the others overall, so the choice should be based on the specific region and scenario studied.

The uncertainty deriving from the use of a climate model over the others propagates to all the other sectors projections, as all sector models are driven by the climate models.

Average Temperature

All models predict an increase in average temperature for all regions in both ssp_{x26} and ssp_{x85}. For all regions, the temperature increase is more significant in the ssp_{x85} scenario than in ssp_{x26}.

The three climate models (mpi, ipsl and gfdl) show good agreement among them and overlap with the mean in all regions and scenarios.

The spread represents the uncertainty range deriving from the different climate model projections and is set at one standard deviation from the mean. Across the studied regions, the average spread ranges between 1.59-2.22 °C in ssp_{x26} and 1.55-2.24 in ssp_{x85}. This means that, on average, each climate model has a $\pm 2^\circ\text{C}$ deviation from the mean of the three models.

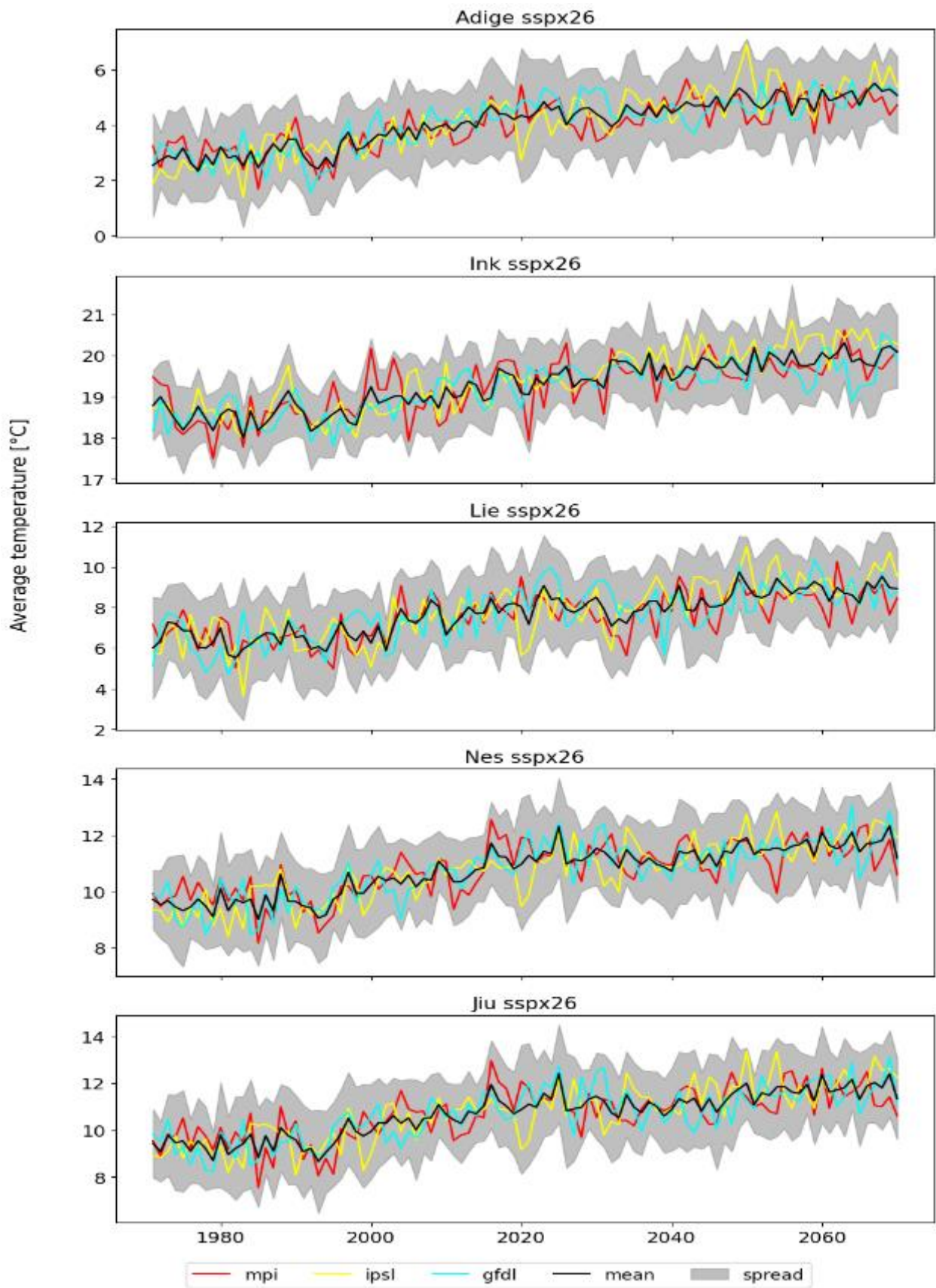


Figure 2. Average temperature [°C] projections for the historical (1971-2014) and sspx26 (2015-2070) scenarios in the MPI-ESM1-2-HR (mpi, red), IPSL-CM6A-LR (ipsl, yellow) and GFDL-ESM4 (gfdl, cyan) in each studied basin. The grey shading represents the spread of the projections and corresponds to one standard deviation from the inter-model mean.

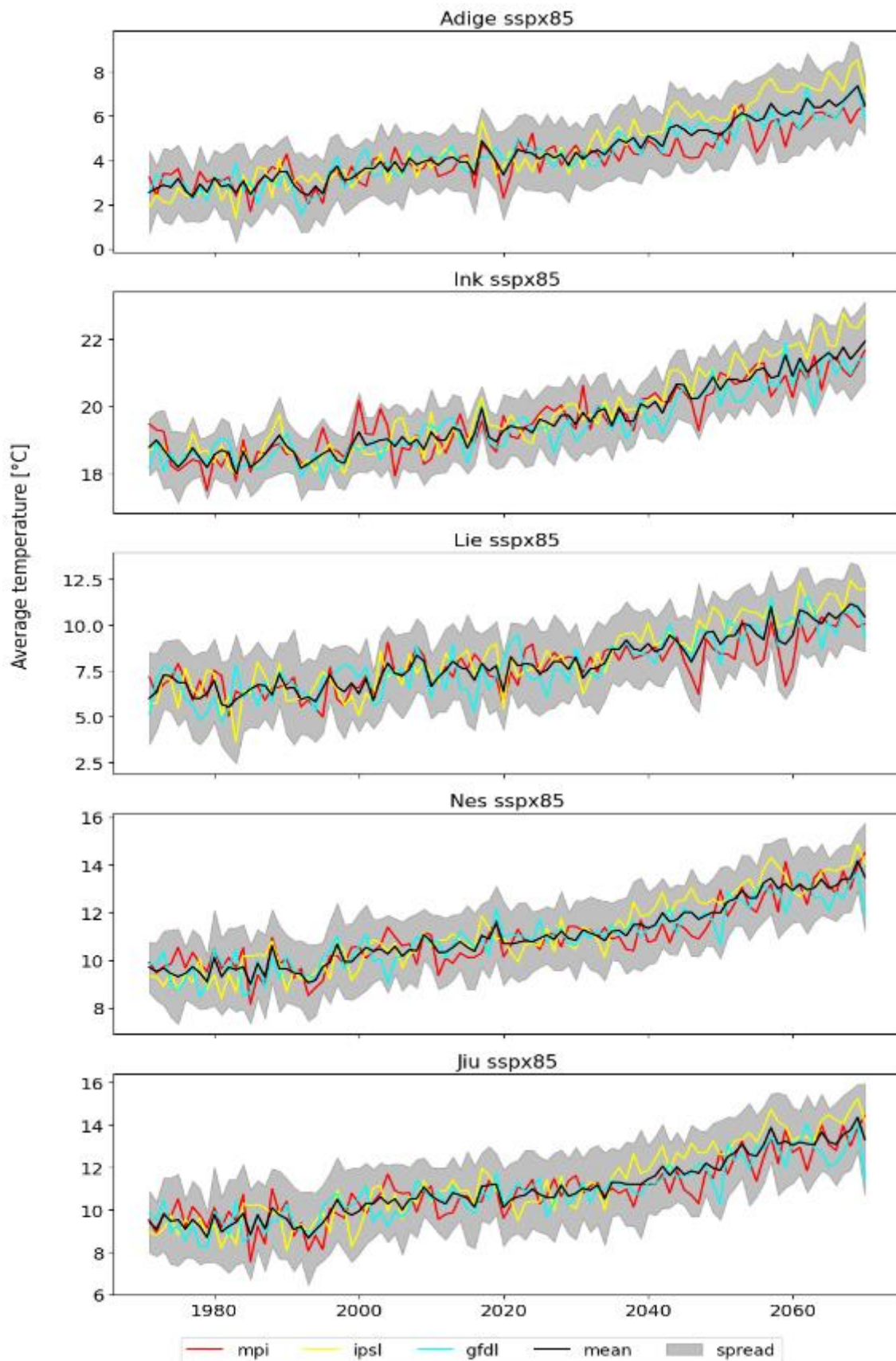


Figure 3. Average temperature [°C] projections for the historical (1971-2014) and ssp85 (2015-2070) scenarios in the MPI-ESM1-2-HR (mpi, red), IPSL-CM6A-LR (ipsl, yellow) and GFDL-ESM4 (gfdl, cyan) in each studied basin. The grey shading represents the spread of the projections and corresponds to one standard deviation from the inter-model mean.

Table 3. Inter-model mean and 95% uncertainty range in mean annual temperature [°C] for the sspx26 and sspx85 scenarios for all the studied regions. The uncertainty is shown in brackets.

	Adi	Jiu	Lie	Nes	Ink
SSPx26	4.1 (3.0)	19.3 (1.8)	7.7 (4.2)	10.7 (3.0)	10.7 (3.6)
SSPx85	4.3 (3.1)	19.6 (1.9)	7.9 (4.2)	11.0 (3.0)	11.0 (3.6)

Total Precipitation

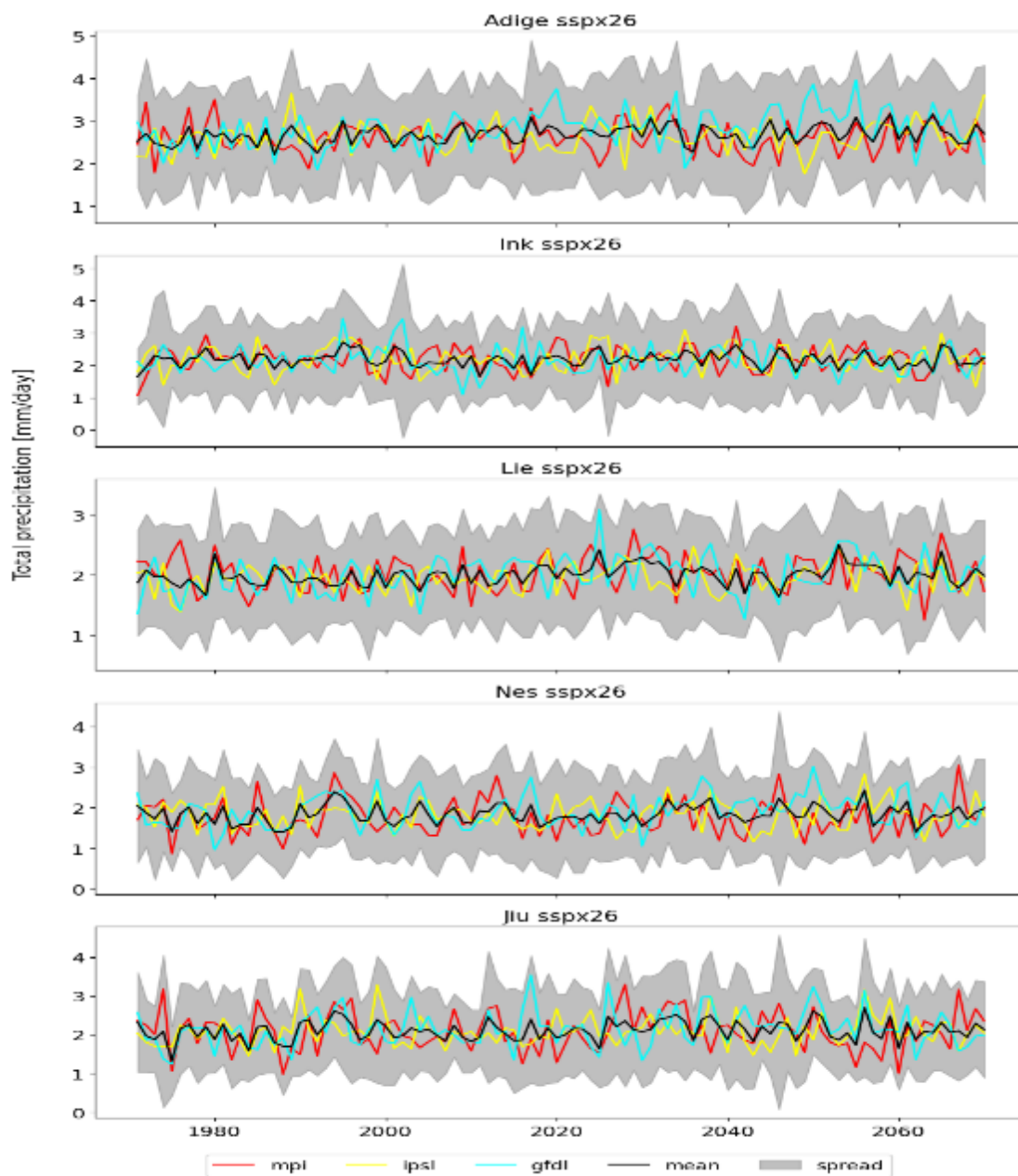


Figure 4. Total precipitation [mm/day] projections for the historical (1971-2014) and sspx26 (2015-2070) scenarios in the MPI-ESM1-2-HR (mpi, red), IPSL-CM6A-LR (ipsl, yellow) and GFDL-ESM4 (gfdl, cyan) in each studied basin. The grey shading represents the spread of the projections and corresponds to one standard deviation from the inter-model mean.

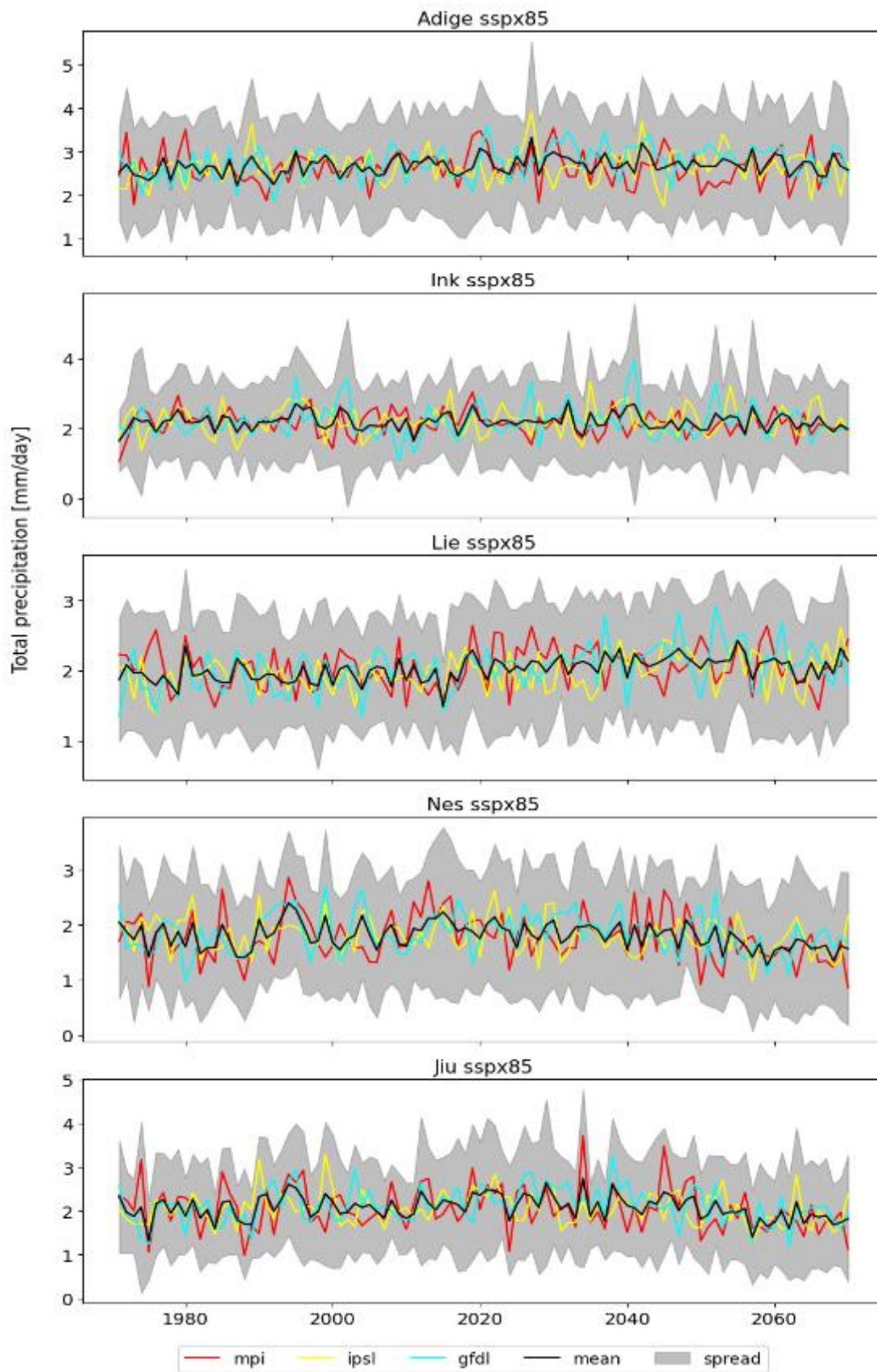


Figure 5. Total precipitation [mm/day] projections for the hisotrical (1971-2014) and ssp85 (2015-2070) scenarios in the MPI-ESM1-2-HR (mpi, red), IPSL-CM6A-LR (ipsi, yellow) and GFDL-ESM4 (gfdl, cyan) in each studied basin. The grey shading represents the spread of the projections and corresponds to one standard deviation from the inter-model mean.



The three climate models (mpi,ipsl and gfdl) show good agreement among them, with mostly consistent overlapping trends in all regions and scenarios.

All regions show a range of interannual variation in the total precipitation mean of 1-1.5 mm/day. None of the regions show a discernible trend in total precipitation in either of the scenarios, with mean values remaining almost the same from the historical period to the second half of the 21st century. A slightly decreasing trend appears in the Nestos and Jiu profiles after 2040, but longer simulations are needed to confirm it with greater certainty.

Table 4. Inter-model mean and 95% uncertainty range in mean daily precipitation [mm/day] for the ssp_{x26} and ssp_{x85} scenarios for all the studied regions. The uncertainty is shown in brackets.

	Adi	Jiu	Lie	Nes	Ink
SSPx26	2.7 (2.5)	2.2 (2.6)	2.0 (1.7)	1.8 (2.2)	2.1 (2.4)
SSPx85	2.7 (2.5)	2.2 (2.6)	2.0 (1.8)	1.8 (2.2)	2.1 (2.4)

3.2 Agriculture

In the NXG project, the agricultural sector is covered by two data sources, i.e., the ISIMP2b/ISIMIP3b database and the SIMETAW_GIS model. The ISIMIP database provides modelling output of agricultural production in terms of crops cultivated for both food and energy purposes at global scale. Four impact-model participate in the ISIMIP simulation round 2b for this sector and twelve for the ISIMIP simulation round 3b:

ISIMIP2b: CLM4.5, *Community Land Model*; GEPIC, *GIS-based EPIC model*; LPJmL, *Lund-Potsdam-Jena managed Land*; PEPIC, *Python-based Environmental Policy Integrated Climate (EPIC) model* (model details at <https://www.isimip.org/impactmodels/>). Within the ISIMIP2b, the models above mentioned generate quantitative information for 12 crops i.e., Cassava, Field Pea, Ground Nuts, Maize, Millet, Rapeseed, Rice, Soy, Sugar Beet, Sugarcane, Sun Flower and Wheat, considering managed in both rainfed (noirr) and in full irrigated conditions (firr).

ISIMIP3b: ACEA; CROVER; CYGMA1p74; DSSAT-Pythia; EPIC-IIASA; LDNDC; LPJ-GUESS; LPJML; PDSSAT; PEPIC; PROMET; SIMPLACE-LINTULS5 Within the ISIMIP3b, the models above mentioned generate quantitative information for 11 crops i.e., Beans, Cassava, Maize, Millet, Potato, Rapeseed, Rice, Sorghum, Soy, Spring wheat and Winter wheat considering managed in both rainfed (noirr) and in full irrigated conditions (firr).

The agricultural model simulations selected so far do either or not consider future CO₂ fertilization changes; provided data can then consistently consider CO₂ concentration in the atmosphere fixed to 2005, i.e., 378.81 ppm, or transient levels following RCPs scenarios (i.e.,

climate and CO₂ scenario: 2005-CO₂). Keep in mind that this alternative scenario is to check the direct effect of CO₂ fertilization on crop physiology. Changes in management up to 2005 are considered also for different socio-economic scenario (i.e., human influence & land-use scenarios in terms of variation of land use, water abstraction, nitrogen deposition and fertilizer input; human influence and land use scenario: 2005CO₂, CO₂). All of these different projections under different co₂ and soc assumptions can be used to characterize uncertainty of impact model projections. Data are delivered yearly per growing season with a resolution of 0.5°x 0.5°.

The variable consolidated from the ISIMP database for the development of agricultural variables for the NXG case studies are:

Planting and maturity dates (short name: *plantday & matday*). Both the planting and the maturity day are expressed as Julian day, i.e., day of the year. The data is available at yearly temporal resolution for CMIP5 (under RCP2.6 and RCP6.0) and for CMIP6 (under ssp26 and ssp85).

Crop Yield (short name: *yield*). The crop yield is expressed in dry matter as tons ha⁻¹ per growing season. The crop model simulations have a global spatial coverage under the assumption that the crops are cultivated everywhere. The data is available at yearly temporal resolution for CMIP5 (under RCP2.6 and RCP6.0) and for CMIP6 (under ssp26 and ssp85).

Biomass Yield (short name: *Biom*): Total Above Ground Biomass Dry Matter Yields is expressed as tons ha⁻¹ per growing season. The data is available at yearly temporal resolution for CMIP5 (under RCP2.6 and RCP6.0) and for CMIP6 (under ssp26 and ssp85).

Potential Irrigation Water Withdrawal (short name: *pirww or pirnreqcum*) The irrigation water withdrawal is expressed in mm of water per growing season. The data refers to irrigation water withdrawn in case of optimal irrigation, in addition to rainfall. The model simulations are under the assumption that there are no losses in water distribution and conveyance and that there is unlimited water supply. The data is available at yearly temporal resolution for CMIP5 (under RCP2.6 and RCP6.0) and for CMIP6 (under ssp26 and ssp85).

Nitrogen application rate (short name: *initr or nincum*) Nitrogen balance: Inputs. The total nitrogen application rate is expressed as kg ha⁻¹ per growing season. The data is available at yearly temporal resolution for CMIP5 (under RCP2.6 and RCP6.0) and for CMIP6 (under ssp26 and ssp85).

Cumulative Nitrogen Losses (short name: *nlosscum*) Nitrogen balance: Losses (growing season sum). The total nitrogen loss rate is expressed as kg ha⁻¹ per growing season. The data is available at yearly temporal resolution for CMIP5 (under RCP2.6 and RCP6.0) and for CMIP6 (under ssp26 and ssp85).

Cumulative Nitrogen Leached (short name: *nleachcum*) Nitrogen balance: Leaching (growing season sum). The total nitrogen leaching rate is expressed as kg ha⁻¹ per growing season. The data is available at yearly temporal resolution for CMIP5 (under RCP2.6 and RCP6.0) and for CMIP6 (under ssp26 and ssp85).

Variable trends and uncertainty

For all regions and scenarios, yield and irrigation requirement projections from agricultural models are compared for the same climate driver (gfdl-esm4), co2 concentration (default) and irrigation practice (firr). In this way, the variability only depends on the internal parametrization and processes of the agricultural models allowing for a direct comparison of their results. Potato, pea and sugarcane projections are not analysed as they are only produced by one sector model, respectively, so their variability corresponds to the superimposed climatic variability.

Yield

Among the yield projections analysed, lpjml often behaves like an overestimating outlier. This is observed for most crops and in all basins except Adige. In contrast, crover often behaves like an underestimating outlier. This is observed for all basins and almost all crops, with very few exceptions. Hence, it is advisable to not rely solely on data from these models as they tend to disagree with the inter model mean. On the other hand, epic-iiasa is often the closest to the inter-model mean and among the models showing the most conservative interannual variability. Thus, the use of data from this model is generally recommended to minimise the potential error magnitude.

As projections show peculiar patterns depending on the basin and scenario, a detailed analysis for each basin is provided below to offer a better explanation of the figures.

Lielupe

Lpjml behaves like an outlier for rice, soy and winter wheat so its use is not advised. For soy and winter wheat all the other models overlap with the mean so they represent an equally reliable option. The same does not apply to rice, where epic-iiasa produces more conservative estimates than promet and pepic, which show strong fluctuations in both the historical and future period.

Ldnc probably offers the most conservative representation of spring wheat as it is very close to the inter-model mean and sits between the two groups of other models above and below the mean.

Cygma-p174 behaves like an outlier in the estimate of sorghum yield with respect to lpjml and lpj-guess. While this might indicate an outlier behaviour for cygma-p174, it is worth noticing that lpjml behaves like an overestimating outlier for other crops, so the same might be true for sorghum. Thus, the user might find lpj-guess as the most reliable data source for this crop. Despite being based on the same land model, lpjml and lpj-guess differ in parameterization, assumptions and internal processes, making their results independent from each other (Rosenzweig et al., 2014).

Two groups of models can be distinguished for the estimate of maize yield: Imdnc,pepic and lpjml projecting values around 3-4 t/ha opposed to crover, promet and epic-iiasa at 1-2 t/ha. Lpjml and epic-iiasa are the closest to the inter-model mean in their groups so the user might opt for one of them. Cross-checking with historical yield data in the basin (if available) is encouraged to assess which of the two groups of models offers the most realistic representation.

Inkomati

Epic-iiasa and lpjml seem the most reliable models for maize projections, as they both fluctuate around the mean showing a relatively stable trend. The use of pepic is not advised as they behave like a strong overestimating outlier. Similarly, the use of promet is not advised due to the strong fluctuations shown, which do not appear in a similar magnitude nor frequency in any of the other models. For opposite reasons, the use of Imdnc is also not advised as it shows an unrealistic flat trend throughout the studied period in both scenarios.

Lpjml and crover appear as the most suitable for rice projections. Again, the use of promet is not advised due to the unrealistic fluctuations shown.

Sugarcane yield results provided for Inkomati are erroneous and flagged in yellow. Fixed yield value for baseline conditions of 19.3 MT, with a decrease projected for 2050 of -4% under ssp26 and -7% under ssp85

For wwh all models but crover and promet show almost perfectly in-phase projections, suggesting relatively high reliability. The same applies to swl, where crover again behaves like a strong outlier but promet is closer to the mean and shows more similar behaviour to the others.

Epic-iiasa, pepic and promet show very similar projections for soy, while lpjml behaves like a strong overestimating outlier.

Due to the large spread among the three models, it is not possible to determine which is the most reliable for sorghum projections. The most conservative approach would entail the preference for lpjml, but while this reduces the chances of error maximization, it does not ensure accuracy of the results.

Adige

For all crops but winter wheat, the use of promet data is not recommended as the model behaves as an outlier and shows strong fluctuations not matched by the rest of the ensemble. The use of crover data is also not advised for any crop but rice, as the model either behaves as an outlier (e.g., soy, swl, wwh) or shows unrealistic fluctuations at individual time steps (e.g., maize).

Lpjml looks like the most robust model overall, providing projections fluctuating around the model mean for all crops but swl, where it is an outlier.

While good agreement is found among the three models for sorghum, the most conservative approach would be using data from lpj-guess, as they have lower interannual variability (i.e., smaller fluctuations) than pepic and lpjml.

The highest level of agreement is found for sorghum and rice (with the exception of promet) projections, suggesting these to be the most reliable in the basin.

Nestos

Except for a few outliers, there is good inter-model agreement for all studied crops. The highest agreement is found for rice and winter wheat, in which apart from promet and lpjml, respectively, all models show similar interannual variability and overlap with the mean.

Good agreement is also found for soy and swh, where all model projections look reliable except for lpjml and crover. The same applies to maize, but with the outliers being pepic, promet and crover.

Good agreement is also found for future (i.e., after 2015) sorghum projections, with all three models converging to a narrow window of values after starting farther away from each other in the historical period.

Jiu

For all crops but maize and rice, lpjml behaves like an overestimating outlier so its use is not advised in the basin.

All other models behave very similarly and show good agreement in terms of variability and magnitude for rapeseed, rice, soy, sunflower and winter wheat. Thus, projections of these crops in this basin can be considered relatively robust.

As for other basins, lpj-guess looks like the most conservative and reliable predictor of sorghum yield.

While all following a similar interannual variability, projections of swh yield show a range of values across the different models. As for other crops in the basin, lpjml might be overestimating swh yield, hence pushing the mean upwards. Thus, epic-iiasa and promet probably offer the most conservative and reliable data.



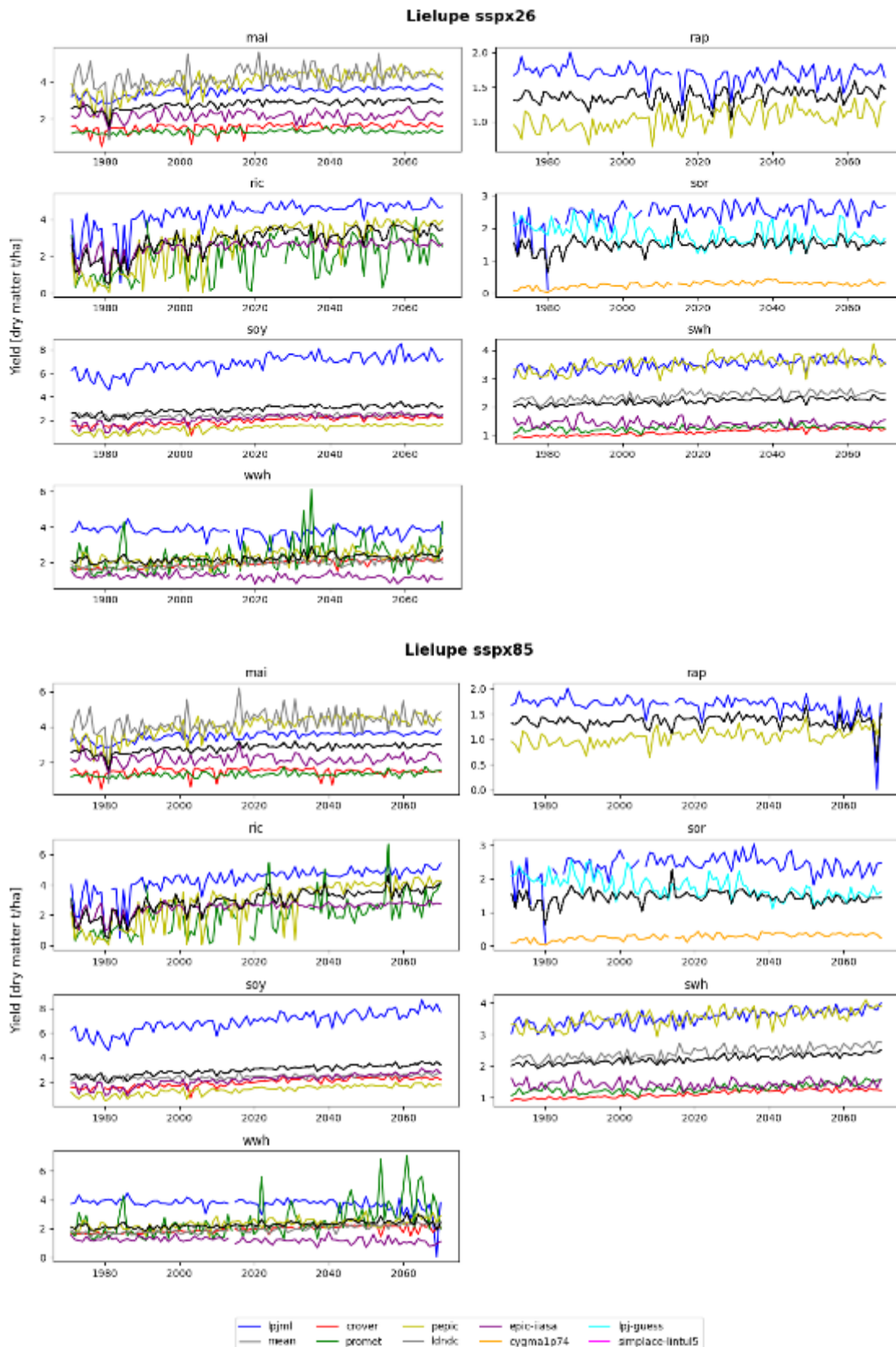


Figure 6. Maize (mai), rapeseed (rap), rice (ric), sorghum (sor), soy, spring wheat (swh) and winter wheat (wwh) yield [dry matter t/ha] projections in the Lielupe basin for the historical, ssp26 (above) and ssp85 (below) scenarios. Each coloured line represents the projection of one agricultural model while the black line represents the inter-model mean.



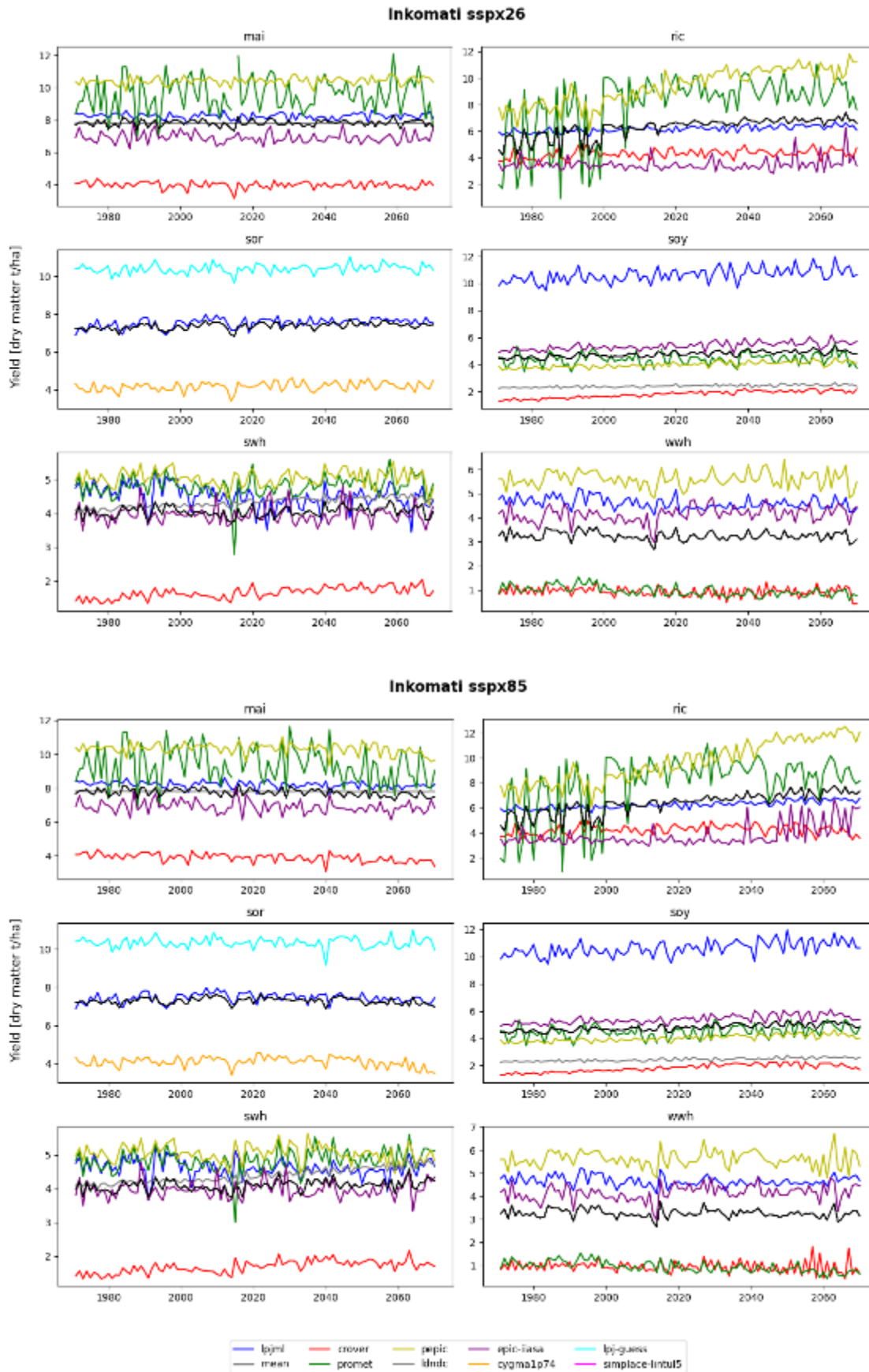


Figure 7. Same as Figure 6, but for Inkomati (rapeseed not available).



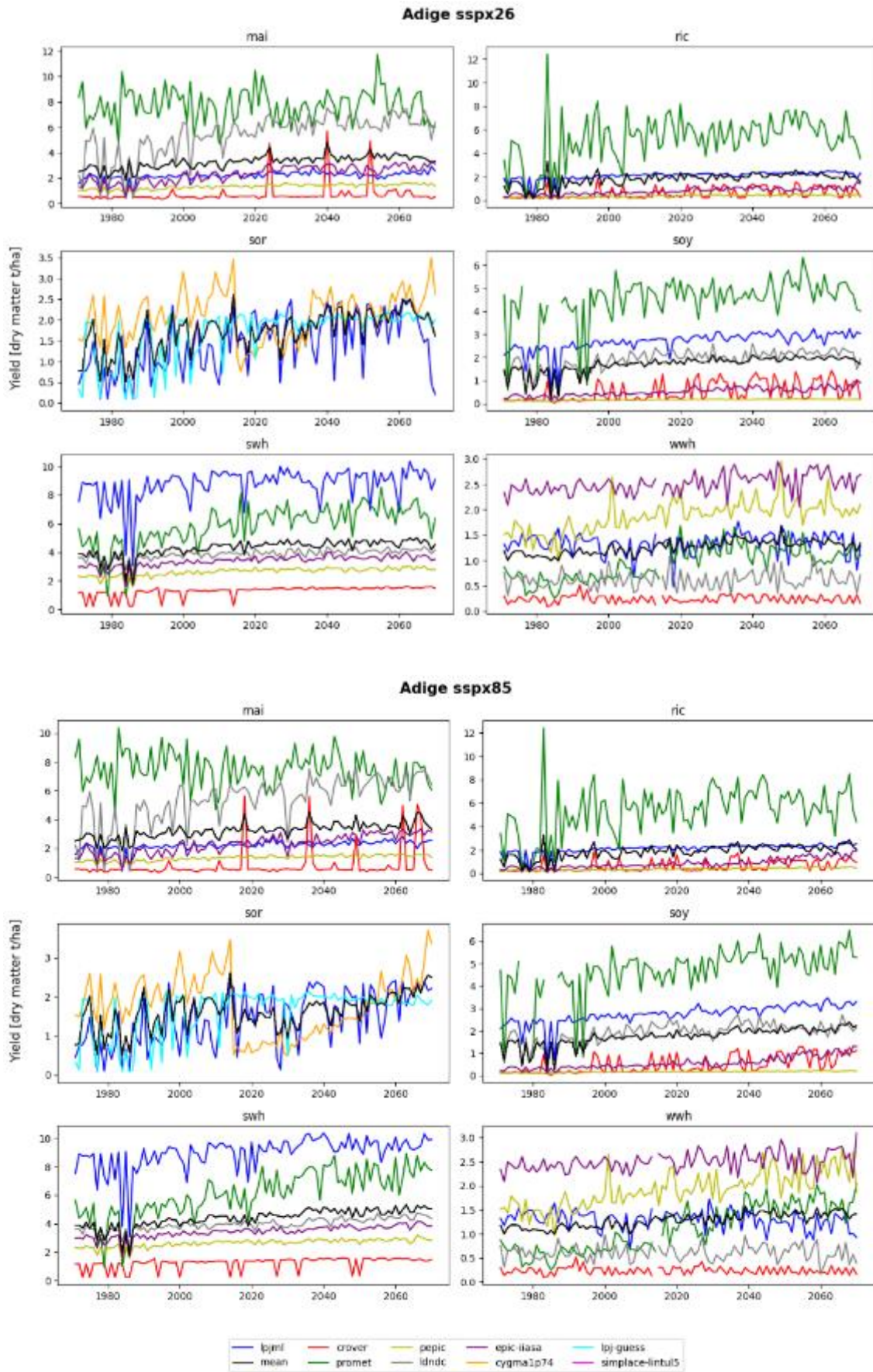


Figure 8. Same as Figure 6, but for Adige (rapeseed not available).



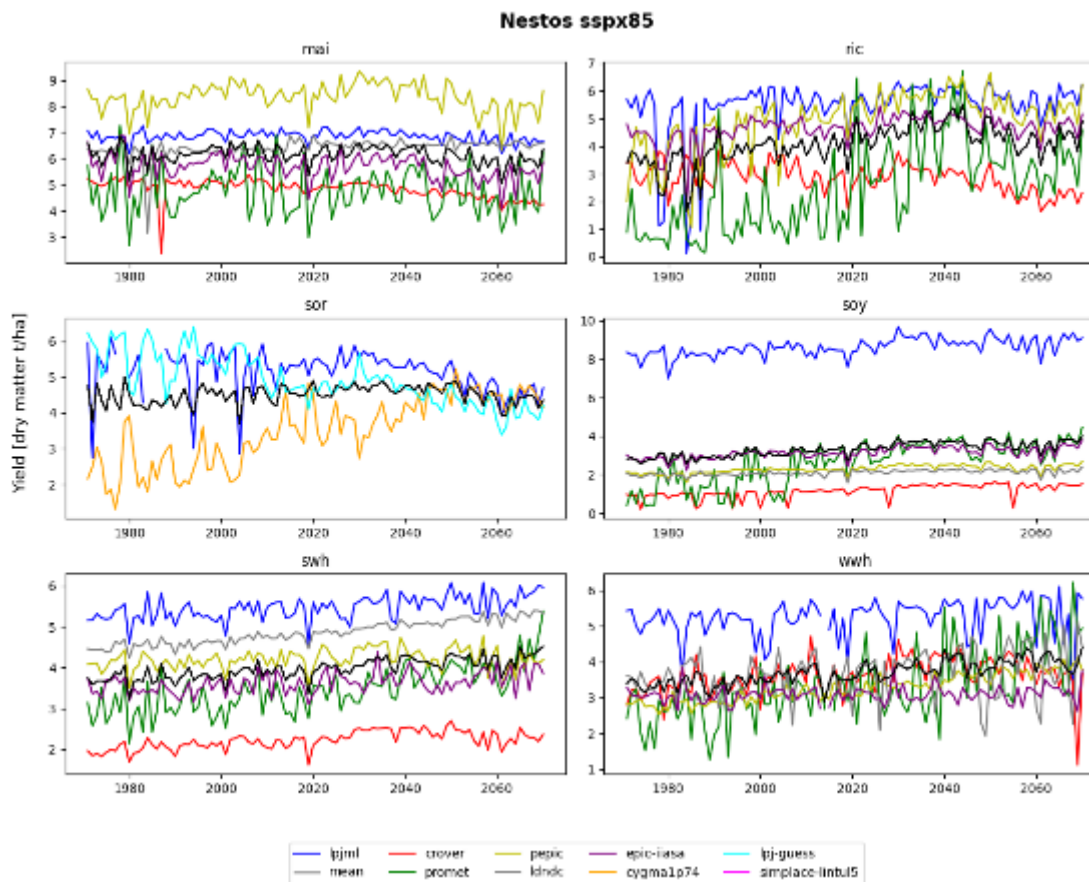
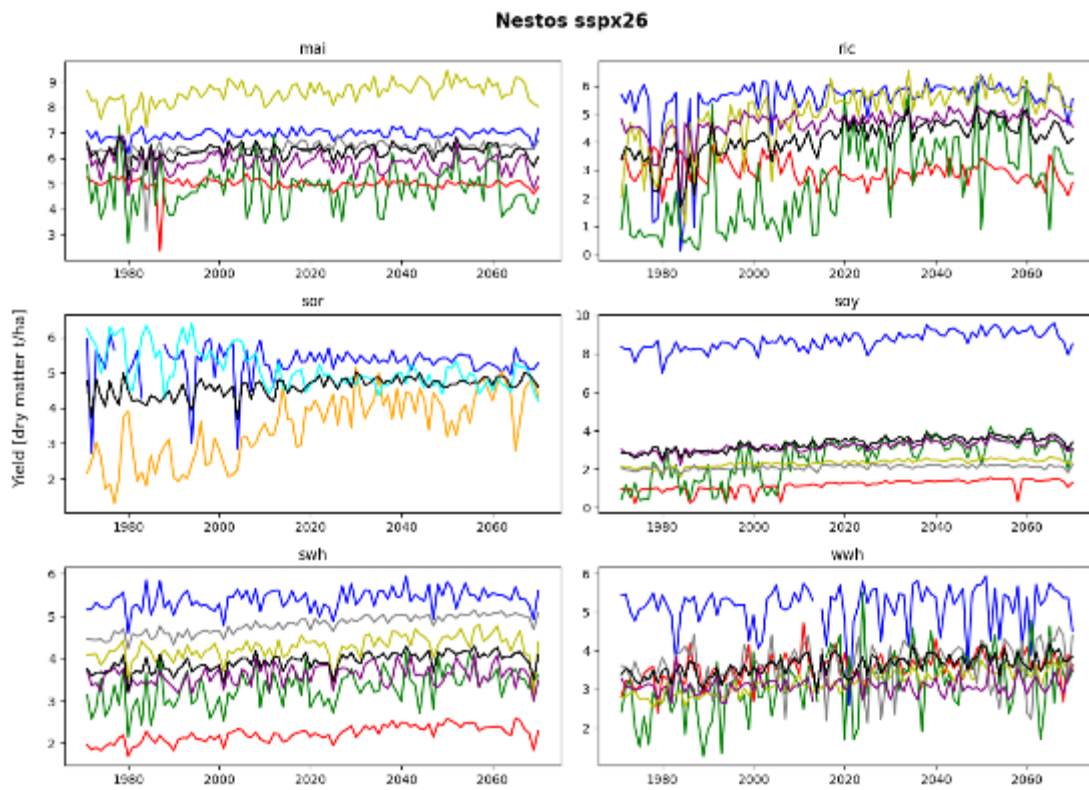


Figure 9. Same as Figure 6, but for Nestos (rapeseed not available).



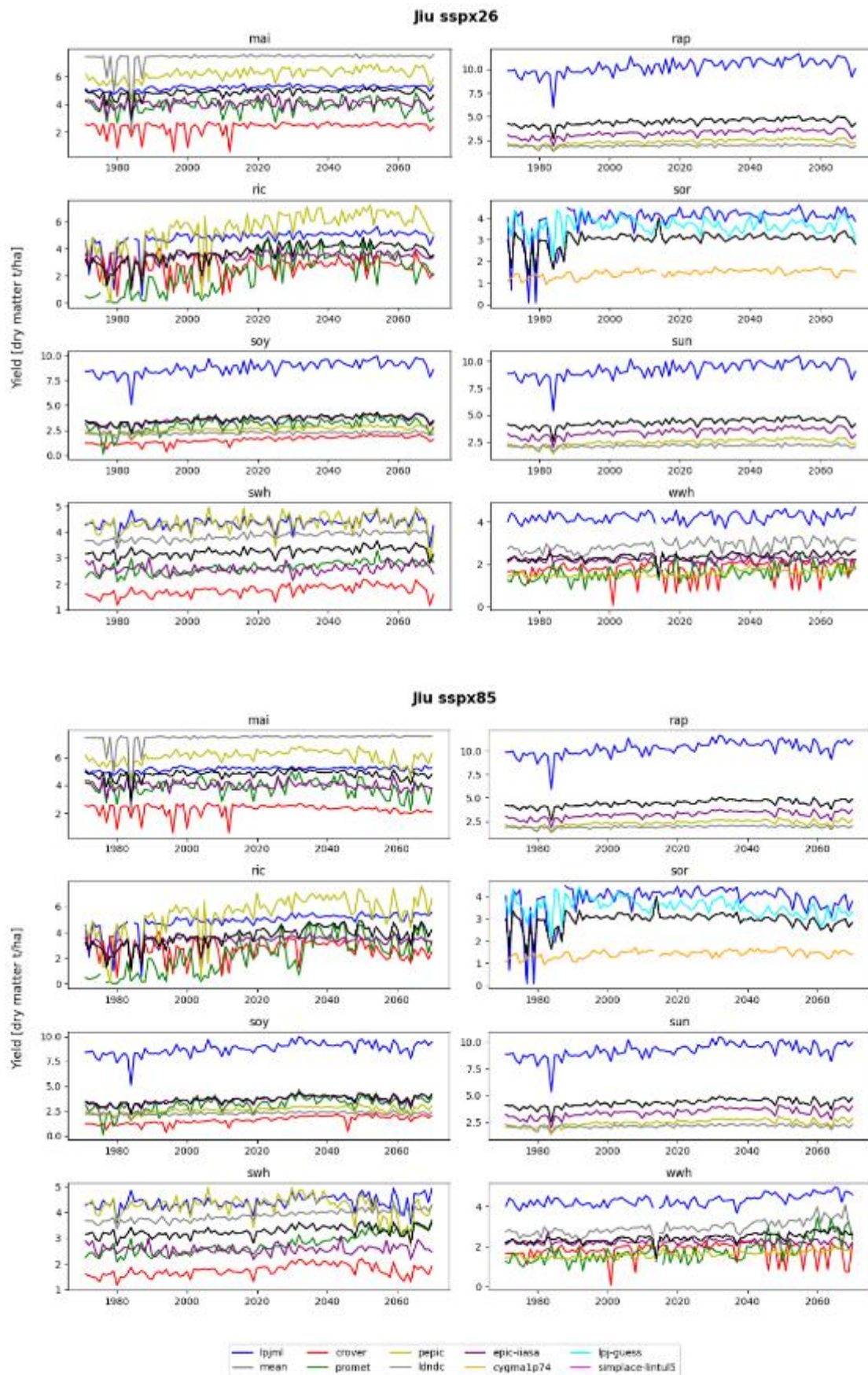


Figure 10. Same as Figure 6, but for Jiu. Here sunflower (sun) projections are also available.



Table 5. Inter-model uncertainty range in crop yields [t/ha] for the ssp26 scenario for all the studied crops and regions. The uncertainty is shown in brackets.

Region/Crop	mai	rap	ric	sor	soy	sun	swh	wwh
Adi	3.3 (5.1)	-	1.8 (3.6)	1.7 (0.9)	1.7 (3.0)	-	4.3 (4.8)	1.3 (1.5)
Jiu	4.8 (3.2)	4.4 (6.7)	3.7 (2.7)	3.0 (2.2)	3.6 (4.7)	4.3 (5.7)	3.2 (2.0)	2.4 (1.9)
Lie	2.8 (2.4)	1.4 (0.6)	2.8 (2.0)	1.5 (1.8)	2.9 (3.9)	-	2.2 (2.0)	2.2 (1.6)
Nes	6.3 (2.6)	-	4.1 (2.7)	4.6 (1.8)	3.3 (4.9)	-	3.9 (2.1)	3.6 (1.6)
Ink	7.8 (4.1)	-	6.2 (4.7)	7.4 (5.0)	4.8 (5.6)	-	4.0 (2.2)	3.2 (3.8)

Table 6. Inter-model mean and 95% uncertainty range in crop yields [t/ha] for the ssp85 scenario for all the studied crops and regions. The uncertainty is shown in brackets.

Region/Crop	mai	rap	ric	sor	soy	sun	swh	wwh
Adi	3.2 (4.9)	-	1.8 (3.7)	1.6 (1.0)	1.7 (3.1)	-	4.4 (5.0)	1.3 (1.6)
Jiu	4.8 (3.3)	4.4 (6.7)	3.7 (2.8)	2.9 (2.2)	3.6 (4.7)	4.3 (5.6)	3.3 (1.9)	2.4 (1.9)
Lie	2.8 (2.4)	1.4 (0.6)	2.9 (2.1)	1.4 (1.8)	3.0 (3.9)	-	2.2 (2.0)	2.3 (1.8)
Nes	6.2 (2.6)	-	4.1 (2.7)	4.5 (1.7)	3.3 (4.9)	-	4.0 (2.1)	3.7 (1.7)
Ink	7.7 (4.1)	-	6.4 (4.7)	7.3 (5.0)	4.8 (5.6)	-	4.1 (2.2)	3.3 (3.8)

Irrigation Requirement (pirnreqcum)

For all regions and crops, most models show a more marked interannual variability in irrigation requirement with respect to yield. Simplace-lintul5 is often the model showing the largest interannual variability, so caution in the use of its data is advised where this trend is not corresponded by other models in the ensemble (as for Inkomati for instance).

Ldncd is a strong outlier in all regions and for most crops. It overestimates the irrigation requirement reaching unrealistic levels, so the use of its data is not recommended. Although to a lesser extent than ldncd, promet also often behaves as an outlier, significantly underestimating the irrigation requirement with respect to the inter-model mean. Therefore, data from this model should also be carefully examined before being used for further analysis.

Apart from the aforementioned issues, the remaining models show good agreement in projection irrigation requirements for all regions and crops, both in terms of magnitude and variability. This indicates that irrigation requirement projections are fairly robust and can be used confidently.

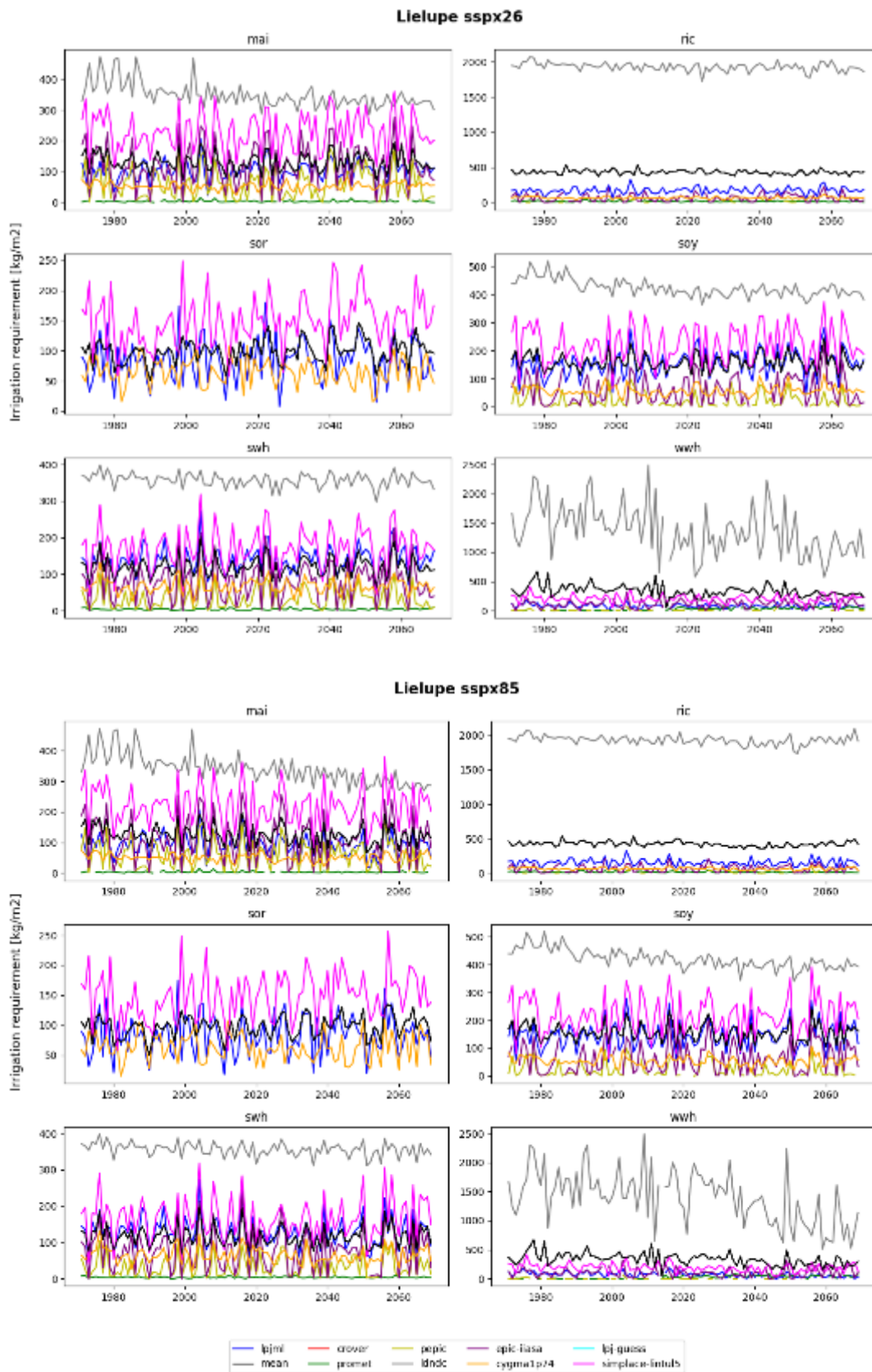


Figure 11. Maize (mai), rapeseed (rap), rice (ric), sorghum (sor), soy, spring wheat (swh) and winter wheat (wwh) irrigation requirement [kg m⁻²] projections in the Lielupe basin for the historical, ssp26 (above) and ssp85 (below) scenarios. Each coloured line represents the projection of one agricultural model while the black line represents the inter-model mean.



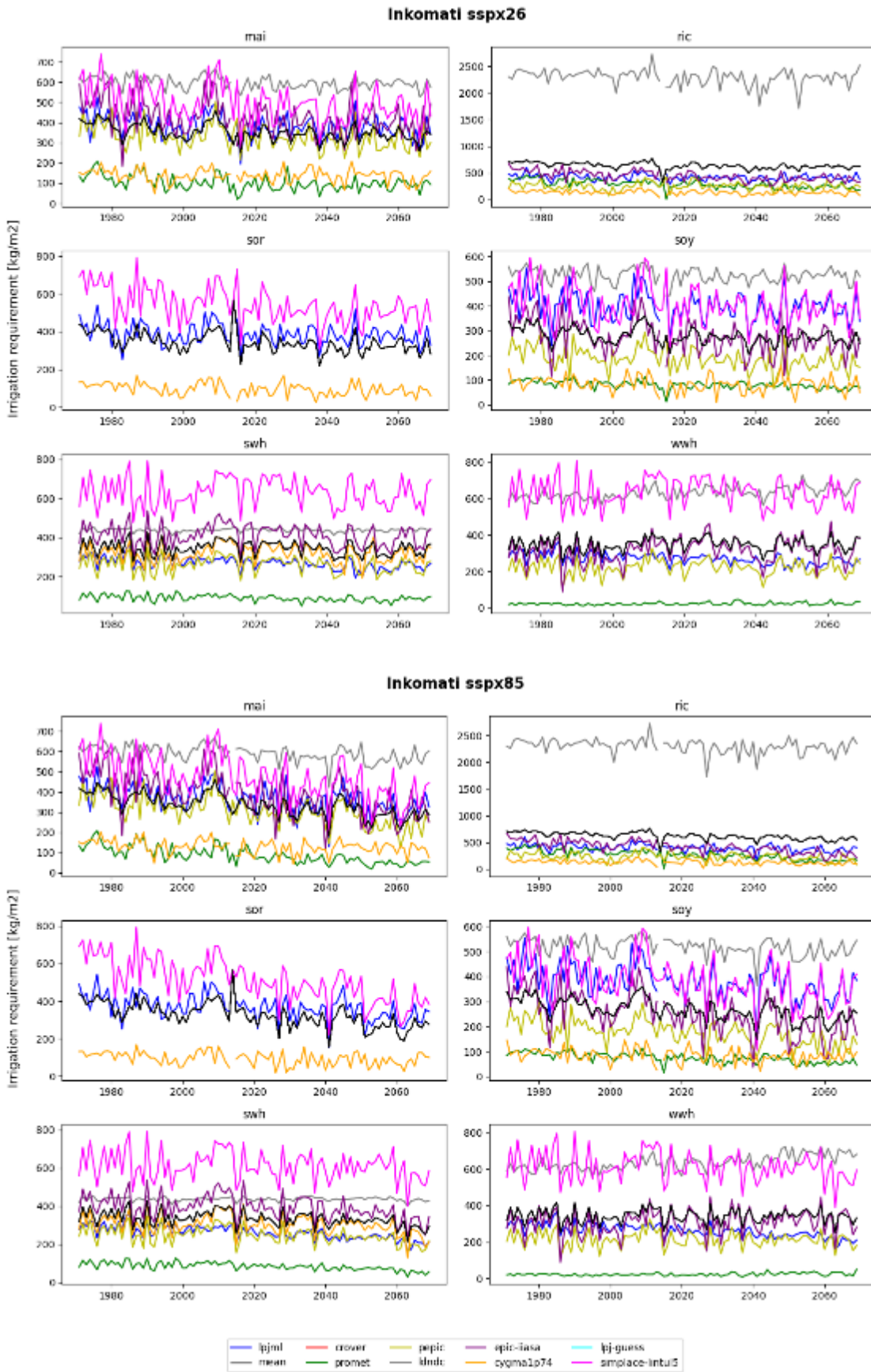


Figure 12. Same as Figure 11, but for Inkomati (rapeseed not available).



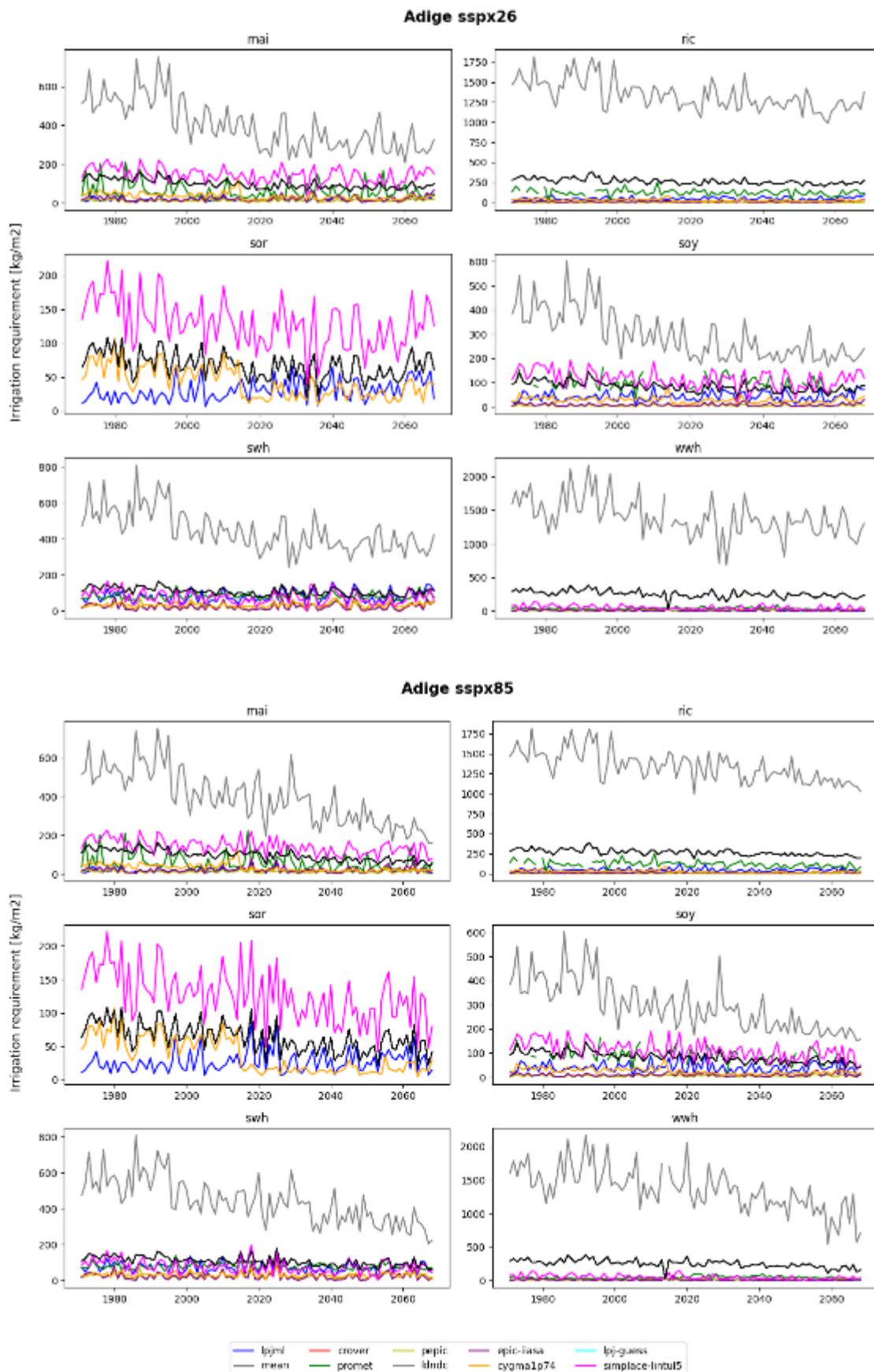


Figure 13. Same as Figure 11, but for Adige (rapeseed not available).



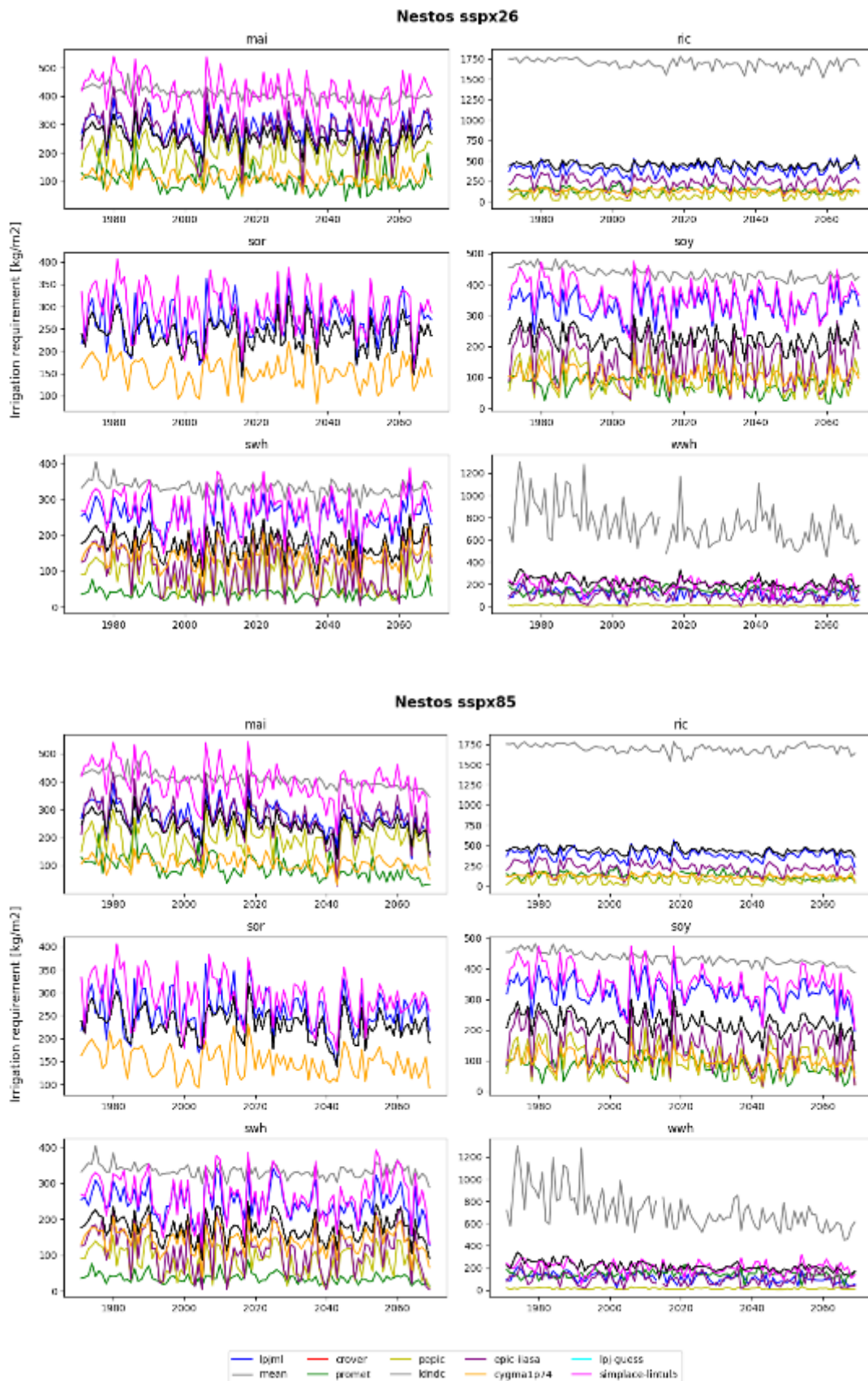


Figure 14. Same as Figure 11, but for Nestos (rapeseed not available).



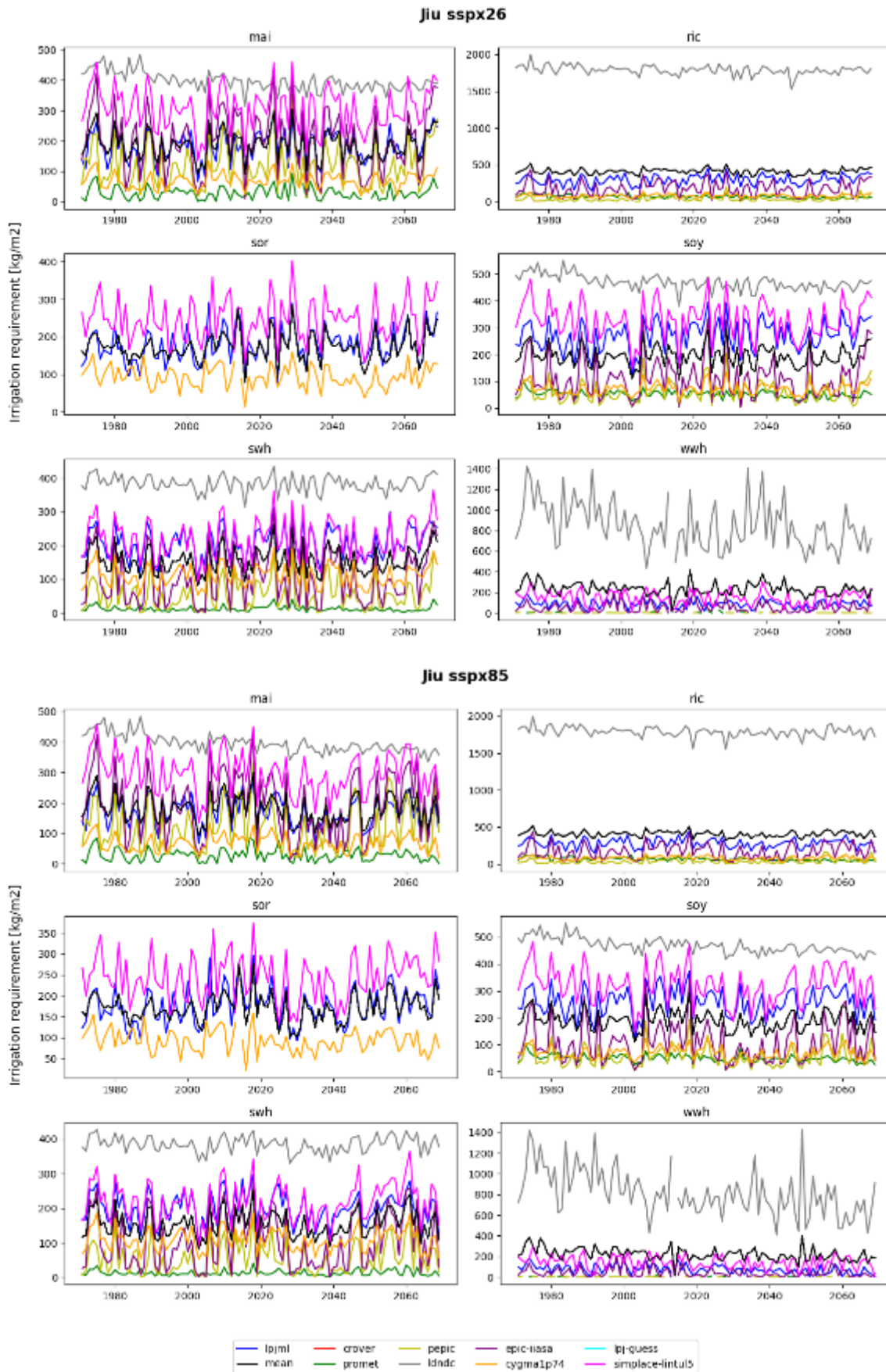


Figure 15. Same as Figure 11, but for Jiu. Here sunflower (sun) projections are also available.



Table 7. Inter-model mean and 95% uncertainty range in crop irrigation requirement [100 kg/m²] for the ssp_{x26} scenario for all the studied crops and regions. The uncertainty is shown in brackets.

Region/Crop	mai	ric	sor	soy	swh	wwh
Adi	1.0 (2.6)	2.6 (9.6)	0.7 (0.9)	0.8 (1.9)	1.1 (2.7)	2.5 (10.0)
Jiu	1.9 (2.5)	4.1 (12.3)	1.7 (1.3)	1.9 (3.0)	1.6 (2.3)	2.3 (6.2)
Lie	1.3 (2.3)	4.3 (14.3)	1.0 (0.8)	1.6 (2.8)	1.2 (2.2)	3.4 (9.8)
Nes	2.6 (2.4)	4.5 (11.2)	2.4 (1.2)	2.2 (2.7)	1.7 (2.0)	2.2 (4.7)
Ink	3.5 (3.4)	6.3 (14.6)	3.4 (3.6)	2.8 (3.2)	3.5 (3.1)	3.5 (4.4)

Table 8. Inter-model mean and 95% uncertainty range in crop irrigation requirement [100 kg/m²] for the ssp_{x85} scenario for all the studied crops and regions. The uncertainty is shown in brackets.

Region/Crop	mai	ric	sor	soy	swh	wwh
Adi	1.0 (2.6)	2.6 (9.7)	0.6 (0.9)	0.8 (2.0)	1.1 (2.7)	2.5 (9.8)
Jiu	1.8 (2.5)	4.0 (12.3)	1.7 (1.3)	1.9 (3.0)	1.5 (2.3)	2.2 (6.0)
Lie	1.3 (2.2)	4.2 (14.3)	1.0 (0.8)	1.6 (2.7)	1.2 (2.2)	3.4 (10.0)
Nes	2.5 (2.4)	4.4 (11.2)	2.3 (1.2)	2.2 (2.7)	1.7 (2.0)	2.1 (4.6)
Ink	3.3 (3.4)	6.2 (14.7)	3.3 (3.4)	2.7 (3.1)	3.3 (3.1)	3.4 (4.3)

3.3 Water

In the NXG project, quantitative information about the water quantity in the selected river basin is provided primarily through the ISIMP database, and for Adige and Nestos case studies by ad-hoc hydrological modelling implementation at basin level by project partners.

The ISIMP database provides modelling output of (eco-)hydrological model across all case studies that include water use simulations from different sectors implemented at global scale. Eight impact-model participate in the ISIMP simulation round 2b for this sector, while so far only 3 models have been able to contribute to ISIMP simulation round 3b.

ISIMP2b: CLM45, H08, JULES-W1, LPJmL, MATSIRO, ORCHIDEE, PCR-GLOBWB, WaterGAP2.

ISIMP2b: CLASSIC, CWatM, H08.

The variable consolidated from the ISIMP database for the development of Water Sectors variables for the NXG case studies are:

Surface runoff (short name: *qs*) The surface runoff is expressed in kg m⁻² s⁻¹ and it is the water that leaves top soil layer (the surface layer), e.g. as overland flow / fast runoff. Data are

available at monthly scale for CMIP5 (under RCP2.6, RCP6.0 and RCP8.5) and for CMIP6 (under ssp26 and ssp85).

Subsurface runoff (short name: *qsb*) The subsurface runoff is expressed in $\text{kg m}^{-2} \text{ s}^{-1}$ and it is the sum of water that flows out from the subsurface layer/s and includes the groundwater layer when present. It equals the groundwater runoff in case of a groundwater layer below only one soil layer. Data are available at monthly resolution. Data are available at monthly scale for CMIP5 (under RCP2.6, RCP6.0 and RCP8.5) and for CMIP6 (under ssp26 and ssp85).

Groundwater recharge (short name: *qr*) The groundwater recharge is expressed and it is water that percolates through the soil layer/s into the groundwater layer. Data are available at monthly scale for CMIP5 (under RCP2.6, RCP6.0 and RCP8.5) and for CMIP6 (under ssp26 and ssp85).

Groundwater runoff (short name: *qg*) The groundwater runoff is expressed in $\text{kg m}^{-2} \text{ s}^{-1}$ and it is the water that leaves the groundwater layer. Data are available at monthly scale for CMIP5 (under RCP2.6, RCP6.0 and RCP8.5) and for CMIP6 (under ssp26 and ssp85).

Potential Evaporation (short name: *potevap*) The potential evaporation is expressed as $\text{kg m}^{-2} \text{ s}^{-1}$. As for the total evapotranspiration, but with all the resistances set to zero, except the aerodynamic one. Data are available at monthly scale for CMIP5 (under RCP2.6, RCP6.0 and RCP8.5) and for CMIP6 (under ssp26 and ssp85).

Total Soil Moisture Content (short name: *soilmoist*) The total soil moisture content is expressed in kg m^{-2} and it is equal to the soil water storage. Data are available at monthly scale for CMIP5 (under RCP2.6, RCP6.0 and RCP8.5) and for CMIP6 (under ssp26 and ssp85).

Total water storage (short name: *tws*) The total water storage is expressed in kg m^{-2} and it is the water storage in all compartments (monthly mean). Data are available at monthly scale for CMIP5 (under RCP2.6, RCP6.0 and RCP8.5) and for CMIP6 (under ssp26 and ssp85).

Wetland storage (short name: *wetlandstor*) The wetland storage is expressed in kg m^{-2} and it is water storage in wetlands (monthly mean). Data are available at monthly scale for CMIP5 (under RCP2.6, RCP6.0 and RCP8.5) and for CMIP6 (under ssp26 and ssp85).

Reservoir storage (short name: *reservoirstor*) The reservoir storage is the water storage in reservoirs (monthly mean). Data are available at monthly scale for CMIP5 (under RCP2.6, RCP6.0 and RCP8.5) and for CMIP6 (under ssp26 and ssp85).

Irrigation water demand = potential irrigation water withdrawal (short name: *pirrww*) Irrigation water withdrawal, assuming unlimited water supply, is expressed in $\text{kg m}^{-2} \text{ s}^{-1}$. Data are available at monthly scale for CMIP5 (under RCP2.6, RCP6.0 and RCP8.5) and for CMIP6 (under ssp26 and ssp85).

Potential irrigation water consumption (short name: *pirruse*) Portion of withdrawal that is evapo-transpired, assuming unlimited water supply, is expressed in $\text{kg m}^{-2} \text{ s}^{-1}$ or mm s^{-1} . Data

are available at monthly scale for CMIP5 (under RCP2.6, RCP6.0 and RCP8.5) and for CMIP6 (under ssp26 and ssp85).

Actual irrigation water consumption (short name: *airruse*) Portion of withdrawal that is evapotranspired, taking water availability into account; if computed, is expressed in $\text{kg m}^{-2} \text{s}^{-1}$ or mm s^{-1} . Data are available at monthly scale for CMIP5 (under RCP2.6, RCP6.0 and RCP8.5) and for CMIP6 (under ssp26 and ssp85).

Actual irrigation water withdrawal (short name: *airrww*) Irrigation water withdrawal, taking water availability into account, is expressed in $\text{kg m}^{-2} \text{s}^{-1}$ or mm s^{-1} . Data are available at monthly scale for CMIP5 (under RCP2.6, RCP6.0 and RCP8.5) and for CMIP6 (under ssp26 and ssp85).

Actual domestic water consumption (short name: *adomuse*) is expressed in $\text{kg m}^{-2} \text{s}^{-1}$ or mm s^{-1} . Data are available at monthly scale for CMIP5 (under RCP2.6, RCP6.0 and RCP8.5) and for CMIP6 (under ssp26 and ssp85).

Actual domestic water withdrawal (short name: *adomww*) is expressed in $\text{kg m}^{-2} \text{s}^{-1}$ or mm s^{-1} . Data are available at monthly scale for CMIP5 (under RCP2.6, RCP6.0 and RCP8.5) and for CMIP6 (under ssp26 and ssp85).

Actual Industrial Water Consumption (short name: *ainduse*) is expressed in $\text{kg m}^{-2} \text{s}^{-1}$ or mm s^{-1} . Data are available at monthly scale for CMIP5 (under RCP2.6, RCP6.0 and RCP8.5) and for CMIP6 (under ssp26 and ssp85).

Actual industrial water withdrawal (short name: *aindww*) is expressed in $\text{kg m}^{-2} \text{s}^{-1}$ or mm s^{-1} . Data are available at monthly scale for CMIP5 (under RCP2.6, RCP6.0 and RCP8.5) and for CMIP6 (under ssp26 and ssp85).

Actual livestock water consumption (short name: *aliveuse*) is expressed in $\text{kg m}^{-2} \text{s}^{-1}$ or mm s^{-1} . Data are available at monthly scale for CMIP5 (under RCP2.6, RCP6.0 and RCP8.5) and for CMIP6 (under ssp26 and ssp85).

Actual livestock water withdrawal (short name: *aliveww*) is expressed in $\text{kg m}^{-2} \text{s}^{-1}$ or mm s^{-1} . Data are available at monthly scale for CMIP5 (under RCP2.6, RCP6.0 and RCP8.5) and for CMIP6 (under ssp26 and ssp85).

All the variables selected so far, consider the effect on vegetation of CO_2 fertilization and their future increasing availability. The socio-economic scenario can be available considering the historical period varying historical land use, nitrogen deposition and fertilizer input (1861-2005; *histsoc*); the 2005 as fixed year and the related values of land use (2005*soc*), nitrogen deposition and fertilizer input. In the ISIMIP 2b water sector, the “human influences” is considered as the human interference directly with the hydrological fluxes of the water cycle for the purposes of e.g., irrigation and domestic water use, manufacturing and livestock production, water management.

Variable trends and uncertainty

For all basins, surface runoff (qs) and groundwater recharge (qr) data for ISIMIP2b and ISIMIP3b models is plotted against the ISIMIP3b inter-model mean (black). ISIMIP2b data are included in the assessment to increase the robustness of the analysis, as only three models of the 3b generation are currently available: cwatm, h08 and classic. As shown in the figures below, the former is only available for the ssp85 scenario.

As for the agricultural variables considered, qs and qr projections of different models are analysed for a fixed climate driver (gfdl-esm4), co2 forcing (default) and societal forcing (2015soc for 3b, not available in 2b). This allows for direct comparison of the model performance and eliminates bias produced by additional parameters.

Surface Runoff

In the ssp26 scenario, the 3b models show good agreement with each other in all regions except Inkomati, where the classic_3b data cannot be considered realistic. At the same time, good agreement is found among the models of the 2b generation for this scenario. Yet, in all basins the two generations of models do not agree with each other, with the 2b generation overestimating the 3b mean by 0.2 to 0.5 mm/day. This difference between generations, combined with the good intra-generation agreement and the low number of 3b models available, complicates the identification of a more reliable dataset. Indeed, it is possible that the 3b generation of models disagrees with the older one due to better parameterization and more accurate design of the internal processes. However, this conclusion is hindered by the very limited number of 3b models available, posing the threat of classic_3b and h08_3b being two underestimating outliers in their generation. Thus, the user is invited to cross-check the projections with historical data whenever possible and choose the models that best reflect them. If observations are not available, the 3b datasets might be preferred to the 2b on the (not foolproof) assumption that a newer generation of models should offer a better representation of the studied phenomenon due to the inherent improvements to the model design.

Similar considerations need to be made for the ssp85 scenario, where the choice is further complicated by the presence of cwatm_3b. Although good agreement is found in most basins between h08_3b and classic_3b, cwatm_3b always overestimates the projections of the other models by 0.1-0.3 mm/day. While cwatm_3b appears as an outlier within the 3b generation of models, its projections are much closer to the models of the 2b generation, as it can be seen by their more frequent overlap with the 3b mean with respect to the ssp26 scenario. Again, this behaviour raises the issue of understanding whether classic_3b and h08_3b are underestimating the projections or, in contrast, cwatm_3b is still affected by the same bias characterising models of the 2b generation. In this case, with the same considerations made for the ssp26 scenario applying, the user might prioritise data of cwatm_3b over the rest, as while being a newer generation model it also shows better agreement with the 2b counterparts.

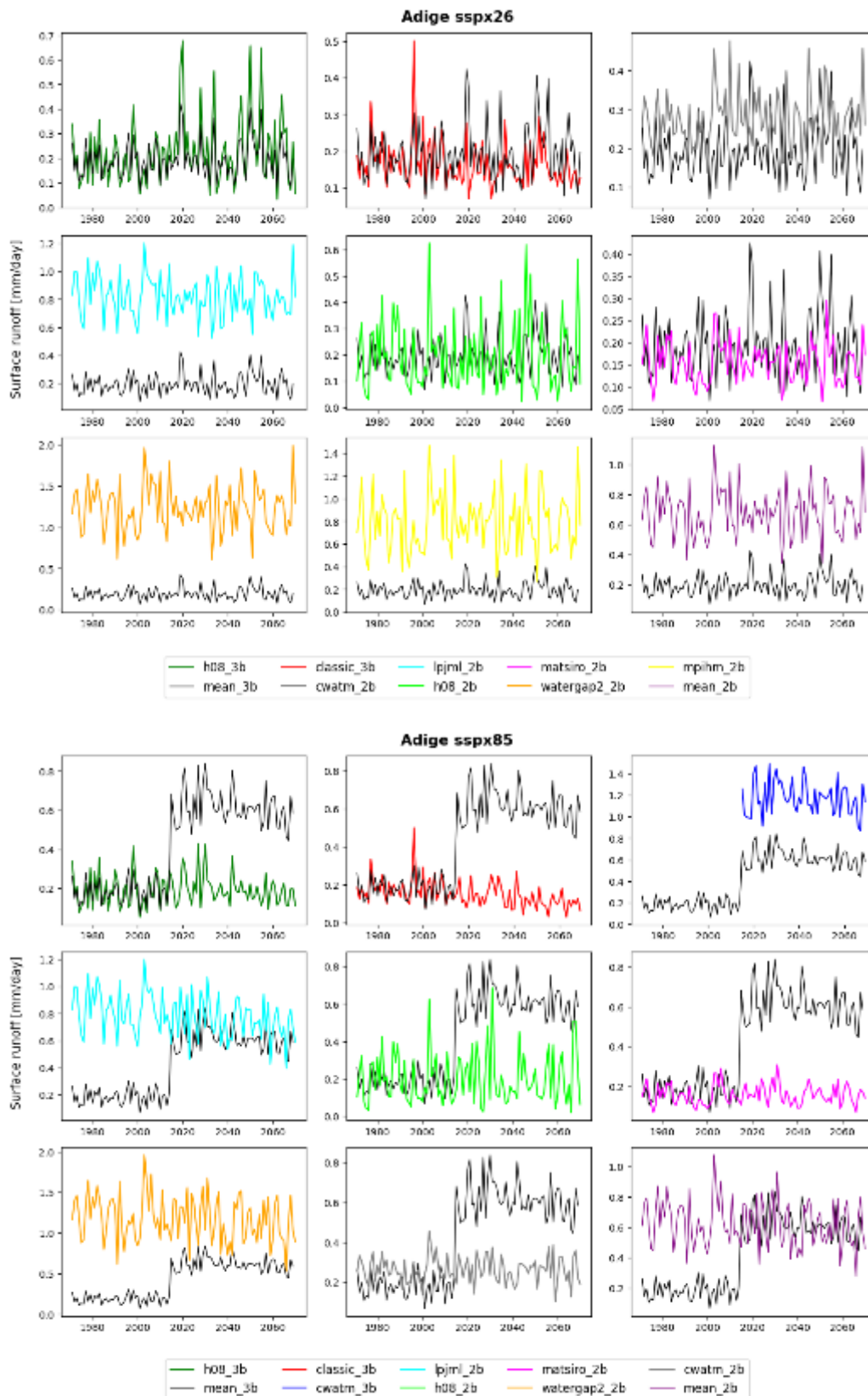


Figure 16. Surface runoff [mm/day] projections for the Adige basin in the ssp26 (above) and ssp85 (below) scenario. In each panel, one of the sector models (coloured) is compared with the inter-model mean of the 3b generation of models.



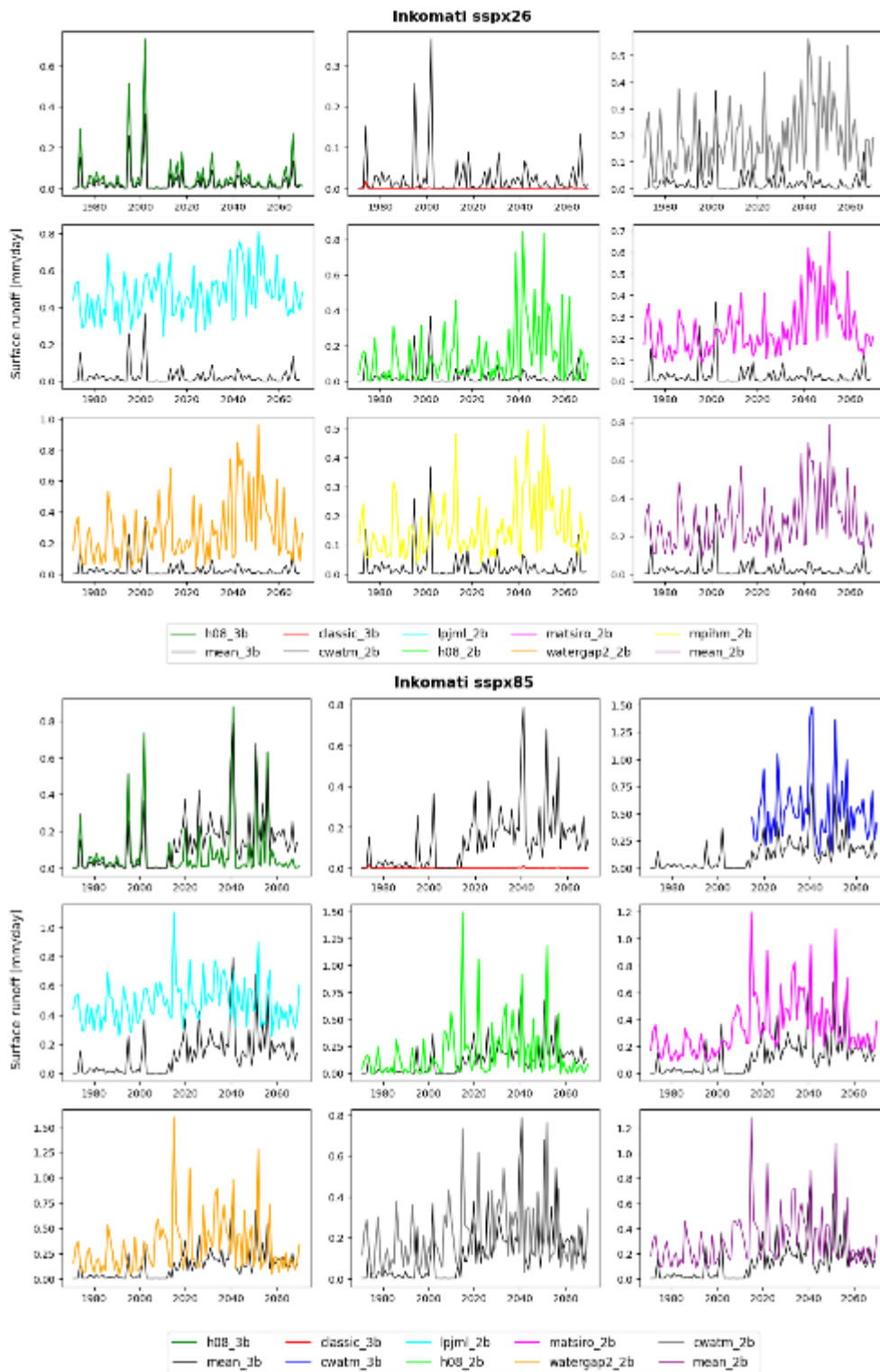


Figure 17. Same as Figure 16, but for Inkomati.



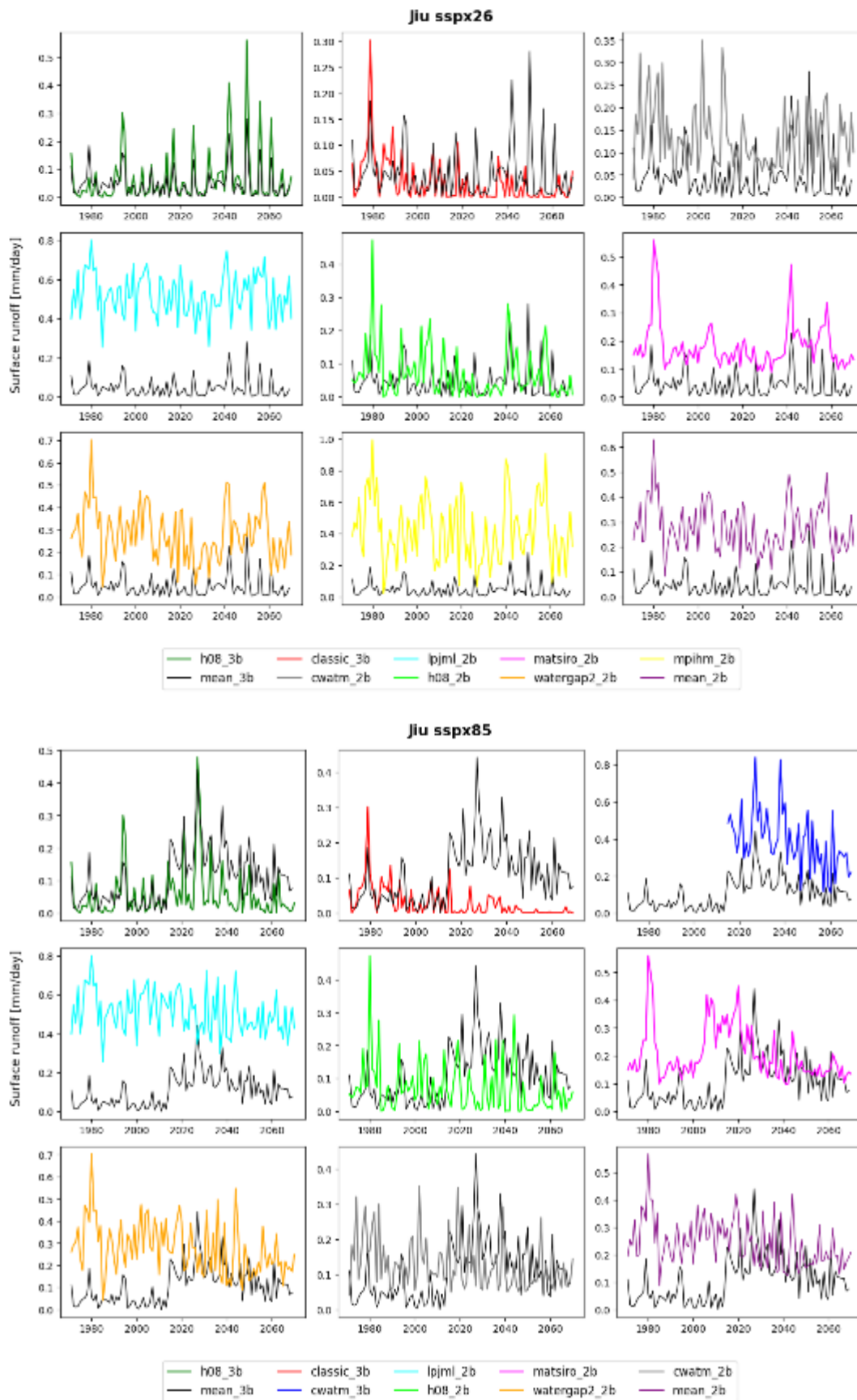


Figure 18. Same as Figure 16, but for Jiu.



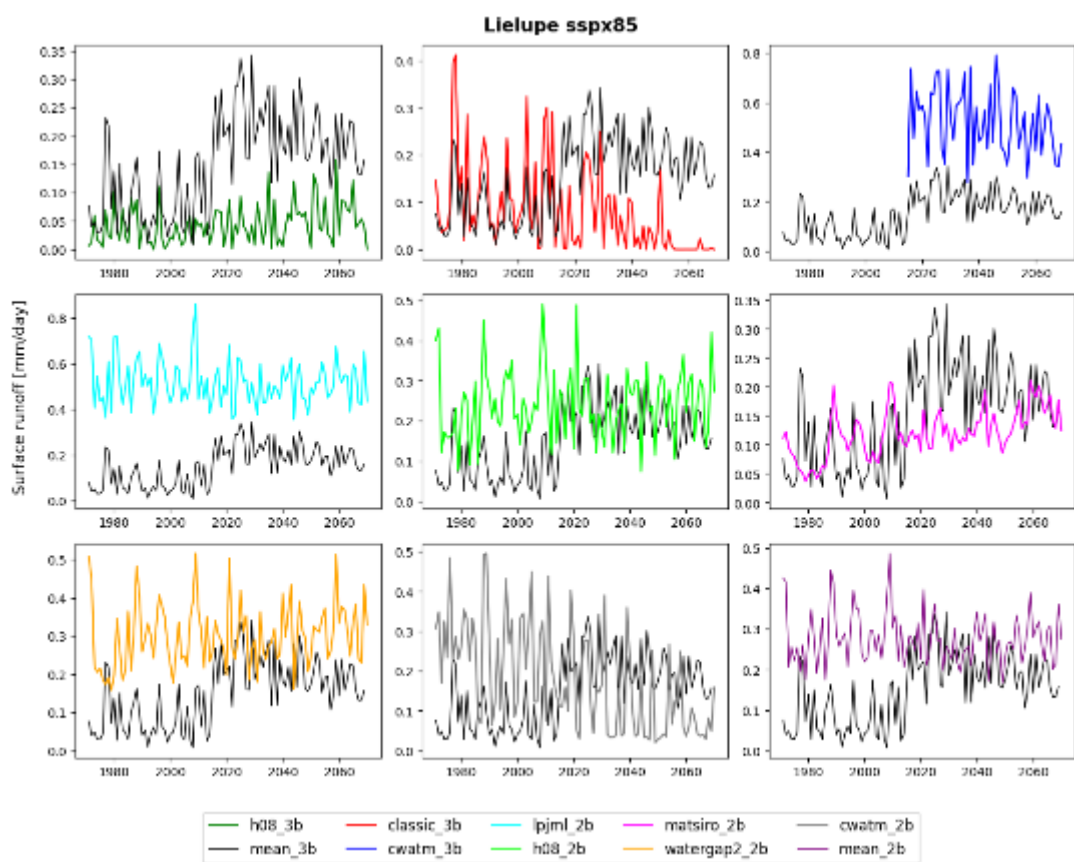
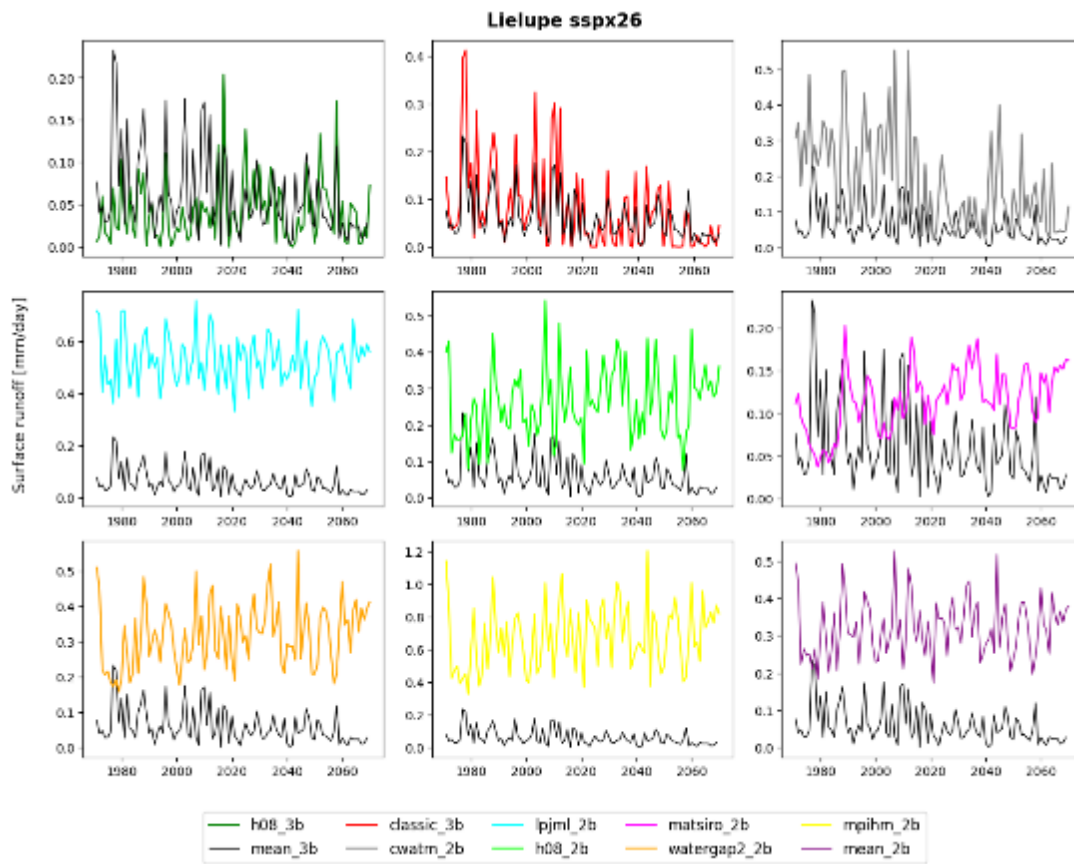


Figure 19. Same as Figure 16, but for Lielupe.



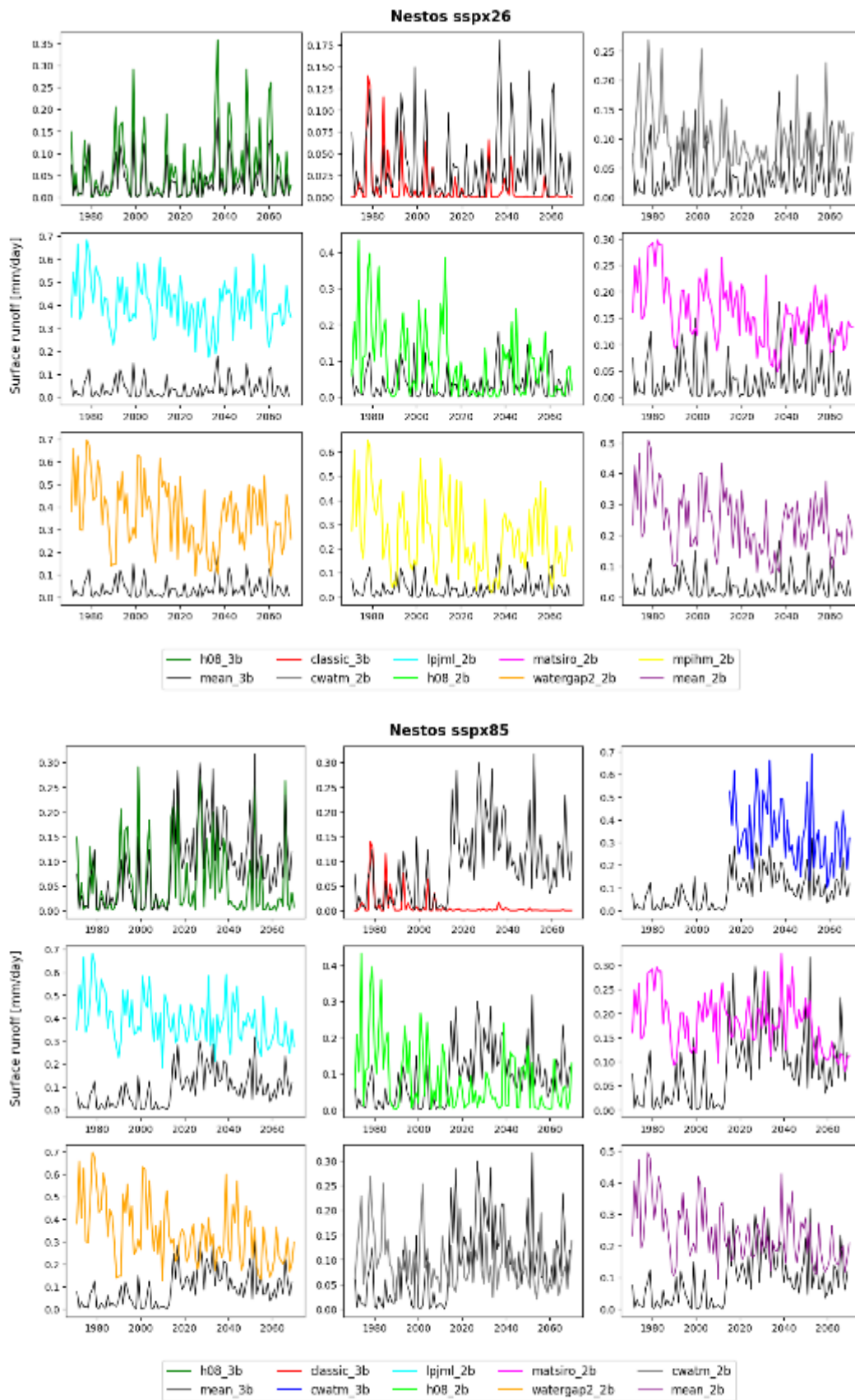


Figure 20. Same as Figure 16, but for Nestos.



Table 9. Inter-model mean and 95% uncertainty range in surface runoff [mm/day] for all regions and scenarios. The uncertainty is shown in brackets.

	Adi	Ink	Lie	Nes	Jiu
SSPx26	0.9 (0.6)	0.3 (0.5)	0.4 (0.5)	0.2 (0.3)	0.3 (0.3)
SSPx85	1.1 (1.2)	0.4 (1.1)	0.4 (0.6)	0.3 (0.4)	0.3 (0.4)

Groundwater Recharge

Very good agreement is generally found between 3b and 2b models for groundwater recharge projections. This applies to all basins and scenarios with the exception of Adige. Here, the 3b mean is pushed downwards by the low values projected by cwatm_3b with respect to h08_3b. As the 2b models projections tend to be in the same order of magnitude as h08_3b (except for matsiro_2b), cwatm_3b can be considered an outlier. This is further suggested by the same level of bias found in the cwatm_2b projection, implying that this family of models fails to adequately represent groundwater recharge in this area.

For all other basins, the 3b and 2b means fluctuate around the same values and often overlap, suggesting relatively high robustness of the groundwater recharge projections. A few models behave like outliers in different basins and their data should be considered carefully.

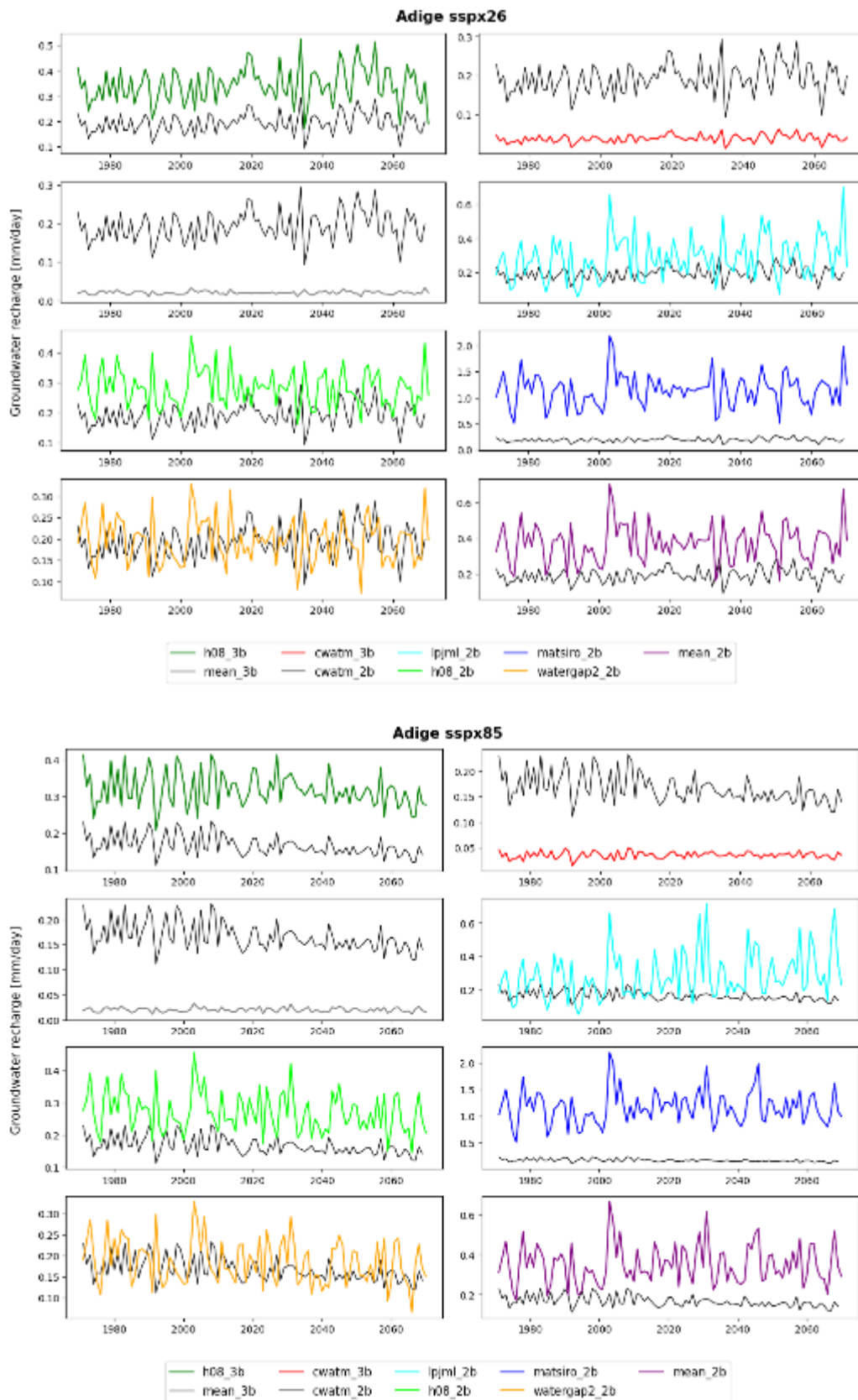


Figure 21. Groundwater recharge [mm/day] projections for the Adige basin in the ssp26 (above) and ssp85 (below) scenario. In each panel, one of the sector models (coloured) is compared with the inter-model mean of the 3b generation of models.



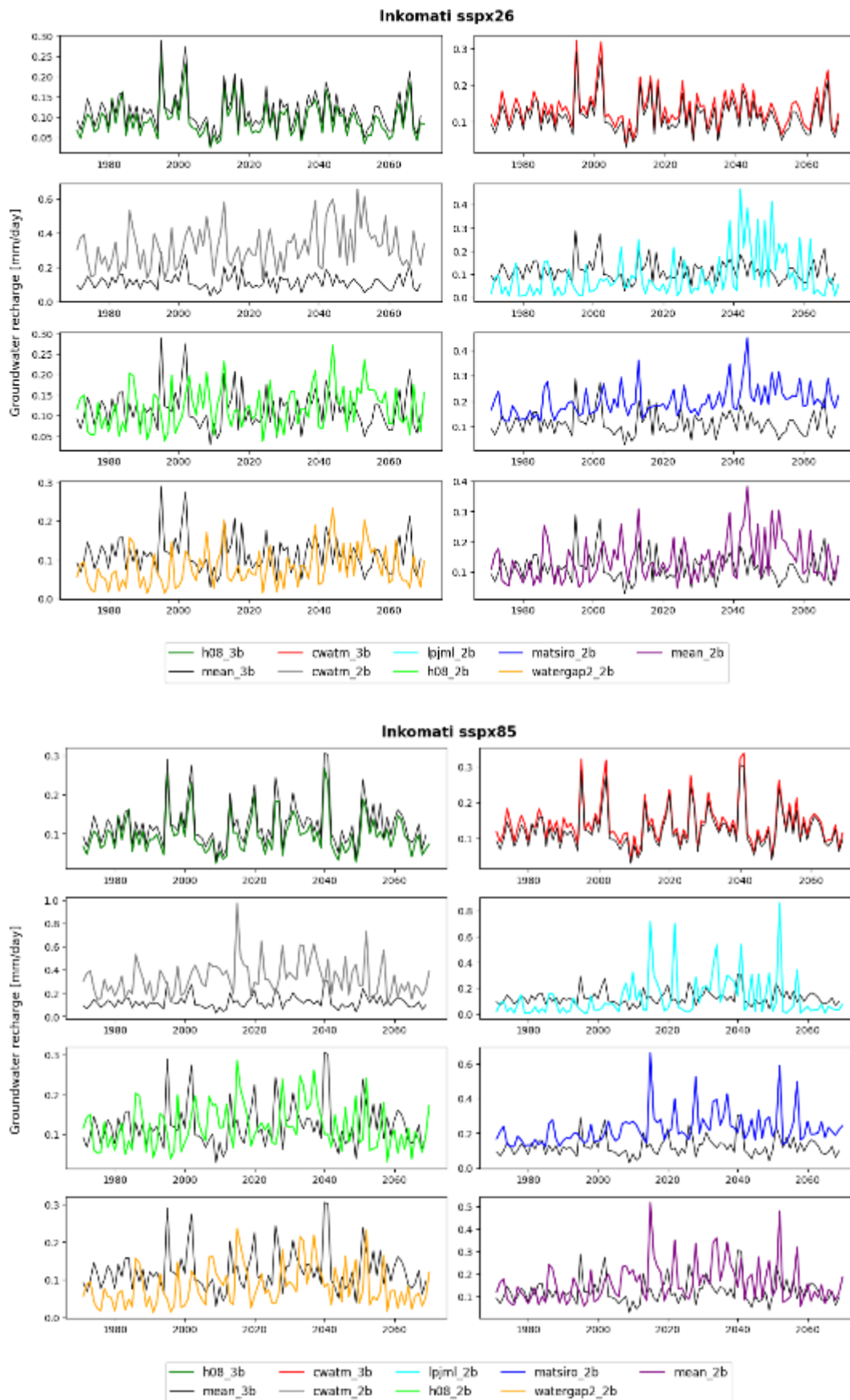


Figure 22. Same as Figure 21, but for Inkomati.



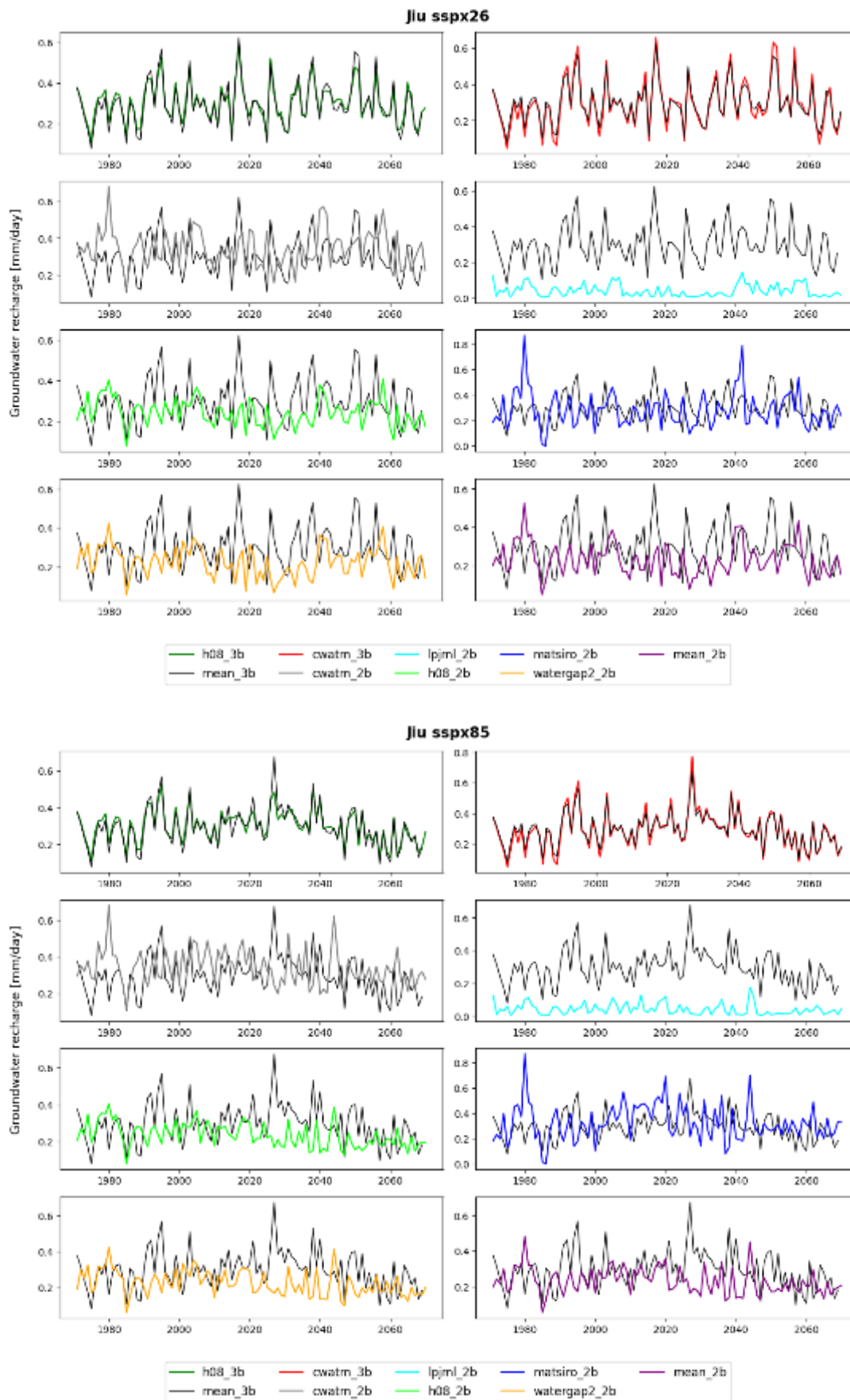


Figure 23. Same as Figure 21, but for Jiu.



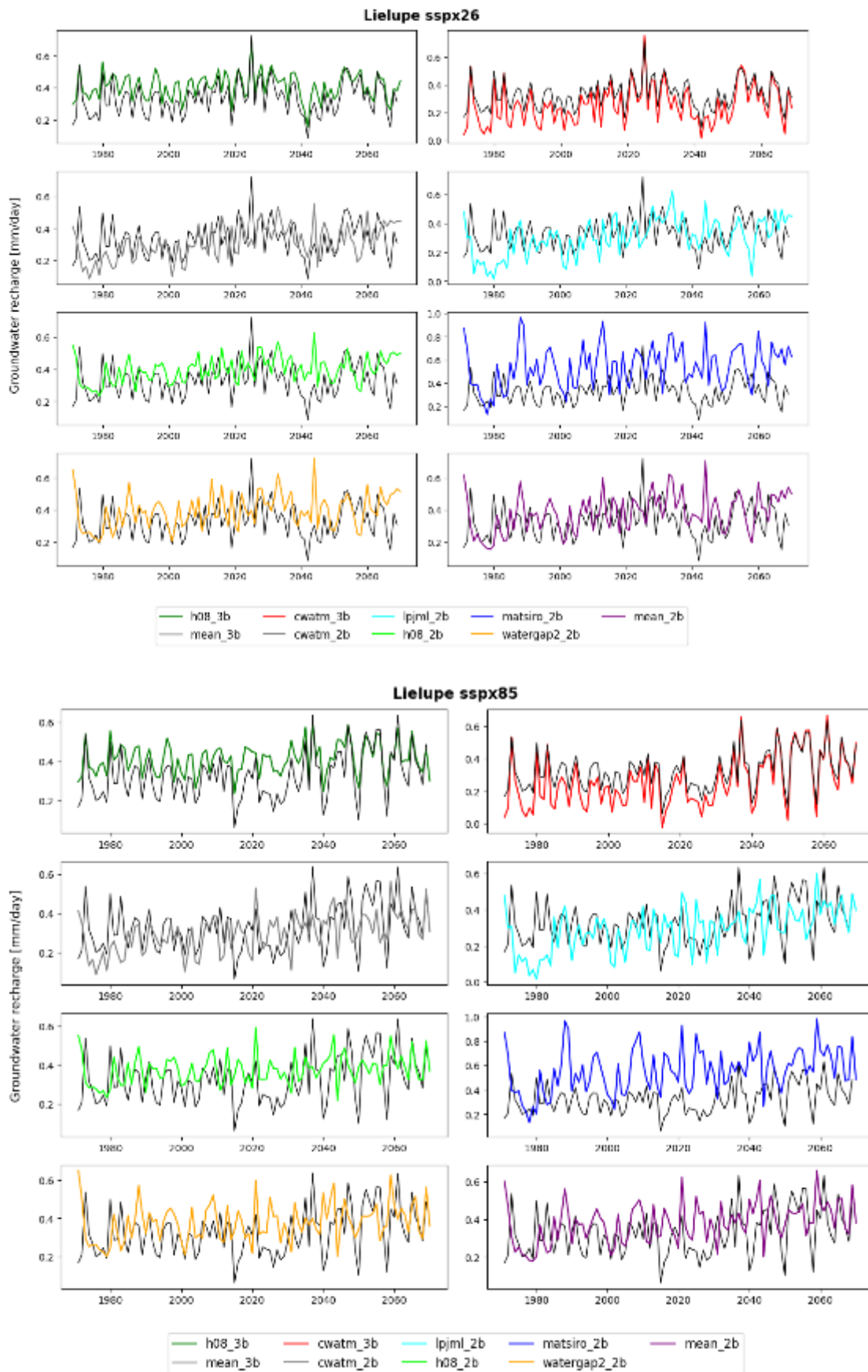


Figure 24. Same as Figure 21, but for Lielupe.



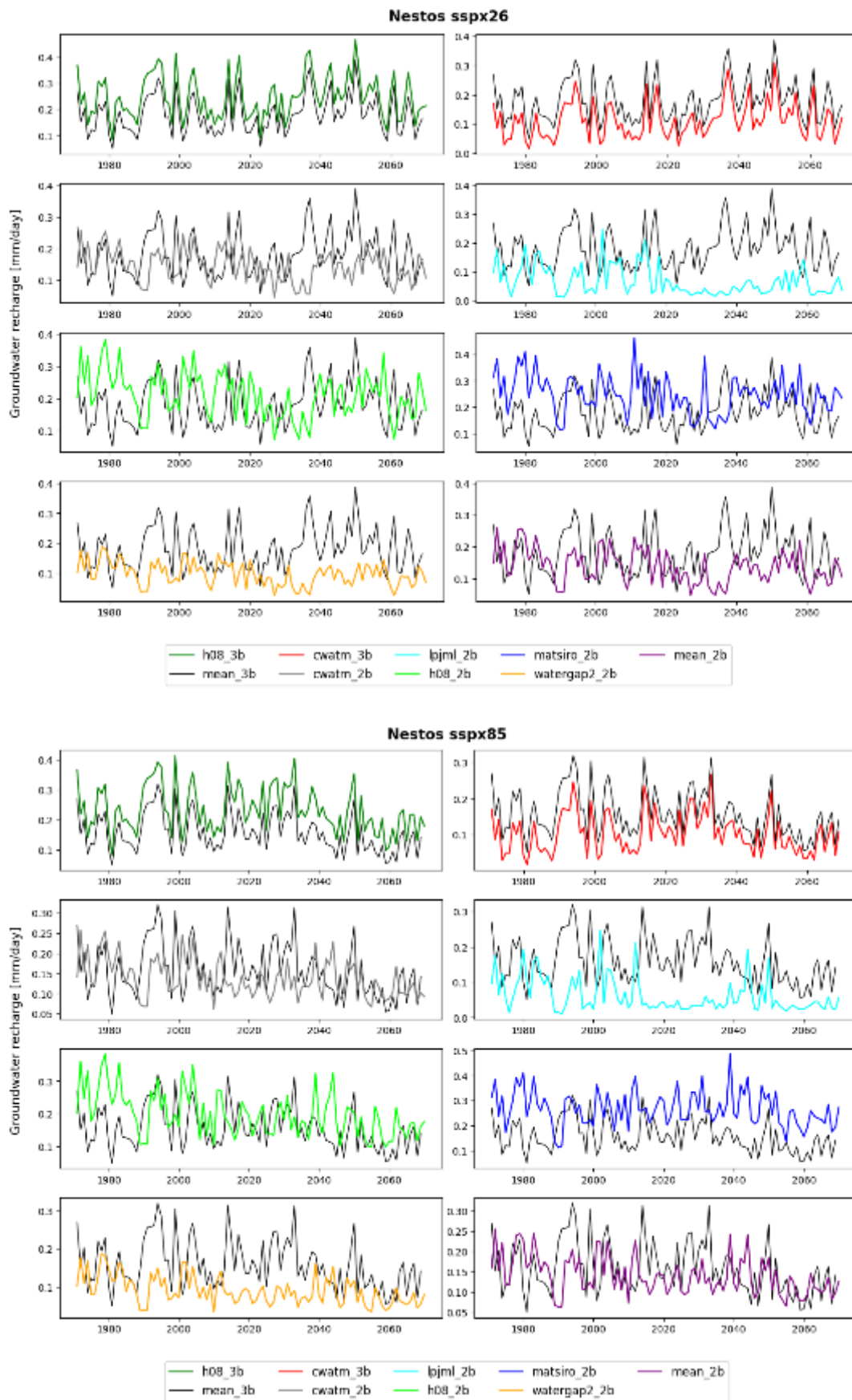


Figure 25. Same as Figure 21, but for Nestos.



Table 10. Inter-model mean and 95% uncertainty range in groundwater recharge rate [mm/day] for all regions and scenarios. The uncertainty is shown in brackets.

	Adi	Ink	Lie	Nes	Jiu
SSPx26	0.6 (0.2)	0.2 (0.3)	0.7 (0.5)	0.3 (0.3)	0.5 (0.4)
SSPx85	0.6 (0.2)	0.2 (0.4)	0.7 (0.6)	0.3 (0.3)	0.5 (0.4)

3.4 Ecosystems/Biomes

The biomes sector covered by the ISIMIP 2b database include sectorial impact elaborated from 6 models (CARAIB, CLM45, JULES, LPJ-GUESS, LPJmL, ORCHIDEE, ORCHIDEE-DGVM), while impact covered by the ISIMIP3b include impact from CLASSIC model.

The variable selected from the ISIMIP database for covering the Biomes sector and subsequently developing the NXG complexity science are:

Carbon Mass in Vegetation (short name: *cveg*) The Carbon Mass in Vegetation is expressed in kg m^{-2} and is available at an annual resolution for the historical and future climate. Values are available in ISIMIP3b for the following Plant Functional Types: c3crop (C3 crops); c3grass (C3 grass species); c4crop (C4 crops); c4grass (C4 grass species); dcdcldbdltr (Broadleaf cold deciduous tree); dcdldrybdltr (Broadleaf drought deciduous tree); dcdndltr (Needleleaf deciduous tree); evgbdltr (Broadleaf evergreen tree); evgndltr (Needleleaf evergreen tree); total (Total, given by combination of Plant Functional Type Grid Fraction)

Carbon Mass in Soil (short name: *csoil*) The Carbon Mass in Vegetation is expressed in kg m^{-2} and is available at an annual resolution for the historical and future periods. Values are available in ISIMIP3b for the following Plant Functional Types: c3crop (C3 crops); c3grass (C3 grass species); c4crop (C4 crops); c4grass (C4 grass species); dcdcldbdltr (Broadleaf cold deciduous tree); dcdldrybdltr (Broadleaf drought deciduous tree); dcdndltr (Needleleaf deciduous tree); evgbdltr (Broadleaf evergreen tree); evgndltr (Needleleaf evergreen tree); total (Total, given by combination of Plant Functional Type Grid Fraction).

Carbon Mass Flux out of Atmosphere due to Gross Primary Production on Land (shortname: *gpp*) The Carbon Mass Flux out of Atmosphere due to Gross Primary Production on Land is expressed in $\text{kg m}^{-2} \text{ s}^{-1}$ and is available at monthly resolution for the historical and future periods.

Carbon Mass Flux out of Atmosphere due to Net Primary Production on Land (shortname: *gpp*) The Carbon Mass Flux out of Atmosphere due to Net Primary Production on Land is expressed in $\text{kg m}^{-2} \text{ s}^{-1}$ and is available at an annual and monthly resolution for the historical and future periods.

Carbon Mass Flux into atmosphere due to total Carbon emissions from Fire (shortname: *fireint or ffire*) Total C emitted from all fires expressed in $\text{kg m}^{-2} \text{ s}^{-1}$ and is available at monthly resolution for the historical and future periods.

Burnt Area Fraction (shortname: *burntarea*) Total area percentage of grid cell that has burned at any time, expressed in % and is available at monthly resolution for the historical and future periods

All the variables selected so far, can consider the effect on vegetation of CO₂ fertilization with co₂ levels fixed at 2005 (2005CO₂ scenarios, no fertilization effects) or with transient level of co₂ (CO₂ scenario, fertilization effect). The socio-economic scenario can be available considering land use, nitrogen deposition, and fertilizer input constant to pre-industrial value (1661-1860; 1860soc); the historical period varying historical land use, nitrogen deposition and fertilizer input (1861-2005; histsoc); the 2005 as fixed year and the related values of land use (2005soc), nitrogen deposition and fertilizer input; the future period varying land use, water abstraction, nitrogen deposition and fertilizer input.

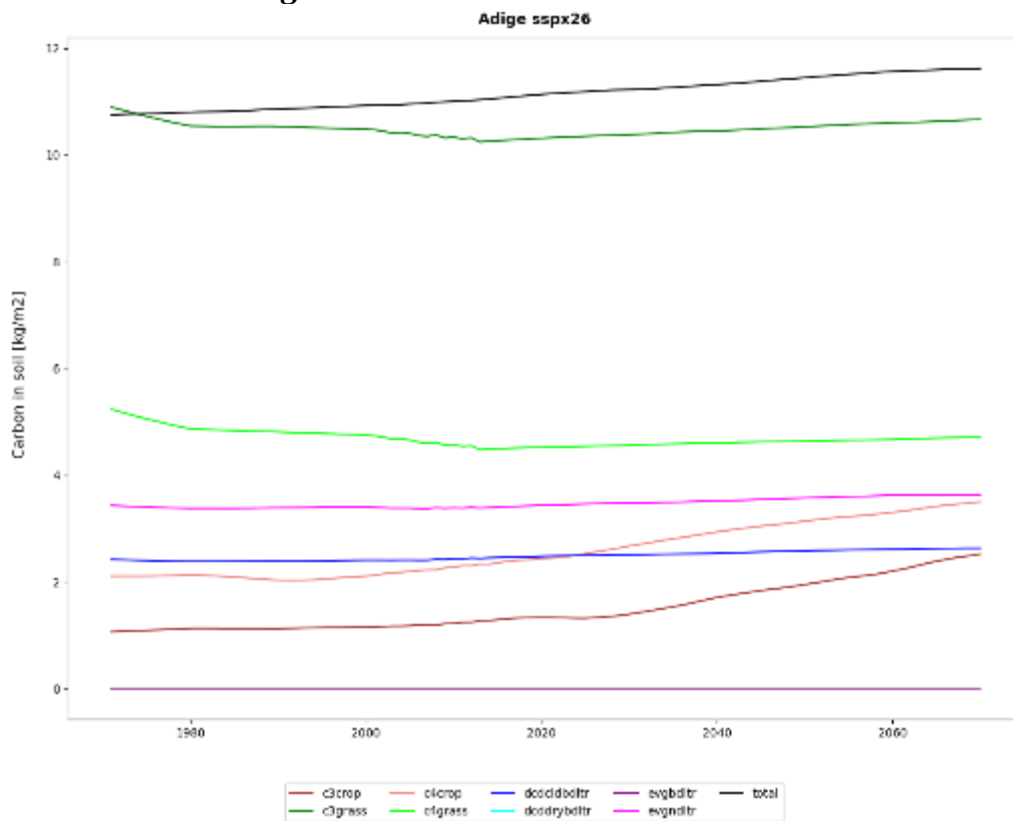
Variable trends and uncertainty

For all basins and scenarios, soil carbon and vegetation carbon storage projections for all available plant functional types (PFT) from the isimip3b model classic were compared and evaluated. The comparison is made for the same climate driver (gfdl-esm4), co₂ concentration forcing (default) and societal forcing (histsoc for historical and 2015soc-from-histsoc for the future scenarios) to exclude bias from external parameters in the comparison. The ‘total’ category does not represent a sum of the carbon stored in each PFT, but the average of each PFT storage weighted by the respective percentage land cover in each grid cell of the region.

In general, the model offers a good representation of carbon dynamics in temperate terrestrial ecosystems. Consistently with the literature, grass PFTs are the main storages of soil carbon while deciduous and evergreen forest types have the largest aboveground C mass (Ciais et al., 2000).

The only anomalous data is the one about the ‘total’ soil and vegetation storage in the Adige basin. For soil storage, the Adige total is higher than any individual PFT, which, given the way the total is calculated, should be impossible (as a weighted average cannot be higher than the highest averaged member). Similarly, for vegetation storage the Adige ‘total’ value shows an unrealistic fluctuation that is not observed in any of the individual PFTs, and which also makes the total reach higher values than *evgndltr* for several years. These anomalies in the ‘total’ values for Adige are unlikely due to an error in the data extraction but are probably caused by a mismatch in the grid cell allocation of land use for this particular dataset. In fact, the vegetation and soil carbon ‘total’ values for Adige do not show these anomalies if the 2015soc societal forcing is considered instead of histsoc and 2015-from-histsoc (not shown). The same difference is found if the *ukesm1-0-ll* climate driver is used instead of *gfdl-esm4* (not shown), suggesting that some internal error has indeed occurred in the calculation of the ‘total’ vegetation and soil carbon storage under the histsoc and 2015soc-from-histoc societal forcings. Therefore, the user is invited to use the 2015soc forcing scenario over the others whenever possible, as this reduces the chances of finding anomalies in the data.

Soil Carbon Storage



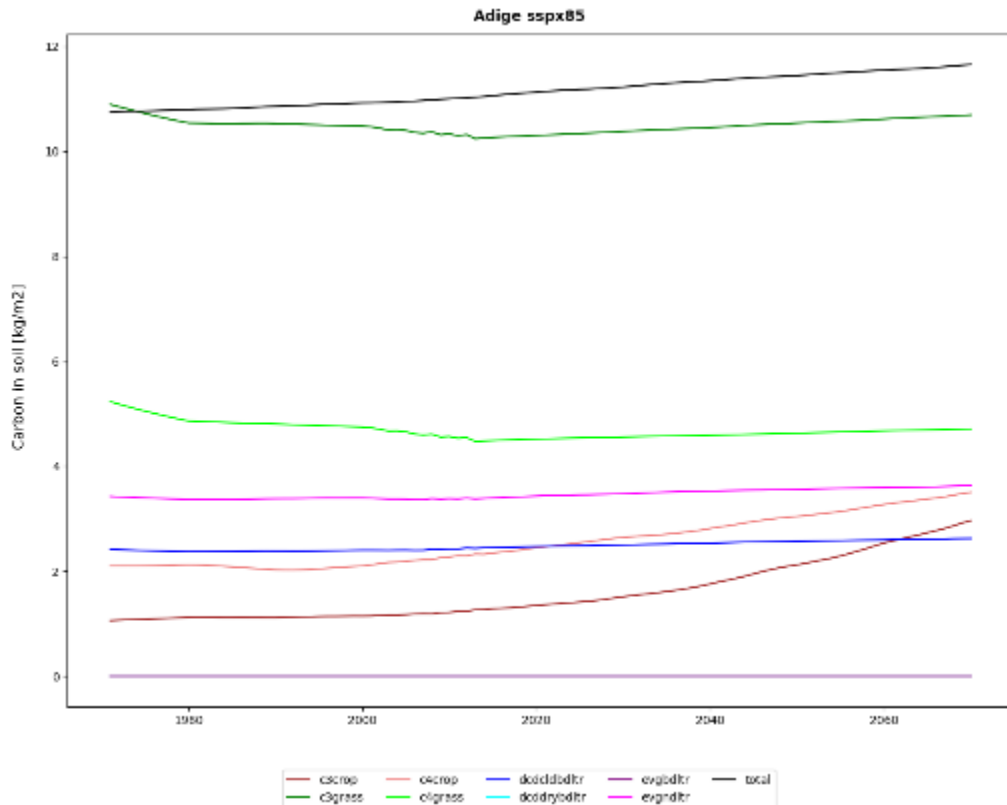
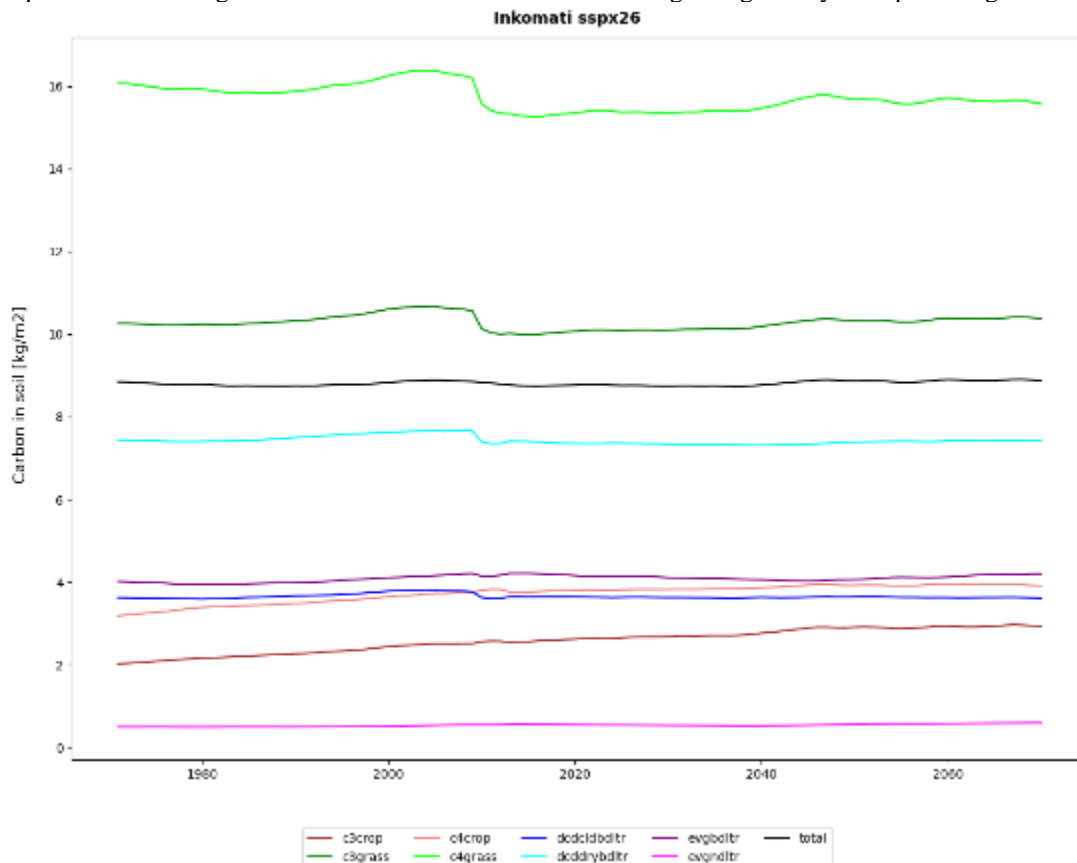


Figure 26. Soil carbon storage [kg m⁻²] in the Adige basin for the ssp26 (above) and ssp85 (below) scenarios for eight plant functional types: c3 crop (brown), c4 crop (orange), c3 grass (dark green), c4 grass (light green), broadleaf cold deciduous tree (dcldbdltr, blue), broadleaf drought deciduous tree (dcddrybdltr, light blue), broadleaf evergreen tree (evgbdltr, purple) and needleleaf evergreen tree (evgndltr, magenta). The total (black) represents the average of the individual PFTs soil carbon storage weighted by their percentage land cover area.



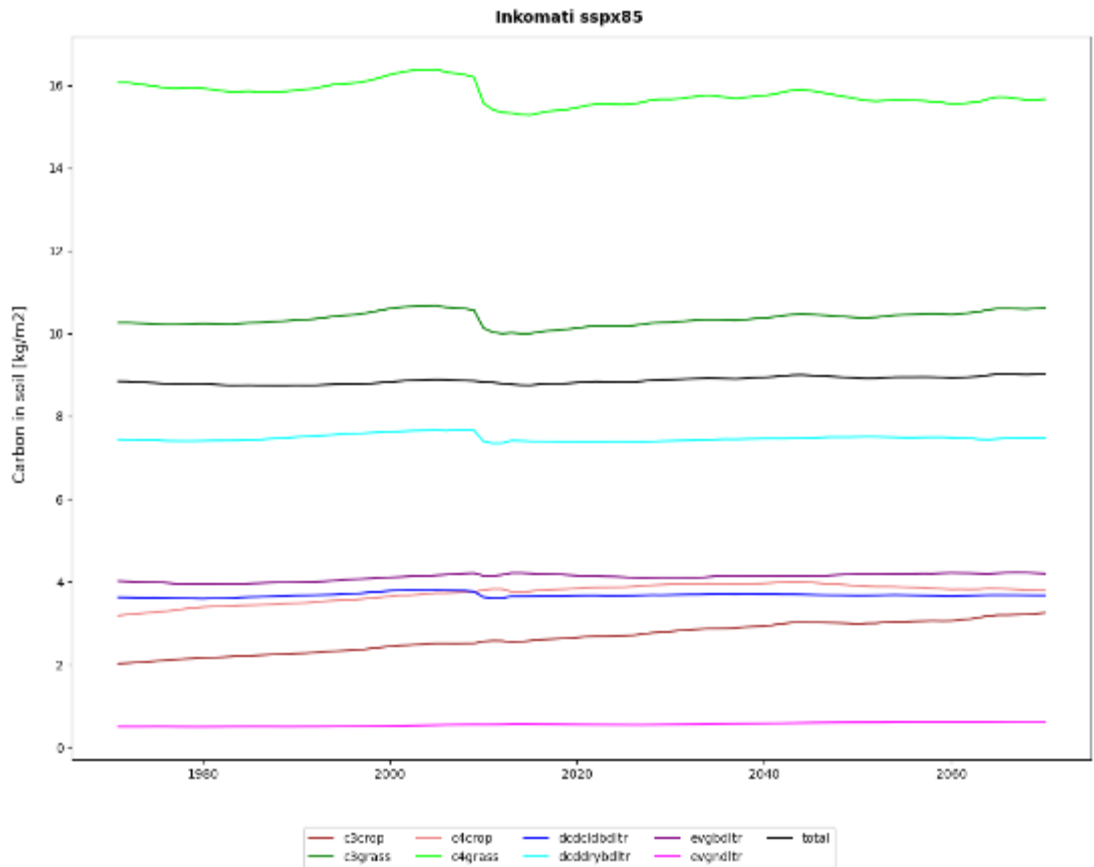
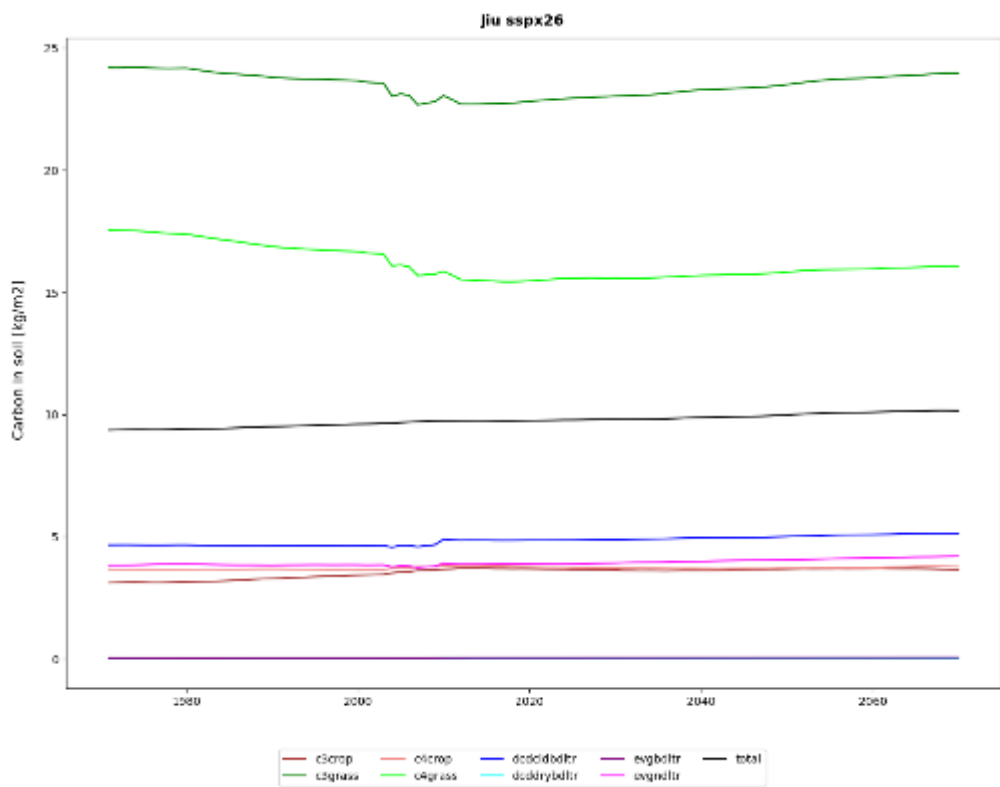


Figure 27. Same as Figure 26, but for Inkomati.



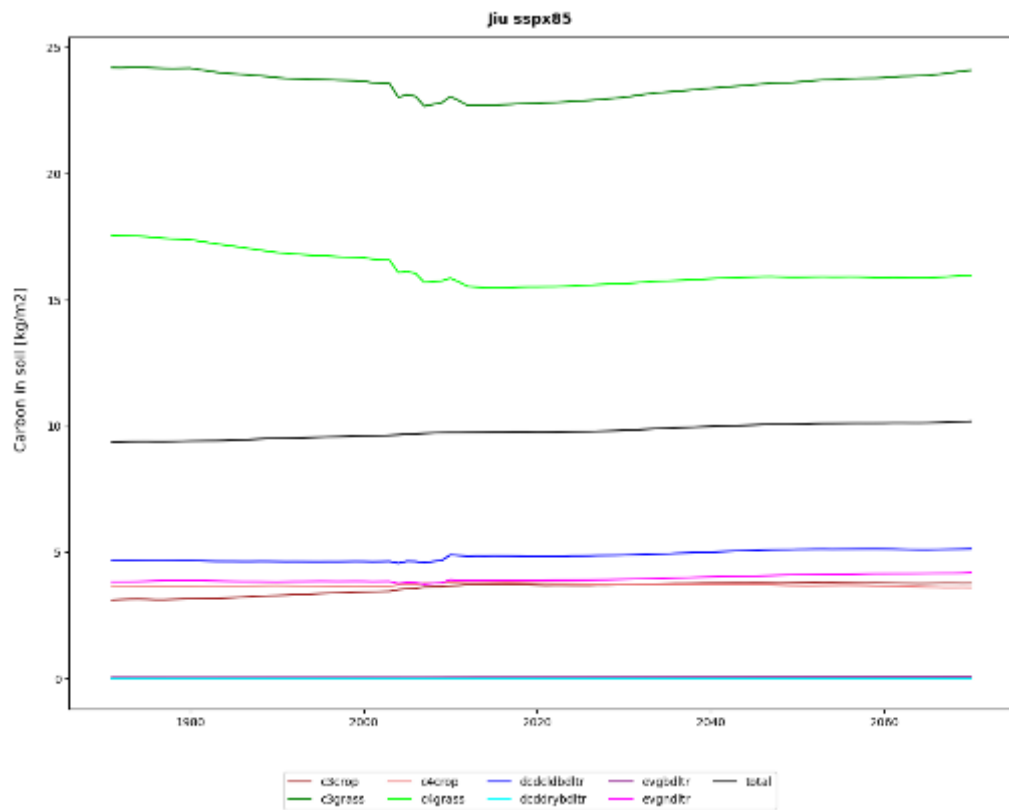


Figure 28. Same as Figure 26, but for Jiu.



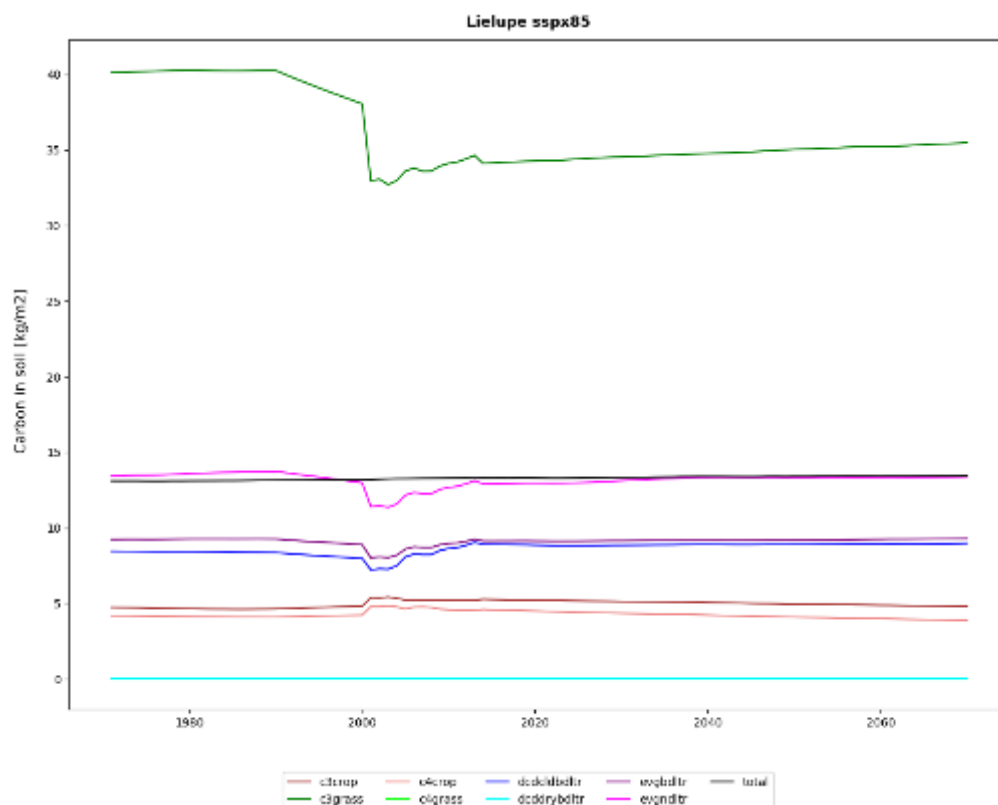
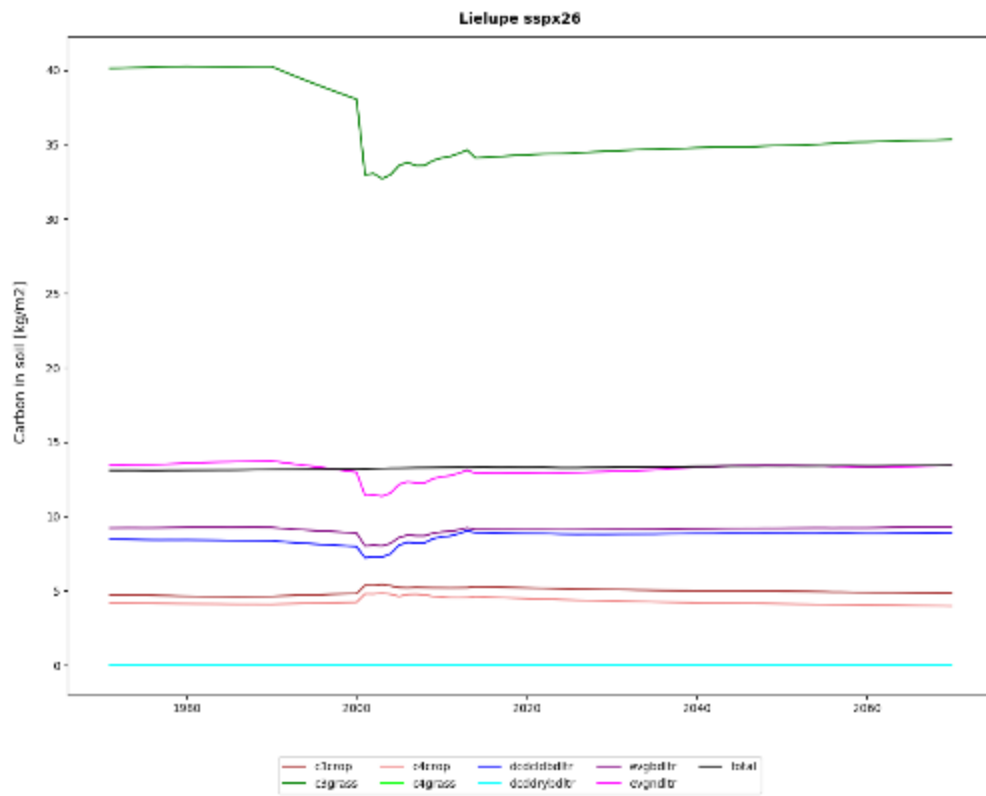


Figure 29. Same as Figure 26, but for Lielupe.



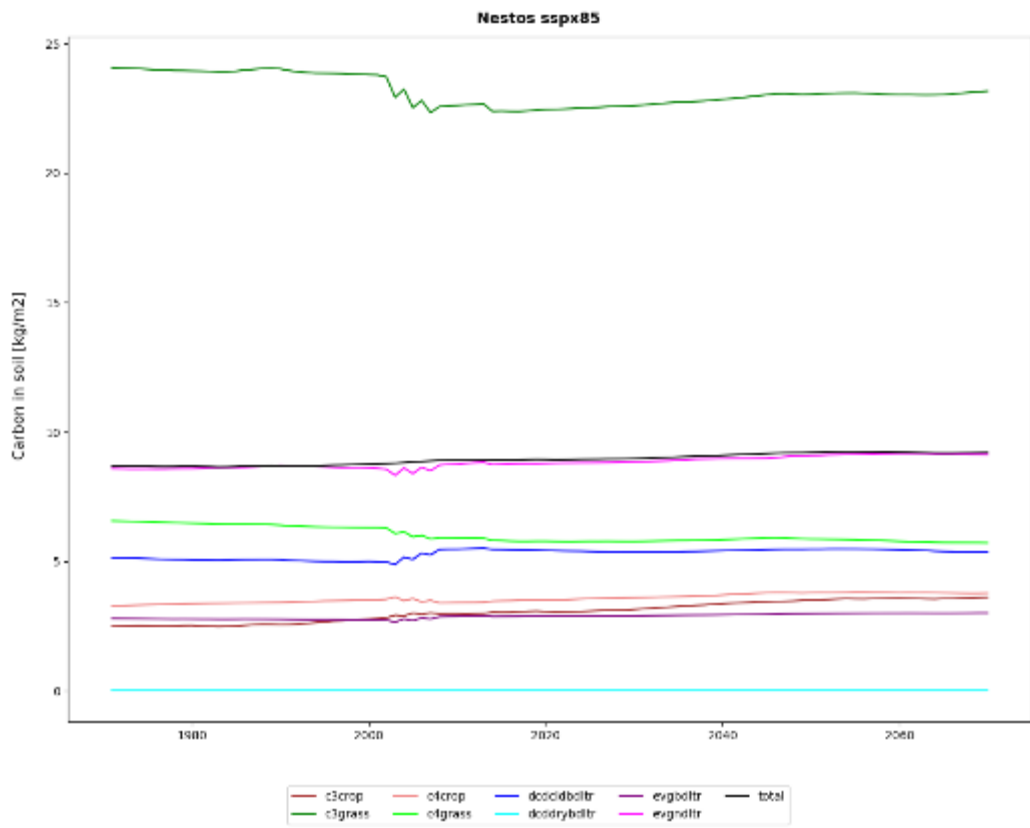
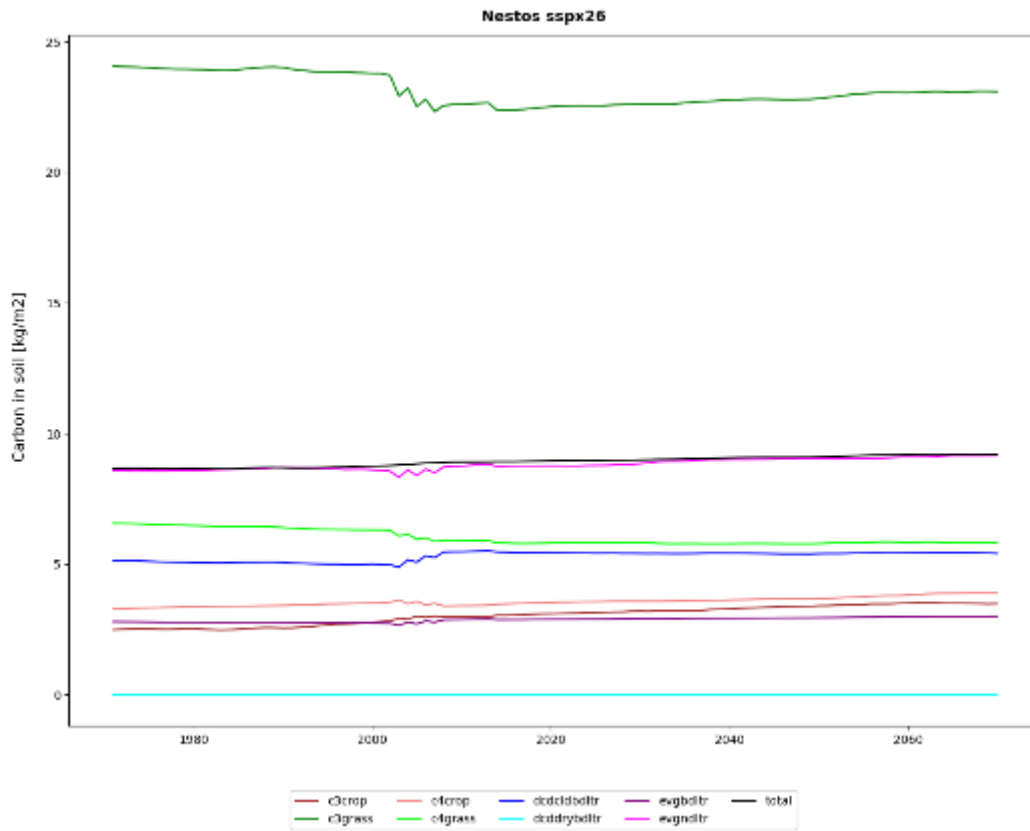


Figure 30. Same as Figure 26, but for Nestos.



Vegetation Carbon Storage

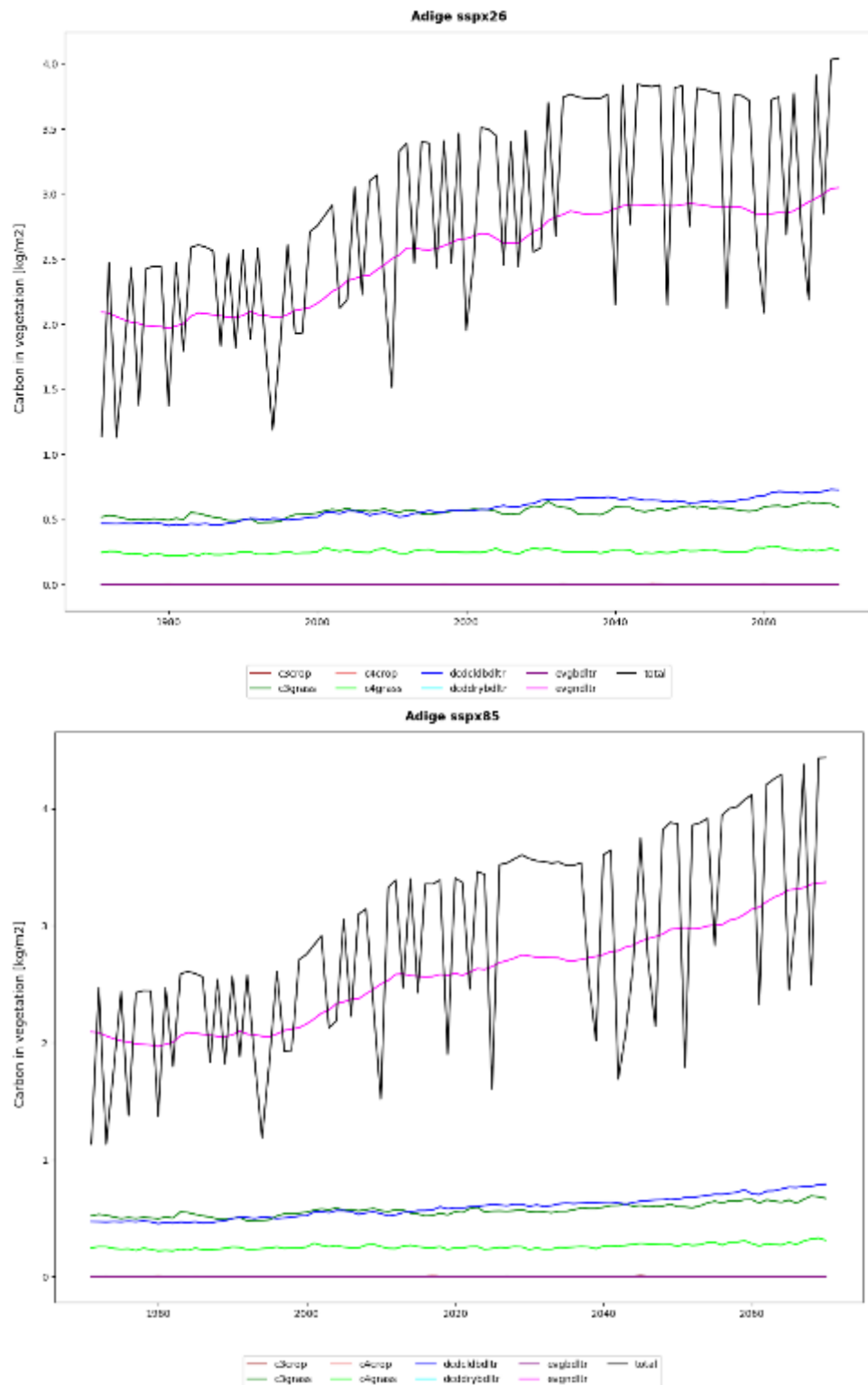


Figure 31. Vegetation carbon storage [kg m⁻²] in the Adige basin for the ssp26 (above) and ssp85 (below) scenarios for eight plant functional types: c3 crop (brown), c4 crop (orange), c3 grass (dark green), c4 grass (light green), broadleaf cold deciduous tree (dclddbdtr, blue), broadleaf drought deciduous tree (dcdrybdtr, light blue), broadleaf evergreen tree (evgbdtr, purple) and needleleaf evergreen tree (evgndtr, magenta). The total (black) represents the average of the individual PFTs soil carbon storage weighted by their percentage land cover area.

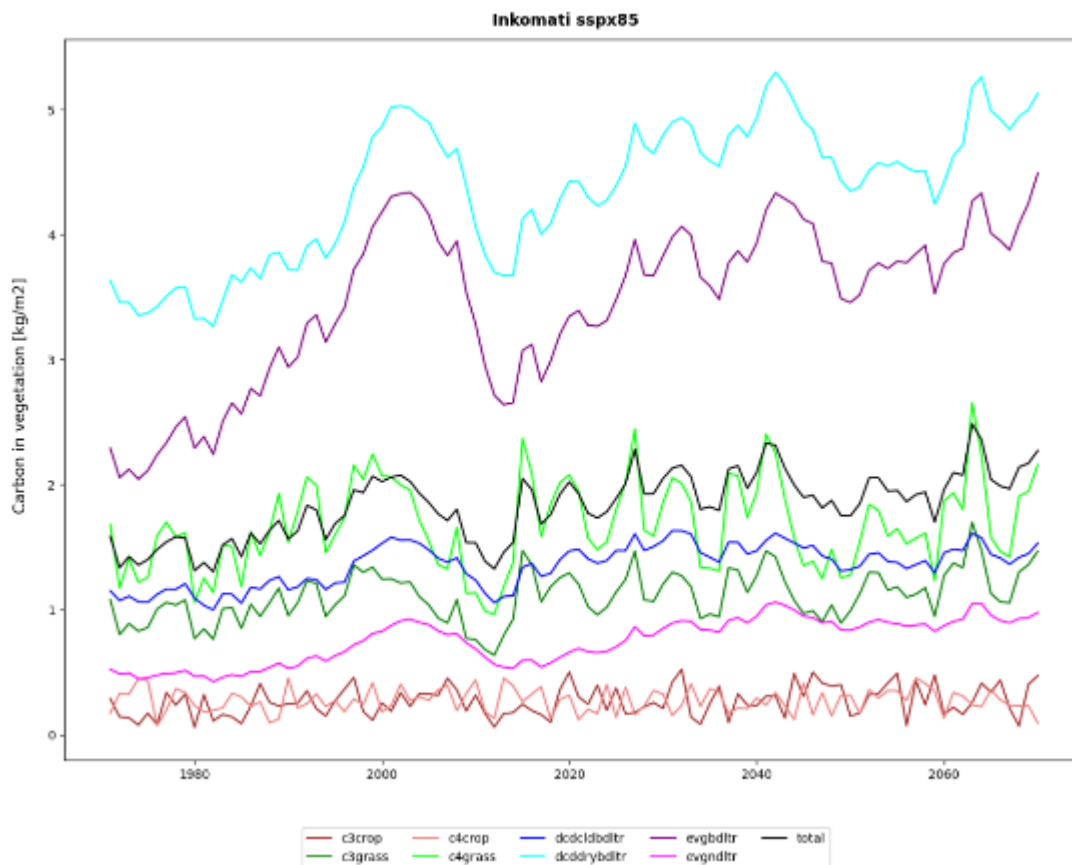
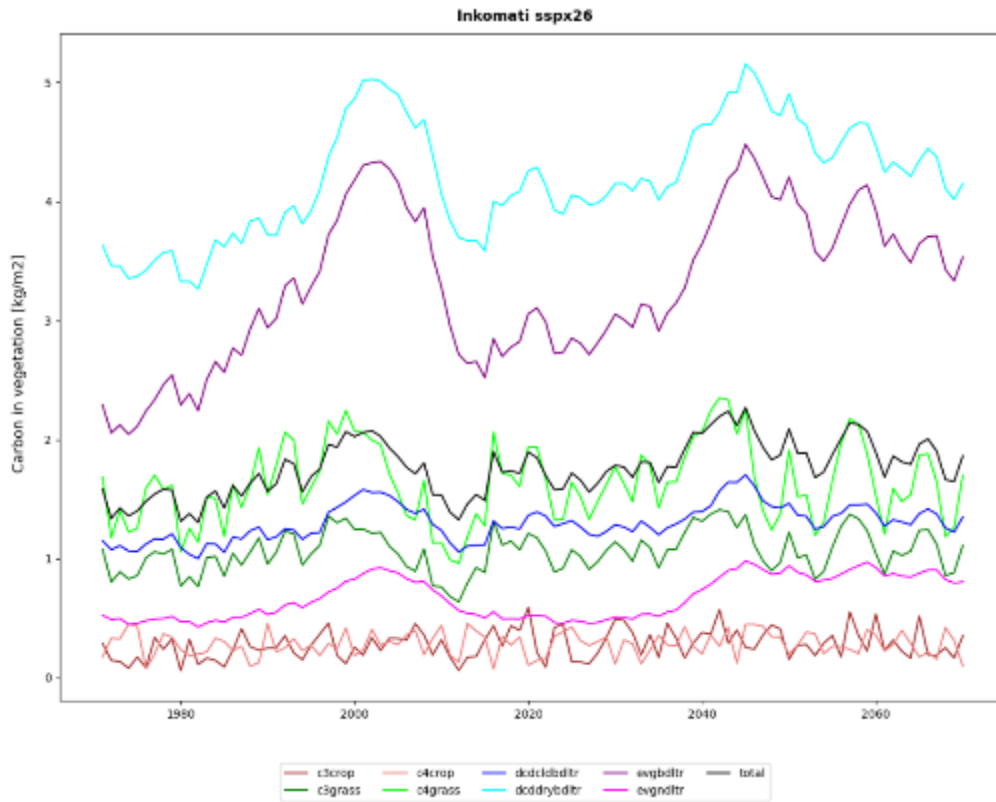


Figure 32. Same as Figure 31, but for Inkomati.



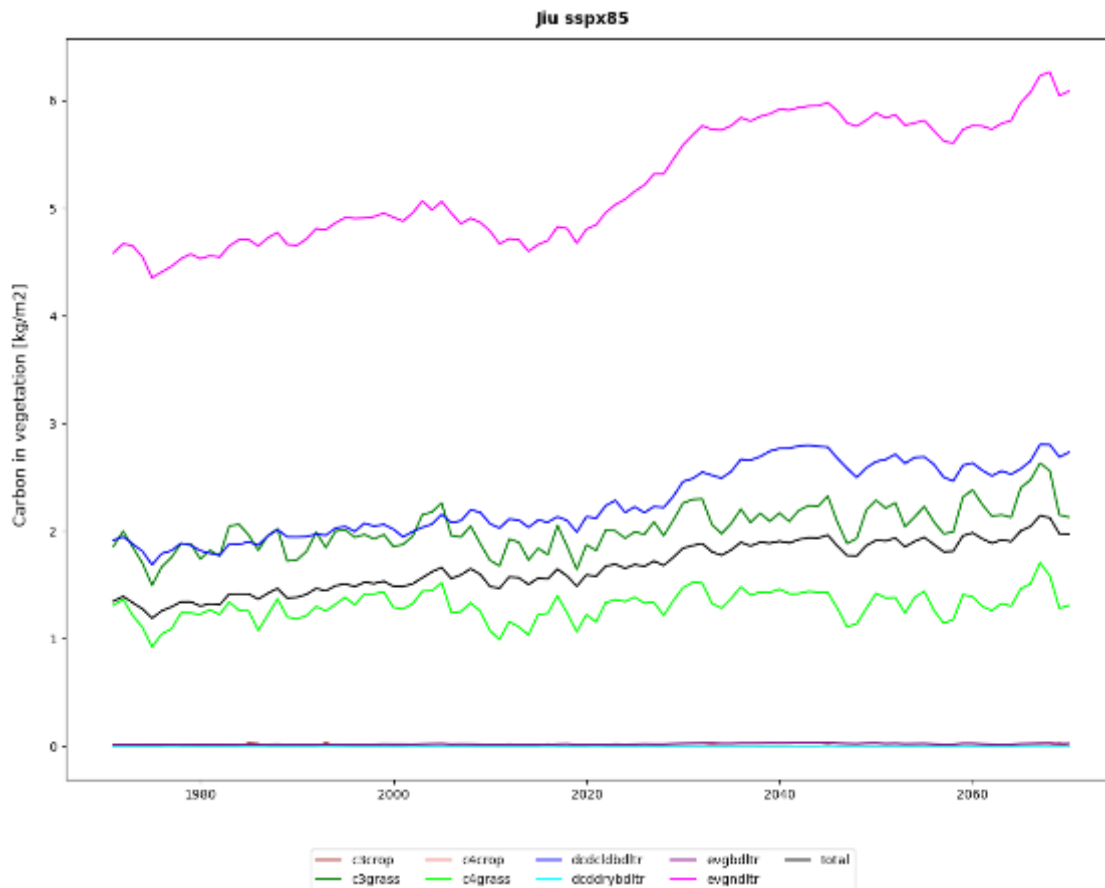
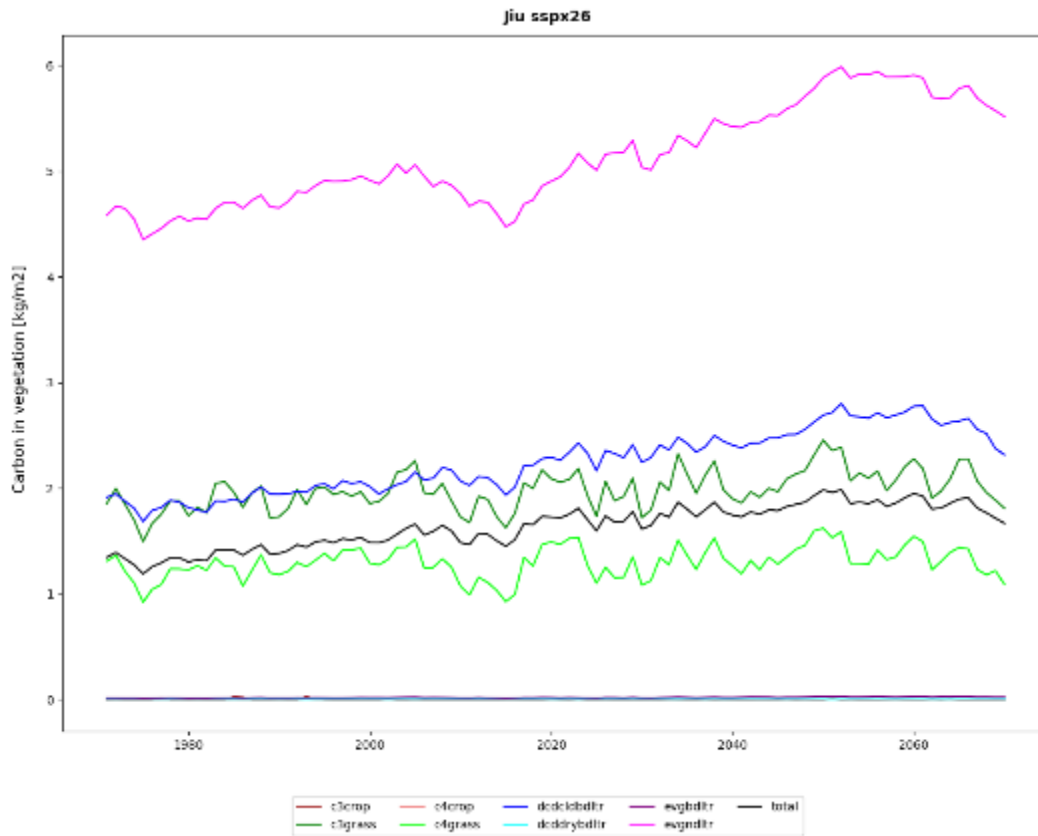


Figure 33. Same as Figure 31, but for Jiu.



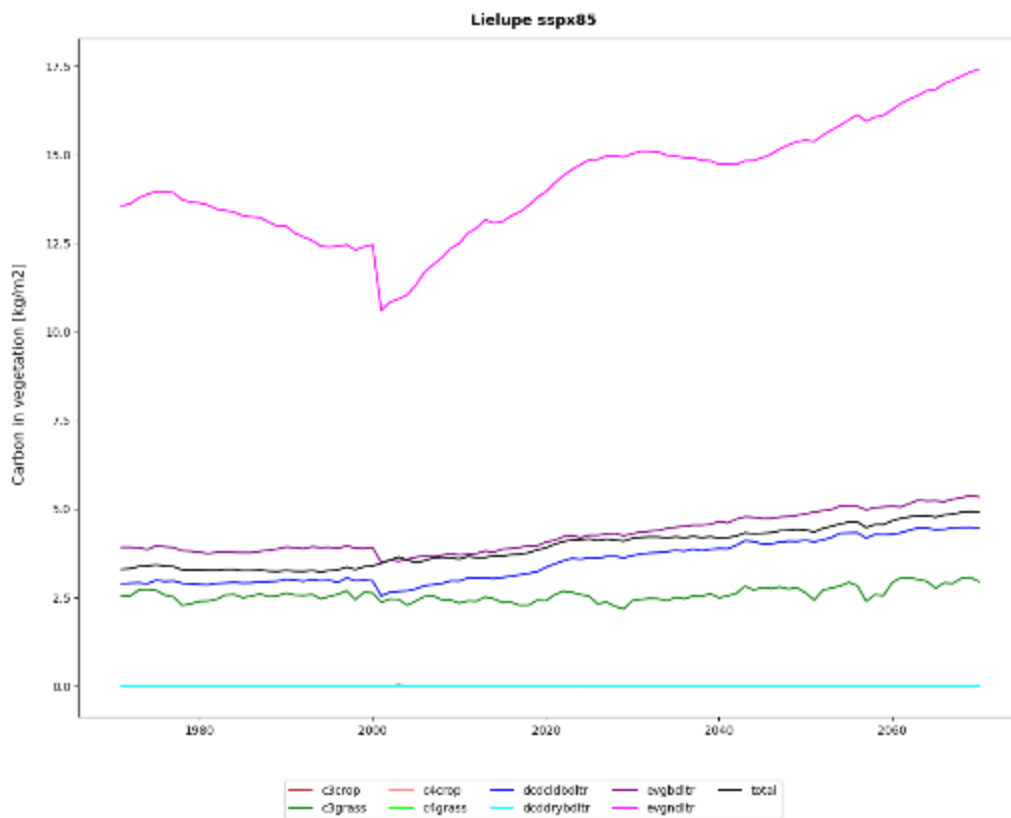
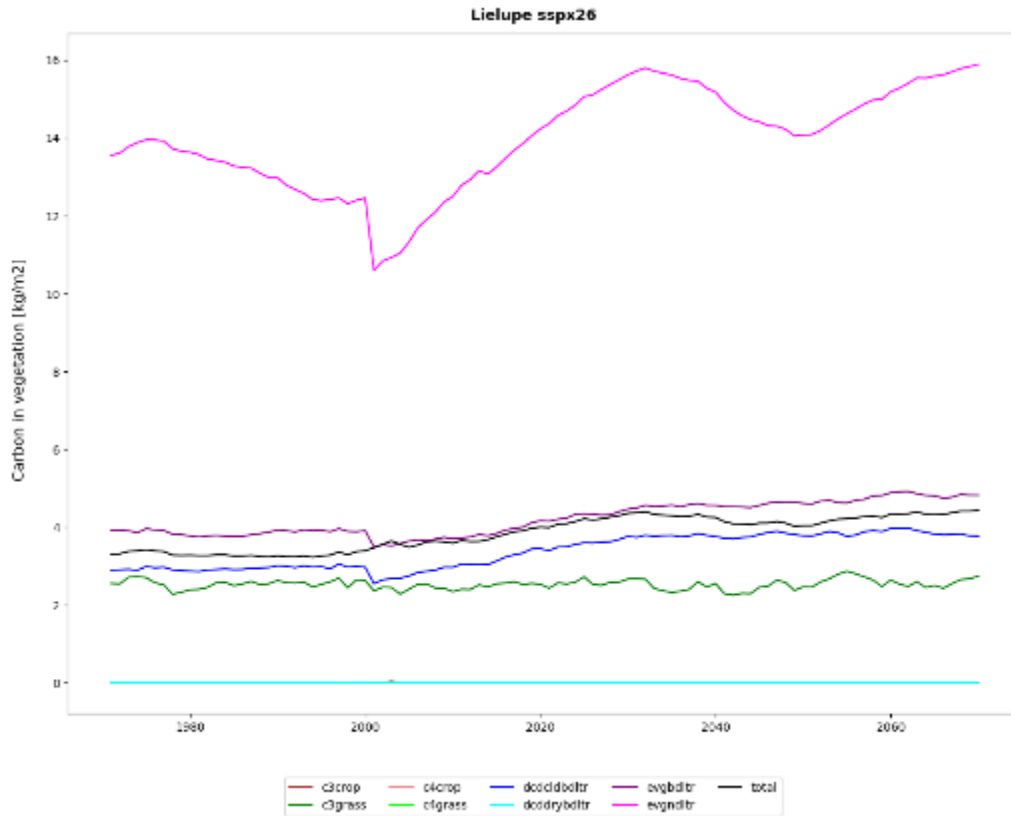


Figure 34. Same as Figure 31, but for Lielupe.



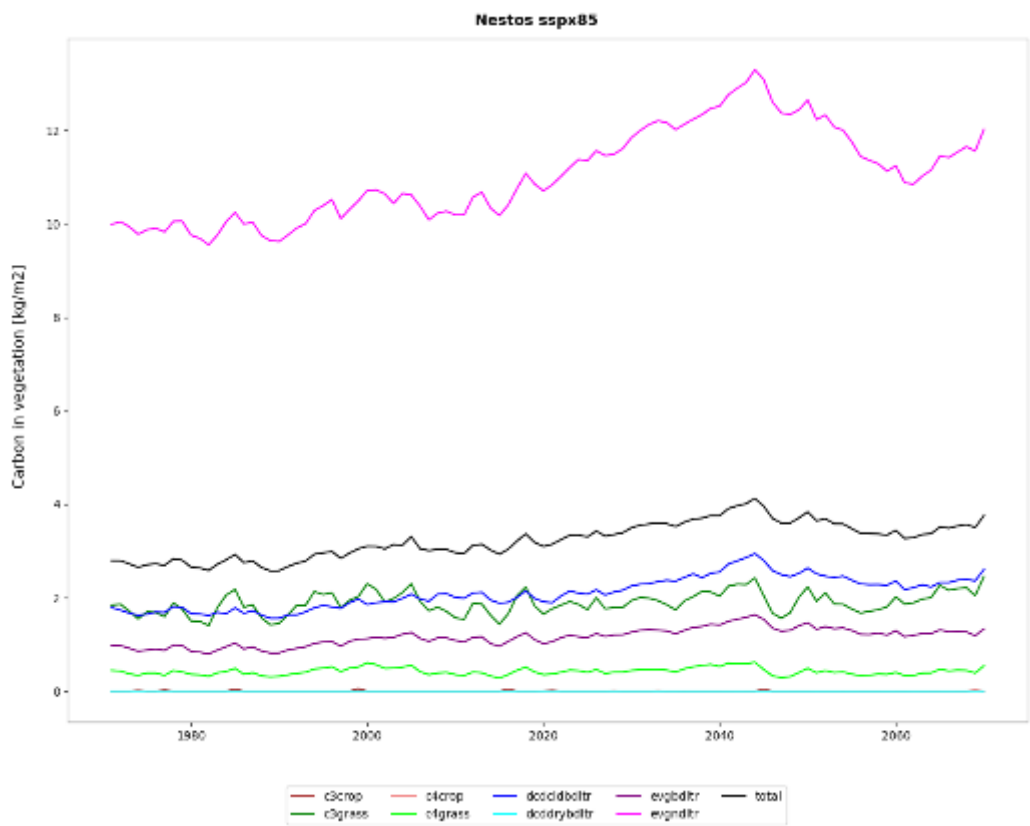
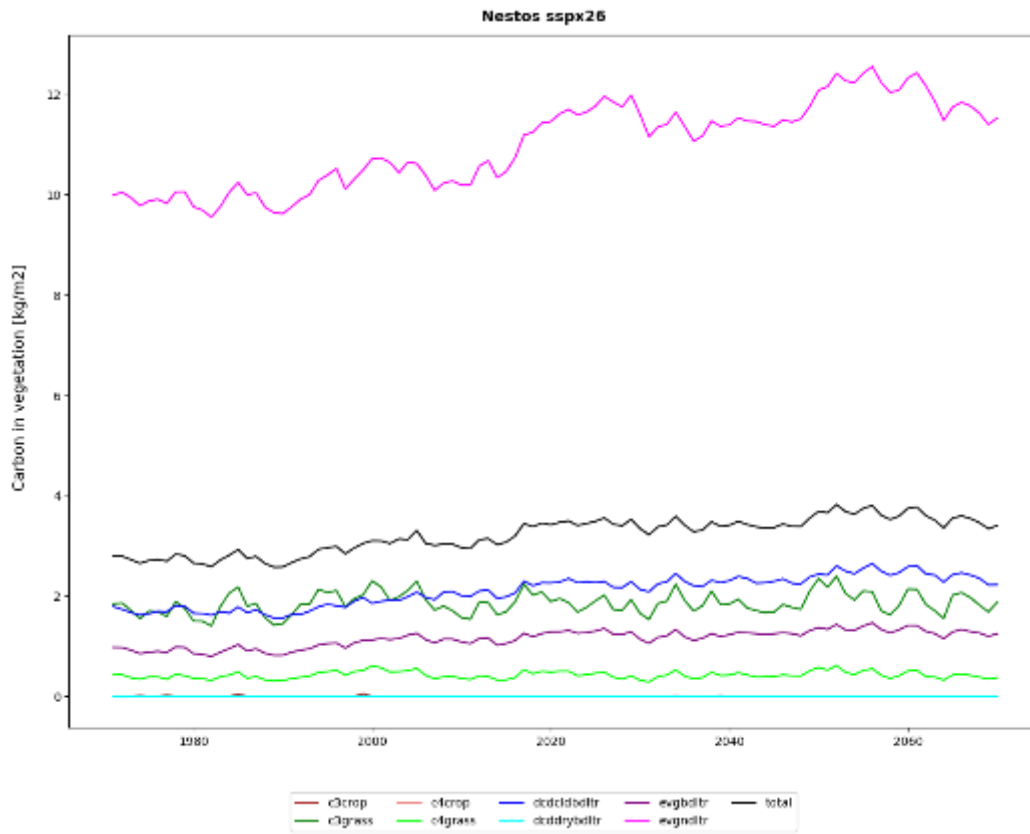


Figure 35. Same as Figure 31, but for Nestos.



4 Land Use

4.1 Land Use Sources Data

Several existing land use data products have been included to define relevant information on spatial distribution and tabular distribution of land uses and main crop types within the case studies. These land use datasets would be particularly relevant in the building of the System Dynamic Modelling and as baseline for the change in future major crop distribution as foreseen by MAGNET-GRID implementation of G-RDEM results.

In principle the CORINE Land Cover (CLC) product provides a pan-European land cover and land use inventory with 44 thematic classes, ranging from broad forested areas to individual vineyards. The product is regularly updated every six years, with the most recent update made in 2018. This latest product has then been considered as detailed land use classification, which offers a detailed description for most case studies in Europe of several major crop types, in addition to other natural, semi-natural, and urban areas. The inventory contains 44 land cover classes. However, the product has a Minimum Mapping Unit of 25 hectares (ha) for areal phenomena and a minimum width of 100 m for linear phenomena. For this reason, other regional land use products may offer a greater and more accurate detail.

For instance, for the Adige case study a new highly detailed land use/landcover map, included in the European Strategy for the Alpine Region (EUSALP), has a spatial resolution of up to 5 m and a temporal extent from 2015 to 2020 (Marsoner et al, 2023). It has a large number of land use classes (65) and high spatial resolution, making it useable by a broad audience for research and management purposes. The dataset combines high-resolution datasets from different sources for the whole alpine region and it is therefore mostly suited to characterize land use and agricultural types of alpine regions.

For the Inkomati case study, a 20 m resolution South African National Land-Cover 2020 (SANLC 2020) dataset has been proposed, which has been generated from automated mapping models, using multi-seasonal 20 m resolution Sentinel 2 satellite imagery. This land use represents the full temporal range of available imagery acquired by Sentinel 2 during the period 01 January 2020 to 31 December 2020, and include a classification of 73 land uses in the full land-cover dataset

Finally, an experimental product developed by JRC has been considered of crops grown in the European Union at 10-m resolution. This map combines Copernicus Sentinel-1 satellite observations and in-situ LUCAS 2018 Copernicus data using machine learning and cloud computing to detect 19 different crop types for year 2018 (d'Andrimont et al 2021). However, limitation on survey information available from the LUCAS dataset implies still a potential inaccuracy in specific areas and further validation against regional statistics is required to determine product accuracy in the NXG case studies.

A more extensive list of land use products and their comparison for uncertainty evaluation is available in ANNEX I.

4.2 Uncertainties in land use downscaling

Uncertainties related to the spatial data employed in the downscaling

For downscaling national land projections to grid cells, MagnetGrid makes use of global spatial datasets (5 arcmin) on land use (base year) and current and future gridded data on agricultural productivity potential. These are very coarse spatial resolution data to work within the river basins borders. In addition, we also add a very limited number of non-agricultural land uses (i.e. water bodies, urban areas and forest areas) to constrain agricultural land allocation. This gives the model more freedom to allocate cropland and grazing grasslands in areas that in theory are not available for agriculture (e.g. peatlands, protected areas, sparse forests). Furthermore, these global spatial datasets, such as MAPSPAM (You et al., 2014) and Irrigation maps (Siebert et al., 2013) are not temporally aligned with the macro-economic model's (G-RDEM) base year (2014). For a further improvement of this study, we suggest that higher resolution data should be employed as well as case-study specific modules implemented in MagnetGrid, (i.e., not using the global version of the downscale modelling).

Uncertainties related to the macro-economic model

The G-RDEM macro-economic model provides land and economic indicators to estimate national level projections on land trends aggregated per agricultural sector considering only two future scenarios (i.e. socio-economic pathways – SPP 2 and 4) of population and Gross Domestic Production (GDP) changes. Additionally, the land dynamics (percentage changes over time) derived from G-RDEM are based on the annual variation of land demand factor per economic activity, without any endogenous integration of land area supply and climate factors, which increase the uncertainty of the G-RDEM output. Therefore, in land use projections based on macro-economic scenarios, the uncertainties on the economic modelling can be very significant and are important to be detected, quantified and compared with other land economic projections. The uncertainties on land use projections driven by macro-economic models are addressed in several studies (Alexander et al., 2017; Popp et al., 2017; Prestele et al., 2016)

Uncertainties related to the land use rules of transition

The non-agricultural land uses are exogenous in the MagnetGrid modelling framework and have no dynamic spatio-temporal variation. This is not realistic as urban areas expand/contract over time as well as other non-agricultural land uses (e.g. forest areas). In this modelling exercise, we assume that non-agricultural land uses are spatially static over time.

Uncertainties related to the suitability and economic land optimization

MagnetGrid utilizes land utility as a suitability factor for land use allocation. The land utility values are based on economic returns per crop, i.e. crop production costs (as function of crop yields), opportunity costs (as function of crop yields) and sunk costs (as function of land area). Hence, the main suitability factors playing a role in the land utility is biophysical. However, other socio-economic parameters might play an important role in calculating the land utility, such as proximity to road network, logistic hubs, and consumer markets (all affecting transportation costs), as well as the farm level economic structure and other indicators of land economic utility (e.g. access to financing, risk aversion, etc.).

Changing base year land data

Although the physically related aspects are the output from MagnetGrid (e.g. crop yield levels, cropland area), the main purpose of using it is to downscale national level projections on percentage changes of land derived from G-RDEM. Hence, the main goal is to inform SDMs on the percentage change of land area within the river basin borders. As mentioned before, unreliable changing rates of land can be produced using MAPSPAM as the agricultural base dataset since it is rather coarse to fit into the river basin borders.

Given that, we use local land area data (from 2015) for the Jiu case study to understand the variation of the land changes between 2015 and 2050. In Figure 11, we compare the development of land change over time in different agricultural sectors in the Jiu basin. For the sectors that normally demand more land (*OilSeeds*, *Cereals* and *Wheat*), MAPSPAM has much lower land available in the base year (total for these sectors=160kha), and consequently shows that land needs to be expanded (approx. between 60% – 160% depending on the sector) until 2050 to meet future production targets (see solid lines in Figure 11). On the other hand, when we use the local data base year (more than 1Mha for all these three sectors), the land demand shows generally decreasing trends in the region except for the *VegFruits* (vegetables and fruits), which land demand is projected to expand more than 3-fold.

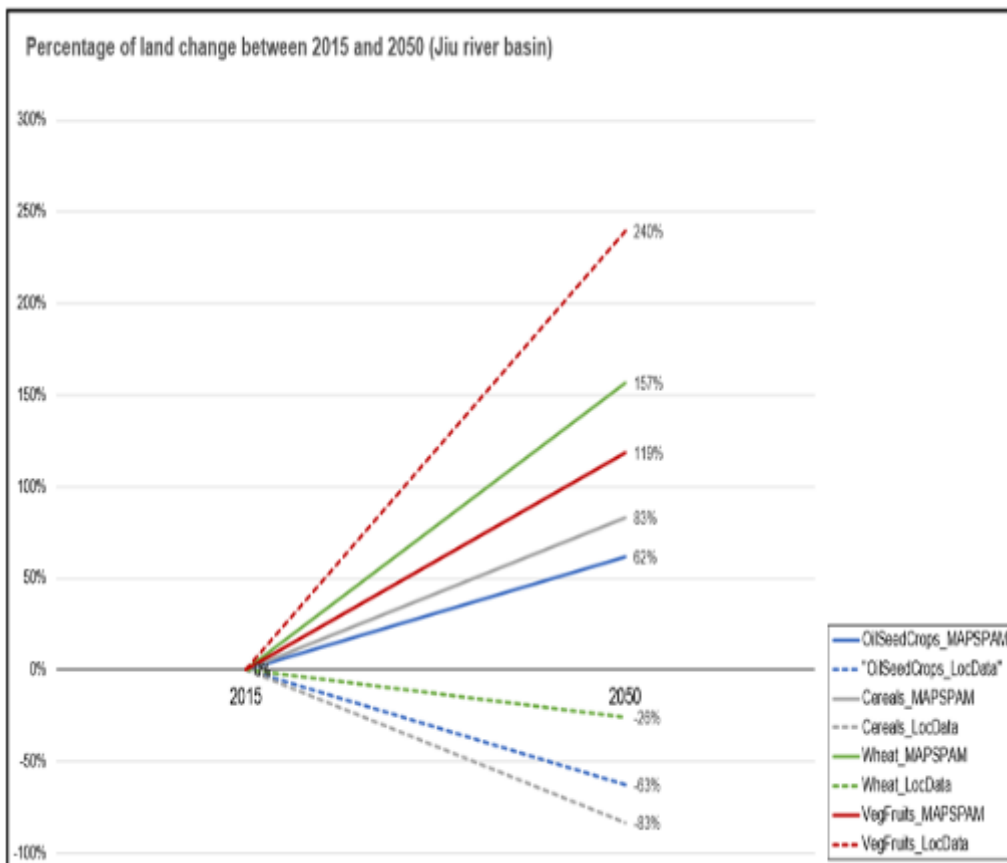


Figure 11. Comparison of land trends in Jiu river basin between 2015 and 2050 (SSP2/RCP2.6), using two different land use area data (MAPSPAM and River basin local data) in the base year.

5 Conclusions and contribution to other project activities

The main aim of this deliverable was to provide knowledge base on data trends and uncertainties, and thus improve confidence levels to facilitate the use and implementation of modelling data for project activities. The presented macro trends from modelling projections display indeed various levels of uncertainties to characterize thematic factors across the WEF Nexus and relevant for project case studies. These depend mostly on divergence between climate projections as drivers to impact models across the Nexus, as well as biases and imperfect/simplified representation of biophysical processes in impact models, and depiction of radiative forcing under low and high-end emission scenarios. All of these factors affect modelling chain through uncertainty propagation in the results. For instance, most models relying on precipitation factors (e.g. hydrological models) tend to propagate and present higher level of uncertainty inherent to higher level of uncertainties of precipitation future trends, while other models more closely dependant on temperature factors (e.g. biomass or crop model) present still significant but lower levels of modelling uncertainties. In fact, the documents describing uncertainty of modelling outputs, together with several interactions with case study responsible, developers and stakeholders, can help clarify but also validate the use and reliability of model outputs. These, for instance can present trends either aligned to mean among uncertainty distribution (rather conservative estimate) or on the edge of distribution (rather as outliers).

The document support information relevant to further interactions with modelling activities in WP3 and WP4 to characterize uncertainties and confidence levels for complexity science modelling and artificial intelligence implementation for policy assessment tools. Furthermore, but also equally important, it aims at more effectively illustrate and support stakeholder's perception of uncertainties, often underrated for risk management, but highly relevant and pertinent to future projections.



References:

- Alexander P, Prestele R, Verburg PH, Arneth A, Baranzelli C, Silva FBE, et al (2017). Assessing uncertainties in land cover projections. *Glob Chang Biol* 2017:767–81. <https://doi.org/10.1111/gcb.13447>.
- Allen R.G., Pereira L.S., Raes D., Smith M. (1998) Crop evapotranspiration: guidelines for computing crop requirements. *Irrig. Drain. Pap. FAO*, 56, p. 300, 10.1016/j.eja.2010.12.001
- Allen R.G., Walter I.A., Elliott R.L., Howell T.A., Itenfisu D., Jensen M.E., Snyder R.L. (2005) The ASCE Standardized Reference Evapotranspiration Equation. American Society of Civil Engineers, Reston, VA
- Allen R.G., Pruitt W.O., Wright J.L., Howell T.A., Ventura F., Snyder R.L., Itenfisu D., Steduto P., Berengena J., Yrisarry J.B., Smith M., Pereira L.S., Raes D., Perrier A., Alves I., Walter I., Elliott R.A. (2006) Recommendation on standardized surface resistance for hourly calculation of reference ETo by the FAO56 Penman–Monteith method
- Almazroui, M., Saeed, F., Saeed, S., Nazrul Islam, M., Ismail, M., Klutse, N. A. B., & Siddiqui, M. H. (2020). Projected Change in Temperature and Precipitation Over Africa from CMIP6. *Earth Systems and Environment*, 4(3), 455–475. <https://doi.org/10.1007/s41748-020-00161-x>.
- Brauman, K. A., Daily, G. C., Duarte, T. K. E., & Mooney, H. A. (2007). The nature and value of ecosystem services: an overview highlighting hydrologic services. *Annu. Rev. Environ. Resour.*, 32, 67–98.
- d’Andrimont, R., Verhegghen, A., Lemoine, G., Kempeneers, P., Meroni, M., van der Velde, m. (2021) From parcel to continental scale – A first European crop type map based on Sentinel-1 and LUCAS Copernicus in-situ observations, *Remote Sensing of Environment*, 266, 112708
- Ciais P., Cramer W., Jarvis P., Kheshgi H., Nobre C., Semenov S., Steffen W. (2000). Chapter 1: Global Perspective. IPCC special report on Land Use, Land-Use Change, and Forestry. Robert T. Watson, Ian R. Noble, Bert Bolin, N. H. Ravindranath, David J. Verardo and David J. Dokken (Eds.) Cambridge University Press, UK. pp 375 Available from Cambridge University Press, The Edinburgh Building Shaftesbury Road, Cambridge CB2 2RU ENGLAND.
- Coppola, E., Nogherotto, R., Ciarlo’, J. M., Giorgi, F., van Meijgaard, E., Kadygrov, N., Iles, C., Corre, L., Sandstad, M., Somot, S., Nabat, P., Vautard, R., Levvasseur, G., Schwingshackl, C., Sillmann, J., Kjellström, E., Nikulin, G., Aalbers, E., Lenderink, G., ... Wulfmeyer, V. (2021). Assessment of the European Climate Projections as Simulated by the Large EURO-CORDEX Regional and Global Climate Model Ensemble. *Journal of Geophysical Research: Atmospheres*, 126(4), e2019JD032356. <https://doi.org/https://doi.org/10.1029/2019JD032356>.
- Diogo V., Hennen W., Verma M., Oudendag D., Kuiper M. (2020). MagnetGrid; Model description and user guide. Wageningen, Wageningen Economic Research, Report 2020-004. 66 pp.; 12 fig.; 2 tab.; 90 ref. <https://edepot.wur.nl/512146>
- Fischer, G., Nachtergaele, F., Prieler, S., Teixeira, E., Tóth, G., Van Velthuisen, Verelst, L., Wiberg, D. (2012). Global Agro-Ecological Zones (GAEZ v3.0): Model Documentation. International Institute of Applied Systems Analysis, Laxenburg, Austria / Food and Agricultural Organization of the United Nations, Rome, Italy. <https://www.gaez.iiasa.ac.at/>

Grizzetti, B., Lanzaova, D., Liqueste, C., Reynaud, A., & Cardoso, A. C. (2016). Assessing water ecosystem services for water resource management. *Environmental Science & Policy*, 61, 194-203.

Guerra E., Ventura F., Spano D., Snyder R.L. (2015) Correcting midseason crop coefficients for climate J. Irrig. Drain. Eng., 141, Article 04014071

Tian H., Liu M., Zhang C., Ren W., Xu X., Chen G., LU (2010) The Dynamic Land Ecosystem Model (DLEM) for Simulating Terrestrial Processes and Interactions in the Context of Multifactor Global Change[J]. *Acta Geographica Sinica*, 65(9): 1027-1047.

Hargreaves G.H., Samani Z.A. (1985) Reference crop evapotranspiration from temperature. *Applied Engineering in Agriculture*, 1, pp. 96-99, 10.13031/2013.26773

Koirala S., Yeh Pat J.-F., OKI Taikan, KANAE Shinjiro (2010) Fully dynamic groundwater representation in the matsiro land surface mode. *Annual Journal of Hydraulic Engineering, JSCE*, Vol.54, 2010, February

Janse, J. H., Kuiper, J. J., Weijters, M. J., Westerbeek, E. P., Jeuken, M. H. J. L., Bakkenes, M., ... & Verhoeven, J. T. A. (2015). GLOBIO-Aquatic, a global model of human impact on the biodiversity of inland aquatic ecosystems. *Environmental Science & Policy*, 48, 99-114.

Lange, S.: Trend-preserving bias adjustment and statistical downscaling with ISIMIP3BASD (v1.0), *Geoscientific Model Development*, 12, 3055–3070, <https://doi.org/10.5194/gmd-12-3055-2019>, 2019

Lange, S.: ISIMIP3BASD v2.5.0, <https://doi.org/10.5281/zenodo.4686991>, 2021.

Lindstöm G, Pers C, Rosberg J, Strömqvist J, Arheimer B (2010) Development and testing of the HYPE (Hydrological Predictions for the Environment) water quality model for different spatial scales. *Hydrol Res* 41(3-4):295-319. doi:10.2166/nh.2010.007

Marsoner, T., Simion, H., Giombini, V. et al. (2023) A detailed land use/land cover map for the European Alps macro region. *Sci Data* 10, 468

Masia S, Trabucco A, Spano D, Snyder S, Susnik J, Marras S (2021) A Modelling platform of Climate risks and crop Water Management at Local and Regional Scale. *Agricultural Water Management*, 255(1–2):107005.

Meinshausen M., Smith S. J., Calvin K., Daniel J. S., Kainuma M. L. T., Lamarque J.-F., Matsumoto K., Montzka S. A., Raper S. C. B., Riahi K., Thomson A., Velders G. J. M. & van Vuuren D. P. P. (2011): The RCP greenhouse gas concentrations and their extensions from 1765 to 2300. *Climatic Change* 109 (1–2): 213–241. doi: 10.1007/s10584-011-0156-z.

Moss R. H., Edmonds J. A., Hibbard K. A., Manning M. R., Rose S. K., van Vuuren D. P., Carter T. R., Emori S., Kainuma M., Kram T., Meehl G. A., Mitchell J. F. B., Nakicenovic N., Riahi K., Smith S. J., Stouffer R. J., Thomson A. M., Weyant J. P., Wilbanks T. J. (2010) The next generation of scenarios for climate change research and assessment. *Nature* 463 (7282): 747–756. doi:10.1038/nature08823.

Müller Schmied et al (2020) The global water resources and use model WaterGAP v2.2d: model description and evaluation. *Geosci. Model Dev.*, 14, 1037–1079, 2021

Popp, A., Calvin, K., Fujimori, S., Havlik, P., Humpenöder, F., Stehfest, E., ... & van Vuuren, D. P. (2017). Land-use futures in the shared socio-economic pathways. *Global Environmental Change*, 42, 331-345.

Portmann F et al (2013) *Environ. Res. Lett.* 8 024023

Prestele R, Alexander P, Rounsevell MDA, Calvin K, Doelman J, Eitelberg DA. (2016). Hotspots of uncertainty in land-use and land-cover change projections : a global-scale model comparison. *Glob Chang Biol* 2016:3967–83. <https://doi.org/10.1111/gcb.13337>.

Rosenzweig, C., Elliott, J., Deryng, D., Ruane, A. C., Müller, C., Arneth, A., Boote, K. J., Folberth, C., Glotter, M., Khabarov, N., Neumann, K., Piontek, F., Pugh, T. A. M., Schmid, E., Stehfest, E., Yang, H., & Jones, J. W. (2014). Assessing agricultural risks of climate change in the 21st century in a global gridded crop model intercomparison. *Proceedings of the National Academy of Sciences*, 111(9), 3268–3273. <https://doi.org/10.1073/pnas.1222463110>.

SANLC 2018 https://egis.environment.gov.za/sa_national_land_cover_datasets

Schaphoff, S., Von Bloh, W., Rammig, A., Thonicke, K., Biemans, H., Forkel, M., Gerten, D., Heinke, J., Jägermeyr, J., Knauer, J., Langerwisch, F., Lucht, W., Müller, C., Rolinski, S., Waha, K. (2018). LPJmL4 – a dynamic global vegetation model with managed land – Part 1: Model description. *Geoscientific Model Development*, 11, 1343-1375.

Schipper, A. M., Hilbers, J. P., Meijer, J. R., Antão, L. H., Benítez-López, A., de Jonge, M. M., ... & Huijbregts, M. A. (2020). Projecting terrestrial biodiversity intactness with GLOBIO 4. *Global Change Biology*, 26(2), 760-771.

Siebert S, Henrich V, Frenken K, Burke J. (2013). Update of the digital global map of irrigation areas to version 5. Rheinische Friedrich-Wilhelms-Universität Bonn, Ger. Food Agric Organ United Nations, Rome, Italy 2013:171.

Snyder R.L., Geng S., Orang M., Sarreshteh S. (2012) Calculation and simulation of evapotranspiration of applied water *J. Integr. Agric.*, 11 (3), pp. 489-501, [10.1016/S2095-3119\(12\)60035-5](https://doi.org/10.1016/S2095-3119(12)60035-5)

Steduto, P., Hsiao, T.C., Raes, D., Fereres, E. (2009) AquaCrop-The FAO Crop Model to Simulate Yield Response to Water: I. Concepts and Underlying Principles. *Agronomy Journal*, 101(3): 426–437. Crop Yield Response to Water. FAO Irrigation and Drainage Paper 66. By P. Steduto, T. C. Hsiao, E. Fereres and D. Raes. Rome, Italy: Food and Agriculture Organization of the United Nations, 2012). pp. 500.

van Vuuren, D. P., J. Edmonds, M. Kainuma, K. Riahi, A. Thomson, K. Hibbard, G. C. Hurtt, T. Kram, V. Krey, J.-F. Lamarque, T. Masui, M. Meinshausen, N. Nakicenovic, S. J. Smith & S. K. Rose (2011): The representative concentration pathways: an overview. *Climatic Change* 109 (1–2): 5–31. doi:10.1007/s10584-011-0148-z.

Weedon, G. P., S. Gomes, P. Viterbo, W. J. Shuttleworth, E. Blyth, H. Österle, J. C. Adam, N. Bellouin, O. Boucher & M. Best (2011): Creation of the WATCH forcing data and its use to assess global and regional reference crop evaporation over land during the twentieth century. *Journal of Hydrometeorology* 12 (5): 823–848. doi: 10.1175/2011JHM1369.1.

You, L., Wood, S., Wood-Sichra, U., Wu, W. (2014). Generating global crop distribution maps: from census to grid. *Agricultural Systems* 127: 53-60. <https://www.mapspam.info/data>



NEXOGENESIS

STREAMLINING WATER RELATED POLICIES



This project has received funding from the European Union's Horizon 2020 research and innovation programme under grant agreement No 101003881

ANNEX I. land use products

Adige case study

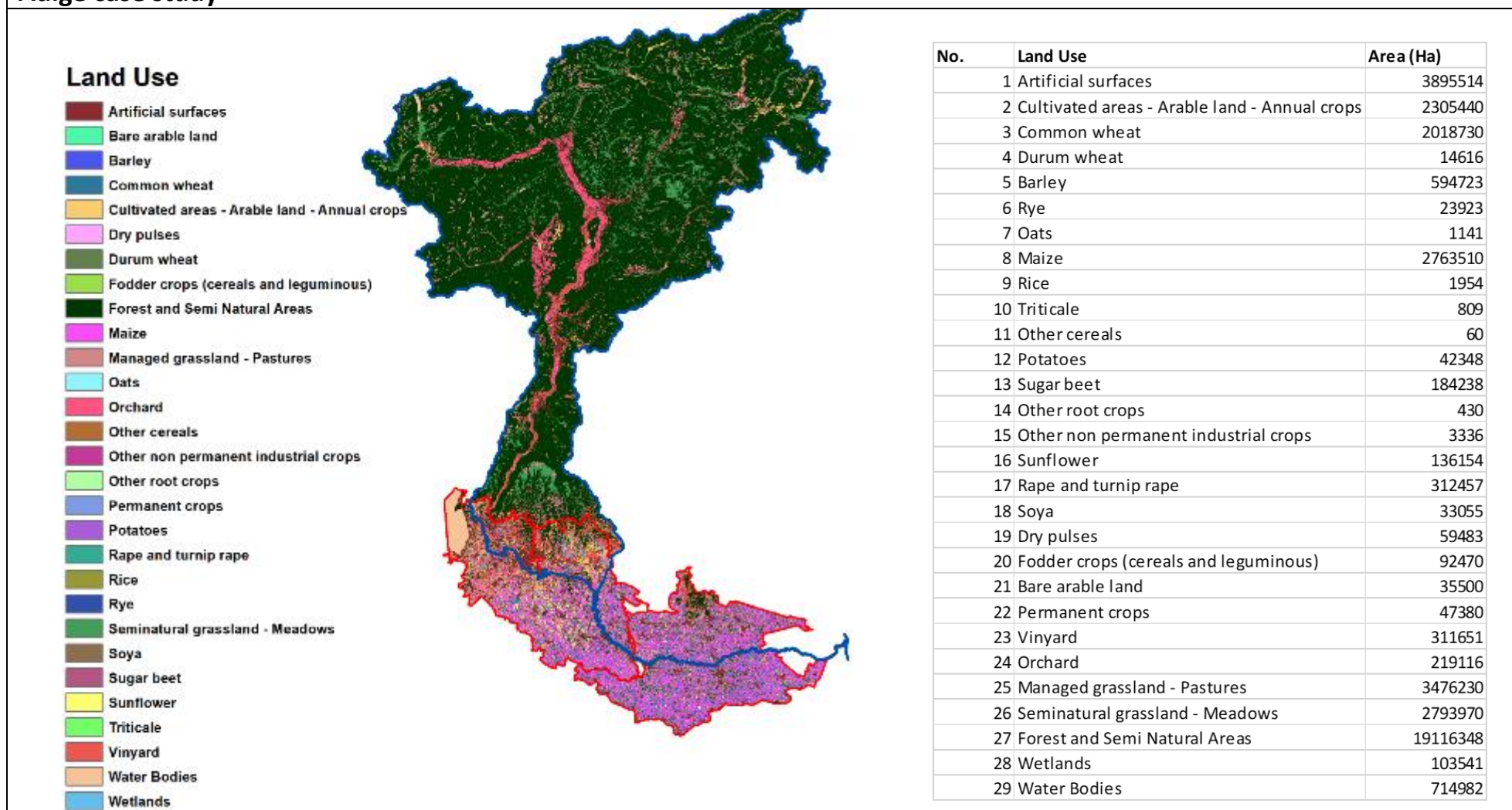
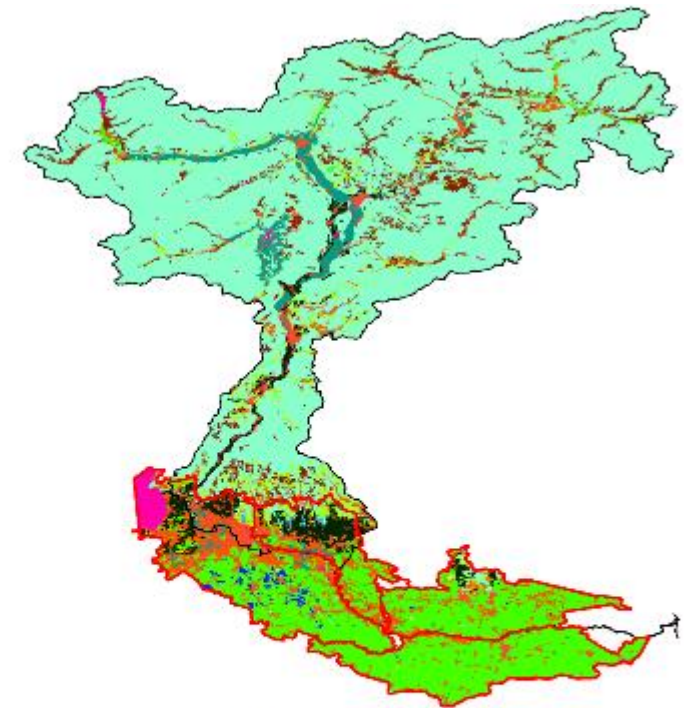


Figure A1. Adige - EUSALP₂ LULC for 2015-2020 with tabulated statistics



No.	Land Use	Area (Ha)
1	Artificial Surfaces	71556
2	Non-irrigated arable land	266075
3	Permanently irrigated land	135
4	Rice fields	5617
5	Vineyards	49724
6	Fruit trees and berry plantations	39547
7	Olive groves	1574
8	Pastures	78154
9	Annual crops associated with permanent crops	32
10	Complex cultivation patterns	61379
11	Land occupied by agriculture (mostly natural vegetation)	48101
12	Forest and Semi Natural Areas	943571
13	Wetlands	416
14	Water Bodies	20874



Land Use

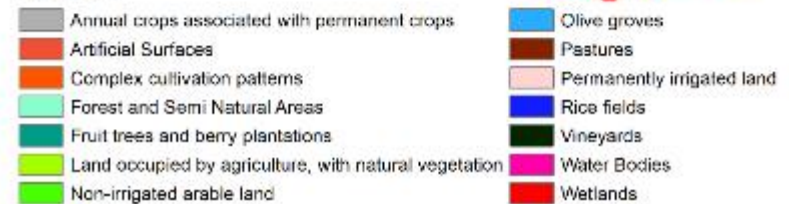
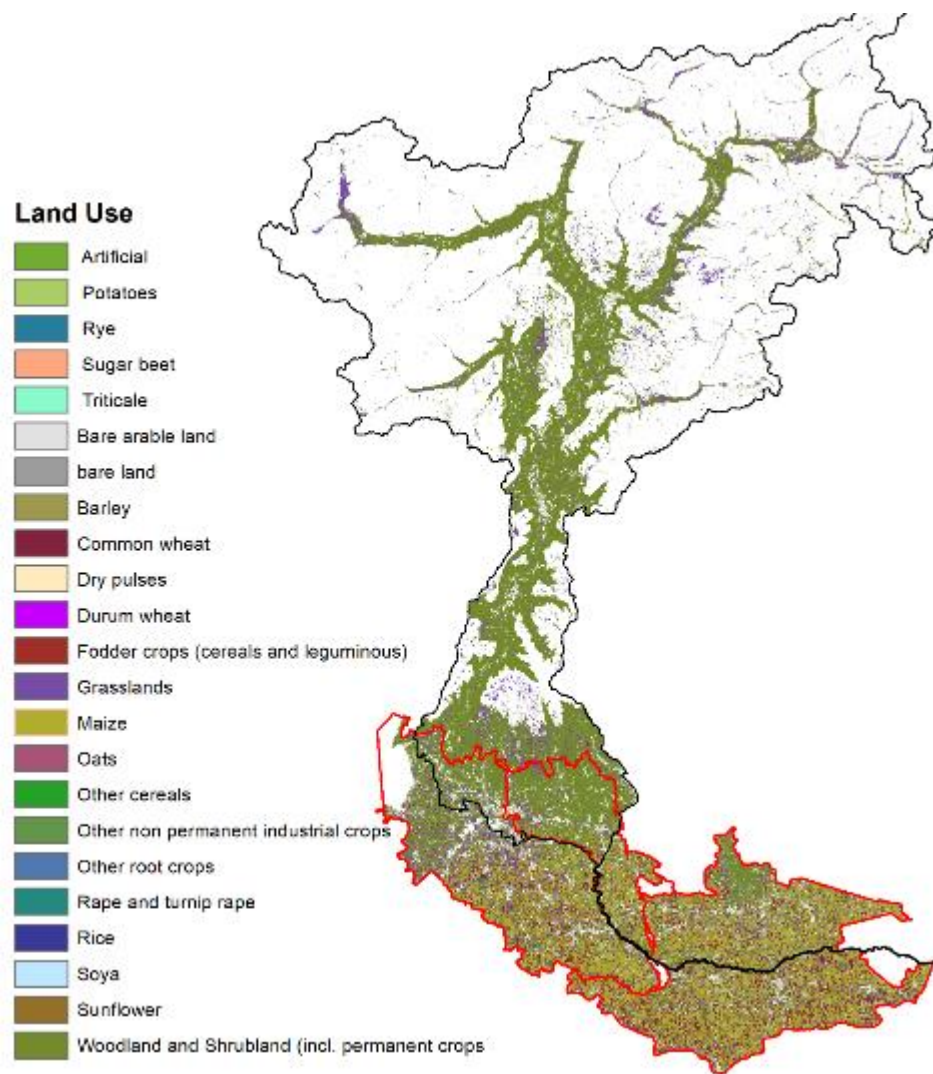


Figure A2. Adige - Corine land cover map for 2018 with tabulated statistics



No.	Land Use	Area (Ha)
1	Artificial	941
2	Common wheat	49019
3	Durum wheat	111
4	Barley	7301
5	Rye	10
6	Oats	10
7	Maize	135251
8	Rice	2
9	Triticale	2
10	Other cereals	0
11	Potatoes	1912
12	Sugar beet	2372
13	Other root crops	3
14	Other non permanent industrial crops	18
15	Sunflower	11635
16	Rape and turnip rape	3572
17	Soya	7194
18	Dry pulses	2522
19	Fodder crops (cereals and leguminous)	4290
20	Bare arable land	244
21	Woodland and Shrubland (incl. permanent crops)	353317
22	Grasslands	84051
23	bare land	82

Figure A3. Adige - EU Crop map for 2018 with tabulated statistics



JIU Case Study

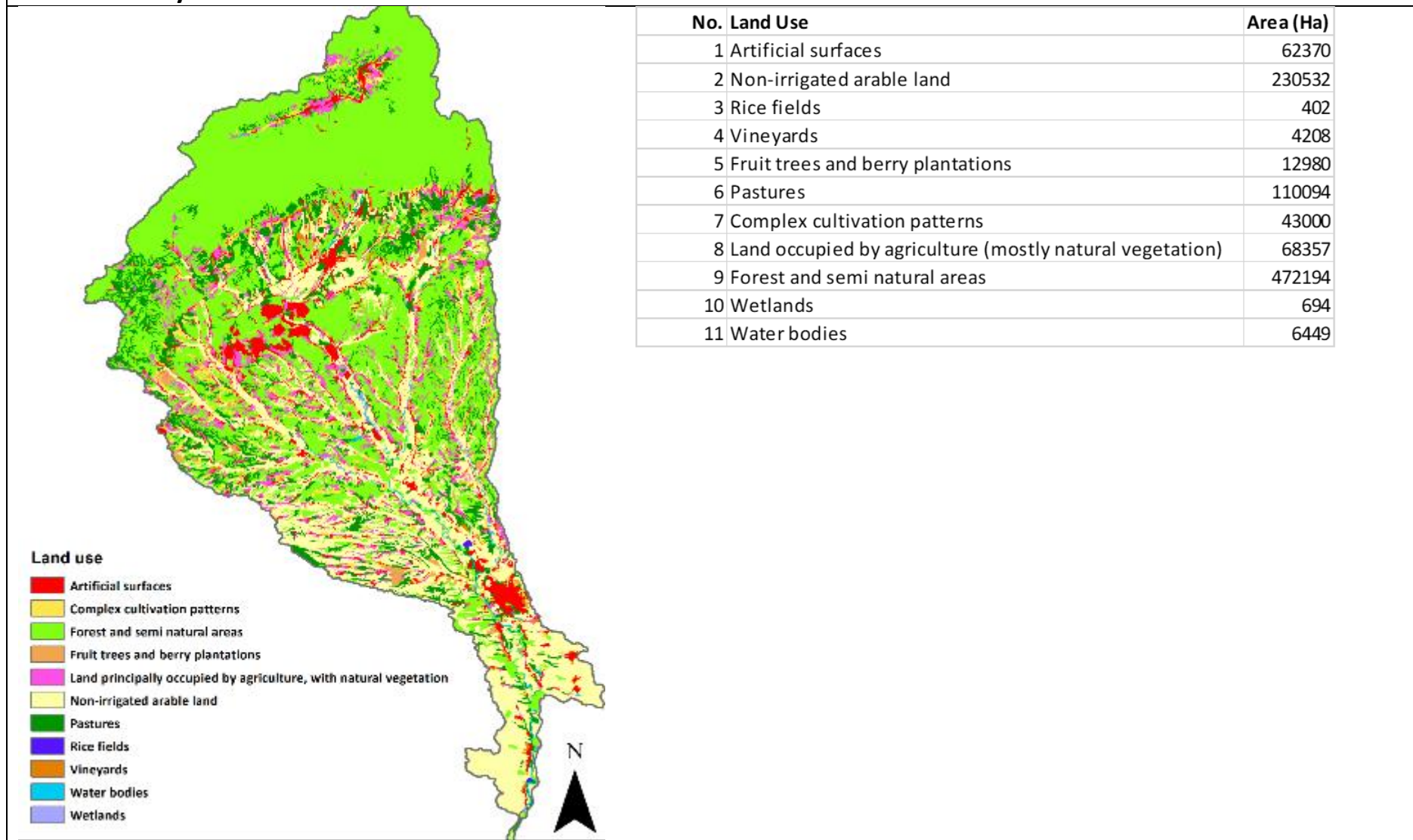


Figure A4. Jiu - Corine land cover map for 2018 with tabulated statistics

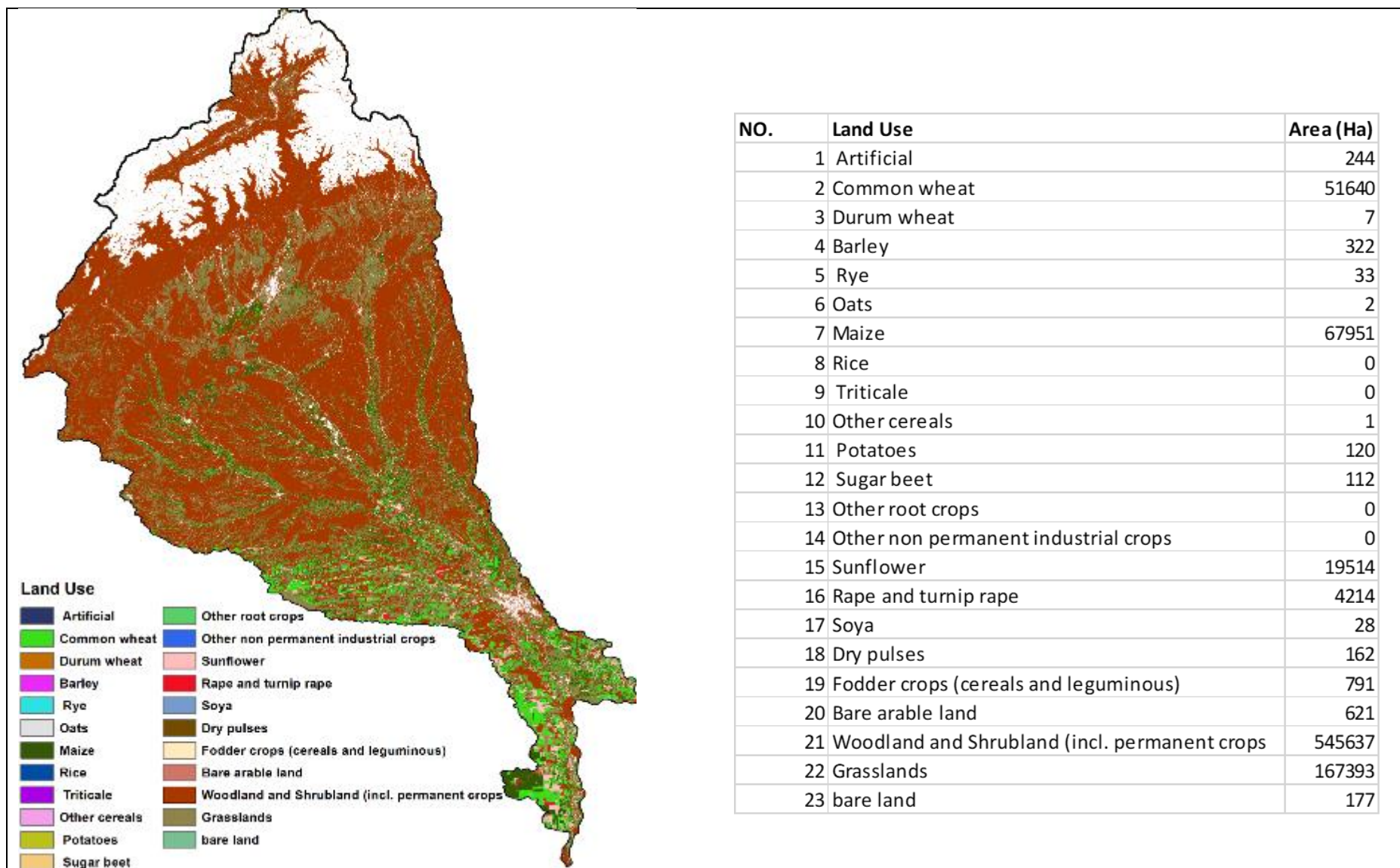
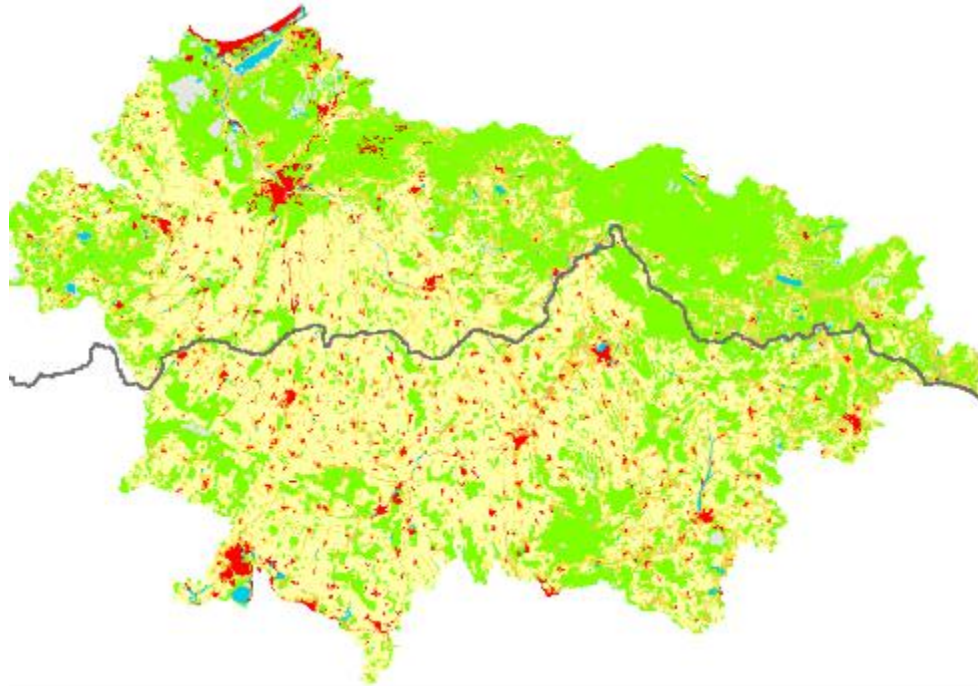


Figure A5. Jiu - EU Crop map for 2018 with tabulated statistics

Lielupe Case Study



Land Use	Area (Ha)
1 Artificial Surfaces	53091
2 Non-irrigated arable land	771055
3 Fruit trees and berry plantations	2260
4 Pastures	87779
5 Complex cultivation patterns	127783
6 Land occupied by agriculture, with natural vegetation	61357
7 Forest and seminatural areas	637053
8 Wetlands	25120
9 Water bodies	16518

Land Use



Figure A6. Lielupe - Corine land cover map for 2018 with tabulated statistics

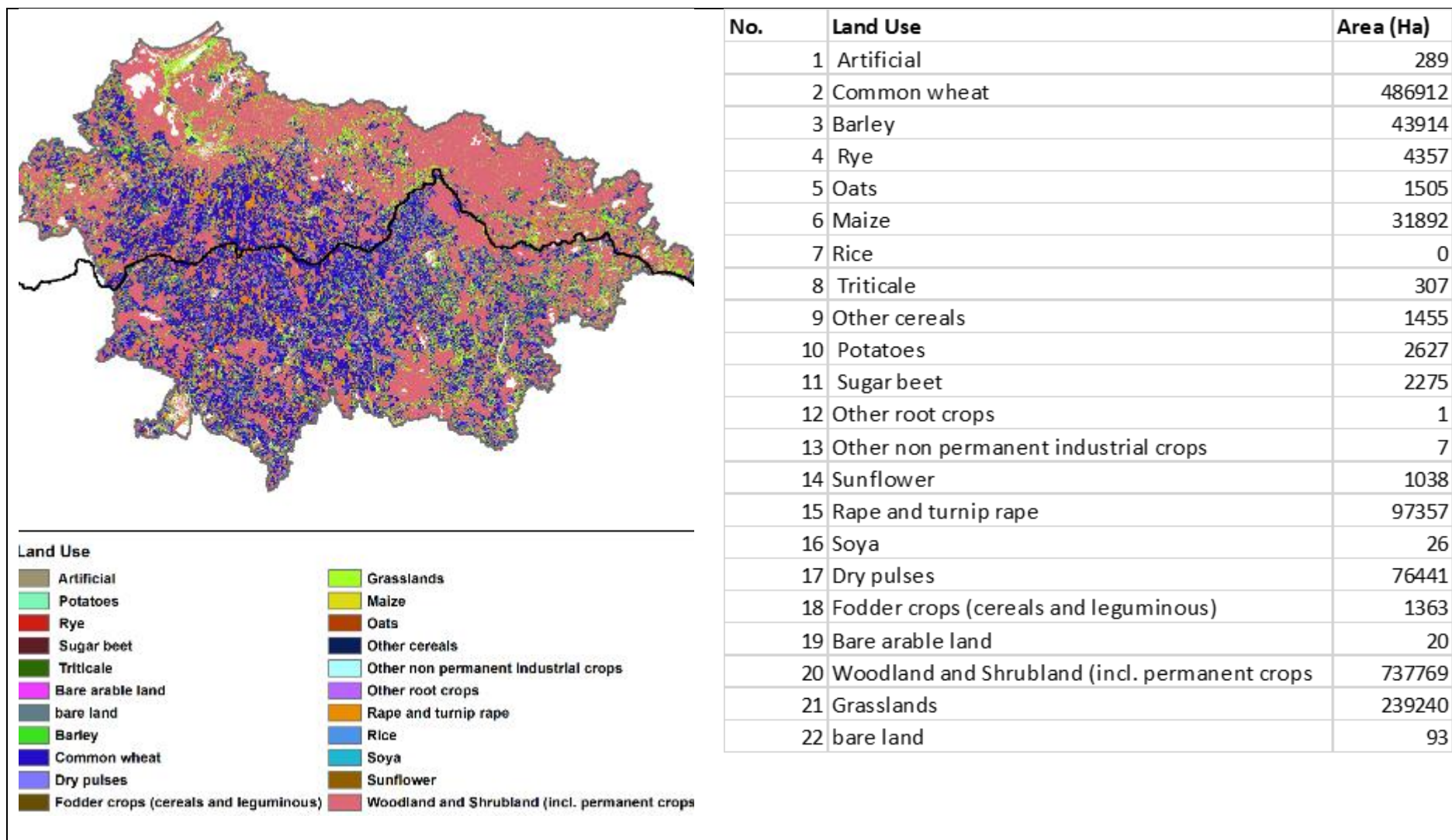
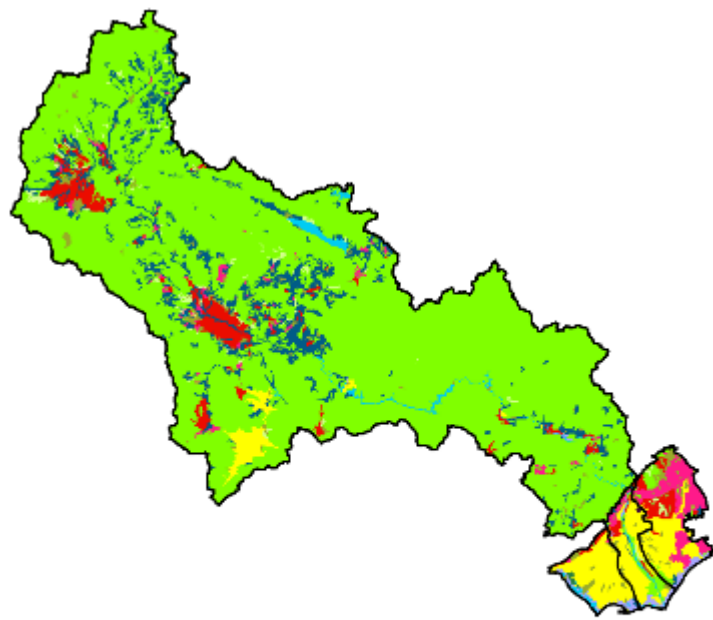


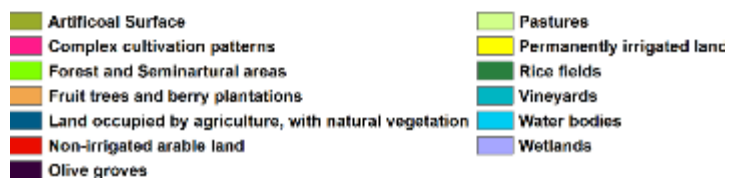
Figure A7. Lielupe - EU Crop map for 2018 with tabulated statistics



Nestos Case Study



Land use



No.	Land use	Area (Ha)
1	Artificial Surface	13365
2	Non-irrigated arable land	25762
3	Permanently irrigated land	39068
4	Rice fields	334
5	Vineyards	106
6	Fruit trees and berry plantations	44
7	Olive groves	138
8	Pastures	6289
9	Complex cultivation patterns	15976
10	Land occupied by agriculture, with natural vegetation	54523
11	Forest and Seminarural areas	515652
12	Wetlands	3639
13	Water bodies	7208

Figure A8 Nestos - Corine land cover map for 2018 with tabulated statistics

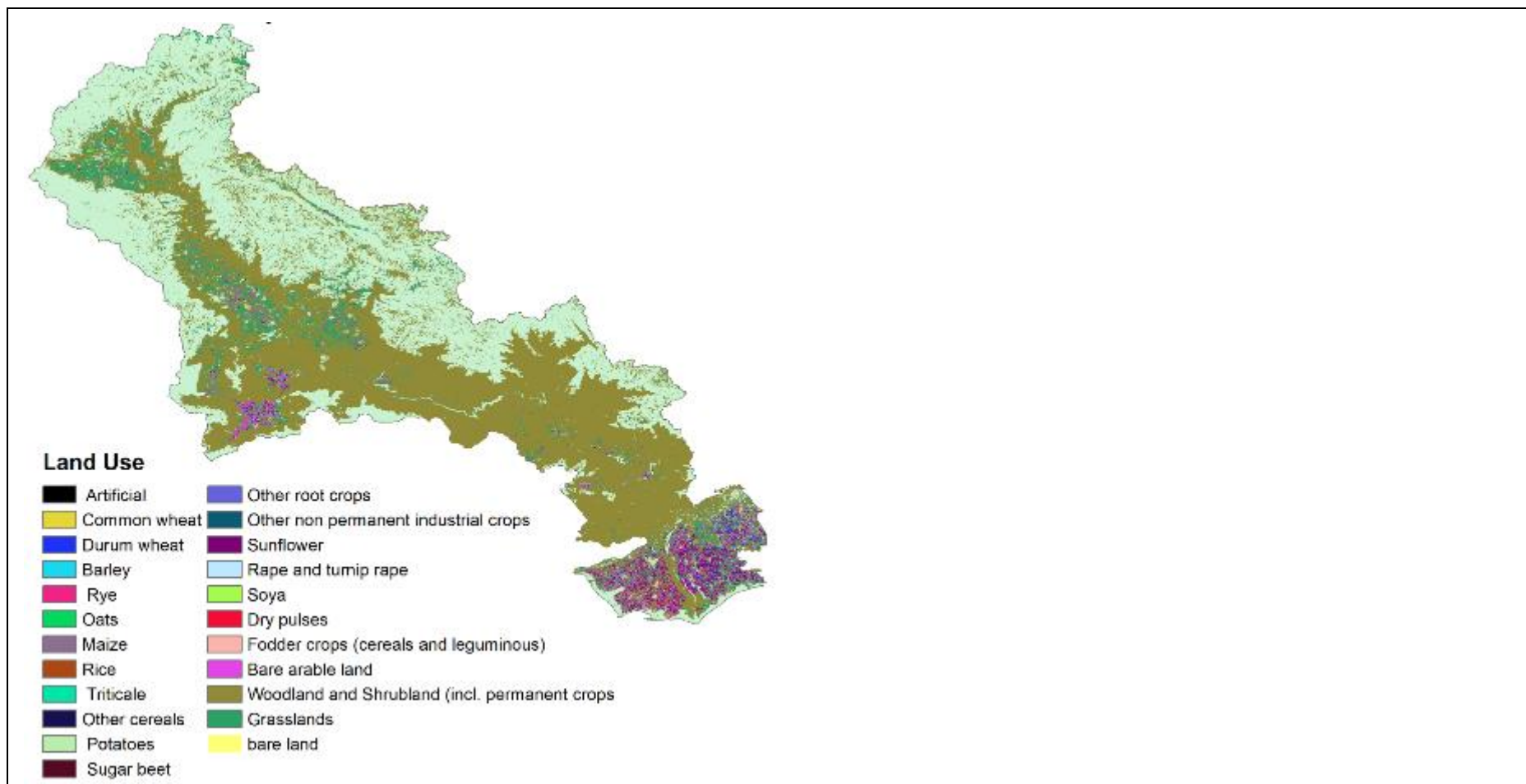
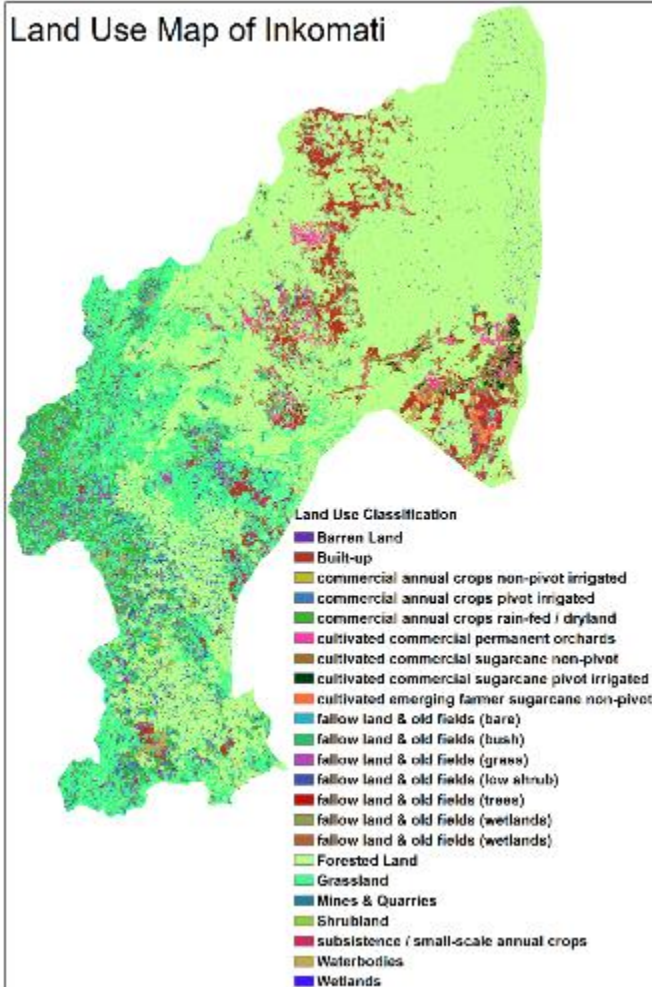


Figure A9. Nestos - EU Crop map for 2018 with tabulated statistics

Inkomati Case Study



No.	Land Use	Area (Ha)
1	Forested Land	2152996
2	Shrubland	25
3	Grassland	775408
4	Waterbodies	23149
5	Wetlands	99245
6	Barren Land	15216
7	cultivated commercial permanent orchards	46894
8	cultivated commercial sugarcane pivot irrigated	10892
9	cultivated commercial sugarcane non-pivot	33679
10	cultivated emerging farmer sugarcane non-pivot	10545
11	commercial annual crops pivot irrigated	9804
12	commercial annual crops non-pivot irrigated	625
13	commercial annual crops rain-fed / dryland	161830
14	subsistence / small-scale annual crops	40268
15	fallow land & old fields (trees)	25256
16	fallow land & old fields (bush)	12621
17	fallow land & old fields (grass)	72497
18	fallow land & old fields (bare)	541
19	fallow land & old fields (low shrub)	16
20	Built-up	142075
21	Mines & Quarries	7151
22	fallow land & old fields (wetlands)	14271

Figure A10. Inkomati - National land cover map for 2020 with tabulated statistics

Responses to reviewer

Deliverable 2.5

The deliverable is submitted on time. There is a clear and consistent coherence between the work

as outlined in the DoA and the results presented in this deliverable.

Recommendations related to this deliverable:

[1] It is necessary to extend the executive summary to include the following:

- A list of the biophysical modelling variables employed for each case study.
- The uncertainty ranges for each variable per a case study.
- The potential mistakes, currently only mentioned.

Response:

The list of specific variables employed, following implementation through System Dynamic Modelling first (WP3), and thereafter through Artificial Intelligence in WP4, is clarified in D3.2 where use of specific biophysical modelling variables for each case study is clarified and justified.

The following text was added to the executive summary (highlighted in red) to indicate main biophysical modelling variables, address uncertainty range and source of potential mistakes:

“In particular, the biophysical modelling variables considered include: mean daily precipitation flux [mm/day], daily maximum and minimum temperature [C] (climate); crop yields [t/ha] and irrigation requirement [kg/m²] (agriculture); surface runoff [mm/day] and groundwater recharge [mm/day] (water); soil carbon storage [kg/m²] and vegetation carbon storage [kg/m²] (ecosystems). Summary tables of mean values and uncertainty ranges are provided for all the studied variables in each case study region. Temperature and precipitation uncertainty ranges are consistent across regions, with model projections mostly agreeing with each other. As expected, higher uncertainty appears for the bio-physical variables, especially those related to water and agriculture. This is due to the higher number of factors affecting the models projections, including model parameterization and design, as well as different response to climatological uncertainty. In most cases the uncertainty range is increased by the presence of one or two models acting as outliers and projecting values significantly different from the rest of the ensemble. Moreover, differences in models behaviour across regions could be dictated by different local conditions, the extent of the studied area and biases in the choice of grid-cells.”

Furthermore, considering necessity of specifying in detail uncertainty ranges of relevant variables, to the table at the end of NEXUS sections values were added defining median and deviance (in brackets) of the ensemble range for the most relevant variable used in the System Dynamic Modelling for each case study.

[2] Disclaimer is missing, please, add.

Response:

A Disclaimer was added at bottom of page 3

[3] Please, indicate all changes in a clear manner, preferably by using a different colour for the text.

It will help to reassess your work accordingly

Response:

All the additions to the text in the deliverable to address reviewer observations are highlighted in red

